

---

This item was submitted to [Loughborough's Research Repository](#) by the author.  
Items in Figshare are protected by copyright, with all rights reserved, unless otherwise indicated.

## **Studies of column packings for polymer separations by size exclusion and interactive chromatography**

PLEASE CITE THE PUBLISHED VERSION

PUBLISHER

© Ana M.C. Montenegro

LICENCE

CC BY-NC-ND 4.0

REPOSITORY RECORD

Montenegro, Ana M.C.. 2019. "Studies of Column Packings for Polymer Separations by Size Exclusion and Interactive Chromatography". figshare. <https://hdl.handle.net/2134/11754>.

This item was submitted to Loughborough University as a PhD thesis by the author and is made available in the Institutional Repository (<https://dspace.lboro.ac.uk/>) under the following Creative Commons Licence conditions.



For the full text of this licence, please go to:  
<http://creativecommons.org/licenses/by-nc-nd/2.5/>

CALL ID NO. DX 72752/82

LOUGHBOROUGH  
UNIVERSITY OF TECHNOLOGY  
LIBRARY

AUTHOR/FILING TITLE

MONTENEGRO, AMC

ACCESSION/COPY NO.

012345/02

VOL. NO.

CLASS MARK

~~27 JUN 1997~~

LOAN COPY

001 2345 02





STUDIES OF COLUMN PACKINGS FOR POLYMER SEPARATIONS BY  
SIZE EXCLUSION AND INTERACTIVE CHROMATOGRAPHY

by

ANA MARIA CELESTINO MONTENEGRO

A Doctoral Thesis

Submitted in partial fulfilment of the requirements for  
the award of Doctor of Philosophy of the Loughborough  
University of Technology.

DECEMBER 1986

Supervisor: J.V. Dawkins, Ph.D.

Department of Chemistry

© by ANA M. C. MONTENEGRO 1986

Loughborough University of Technology Library	
Date	Feb 87
Class	
Acc. No.	012345/02

To my parents for their  
cooperation, comprehension and  
continous encouragement.

## ACKNOWLEDGEMENTS

I would like to thank my supervisor, Dr. J. V. Dawkins, for his useful recommendations and interest shown in this research.

I also wish to thank my employers, Instituto de Atividades Espaciais, Centro Tecnico Aeroespacial, for the financial support of this Ph.D. programme.

Thanks are also due to all my colleagues who made my time at Loughborough enjoyable and especially to Mr. I. Hovell for typing this thesis and for his continuous encouragement.



## ORIGINALITY

All the work presented in this thesis has been carried out by the author except where acknowledged and has not previously been presented for a degree at this University or any other institution.

## ABSTRACT

The chromatographic behaviour of a new column packing for high performance size exclusion chromatography based on crosslinked polyacrylamide particles was studied. Experimental retention data for poly(ethylene glycol) and poly(ethylene oxide) standards in water and water-methanol mixtures showed that the separation mechanism is size exclusion, since a universal calibration plot based on hydrodynamic volume was obtained. For polysaccharide standards in water and water-methanol (80/20), the universal calibration was valid for molecular weights above  $4 \times 10^5$ . Below this value, secondary mechanisms appear to be taking part in the separation since water-methanol (80/20) is a poor solvent for polysaccharides. Crosslinked polyacrylamide packings showed an interactive behaviour with tetrahydrofuran and dimethylformamide as eluents with polystyrene and poly(ethylene glycol)/poly(ethylene oxide) standards and the universal calibration was not valid.

Experimental plate height data for poly(ethylene glycol) standards in water demonstrated a predominance of dispersion caused by solute mass transfer in the stationary phase for crosslinked polyacrylamide packings. The plate height results provided reliable values for the polydispersity of poly(ethylene glycol) standards corrected for axial dispersion.

A system was developed to perform off-line and on-line multidimensional chromatography by coupling a size exclusion column with an interactive column. The results obtained for the analysis of poly(styrene-co-n-butyl methacrylate) copolymers showed that separations

according to copolymer composition can be achieved both with crosslinked polystyrene and crosslinked polyacrylamide packings as interactive columns and mixtures of tetrahydrofuran-heptane and tetrahydrofuran-isopropanol as eluents.

## CONTENTS

	<u>PAGE</u>
<u>CHAPTER 1 - INTRODUCTION</u>	
1.1 Development of column packings for high performance liquid chromatography	1
1.1.1. Microparticulate packings	2
1.1.2. Liquid-solid Chromatography	3
1.1.3. Bonded-phase Chromatography	3
1.1.3.1 Reversed phase	6
1.1.3.2 Normal phase	6
1.1.4. Ion Exchange Chromatography	7
1.1.5. Size Exclusion Chromatography	8
1.1.5.1 Organic	9
1.1.5.2 Aqueous	9
1.2 Calibration of size exclusion chromatography systems	12
1.2.1. Size exclusion chromatography separation mechanism	12
1.2.2. Molecular Weight determination	15
1.2.3. Calibration with narrow molecular weight standards	17
1.2.4. Calibration with broad molecular weight standards	18
1.2.5. Universal Calibration	19
1.3 Secondary effects	22

	<u>PAGE</u>
1.3.1. Mixed eluents	15
1.3.2. Adsorption and partition	24
1.3.3. Ionic effects	26
1.3.4. Concentration effects	28
1.4 Axial Dispersion	29
1.4.1. Plate height	29
1.4.2. Column dispersion processes	32
1.4.3. Correction for axial dispersion	36
1.5 Multidimensional Chromatography	38
1.5.1. Separation methods	38
1.5.2. Off-line	42
1.5.3. On-line	42
1.5.4. Applications for polymer analysis	44
1.6 Aims of the present work	51
 <u>CHAPTER 2- EXPERIMENTAL</u>	
2.1 Materials	53
2.1.1 Solvents	53
2.1.2 Solutes	54
2.1.2.1 Polymer standards and low molecular weight solute	54

	<u>PAGE</u>
2.1.2.2 Styrene-n-butylmethacrylate copolymers	56
2.2 Chromatographic equipment	58
2.2.1 Instrument 1	58
2.2.2 Instrument 2	58
2.2.3 Instrument 3	59
2.2.4 High temperature size exclusion chromatography	62
2.3 Chromatographic operating procedures	63
2.3.1 Size exclusion chromatography	63
2.3.2 Multidimensional chromatography	63
2.3.2.1 Off-line technique	63
2.3.2.2 On-line technique	64
2.4 Columns	67
2.5 Data analysis	69
2.5.1 Retention volumes	69
2.5.2 Calibration curves	70
2.5.3 Molecular weights	72
2.5.4 Column efficiency	72
2.6 Viscosity measurements	73

	<u>PAGE</u>
2.7 Ultraviolet analysis	75
 <u>CHAPTER 3 - RESULTS and DISCUSSION</u>	
3.1 Sample preparation	76
3.1.1 Concentration effects	76
3.1.2 Sample dissolution	78
3.2 Calibration for crosslinked polyacrylamide columns	80
3.2.1 Calibration for different polymers	80
3.2.2 Calibration in aqueous solvents	91
3.2.3 Calibration in organic solvents	105
3.3 Column efficiency	113
3.3.1 Dispersion mechanisms	113
3.3.2 Diffusion coefficient	124
3.3.3 Polydispersity	129
3.4 Preliminary studies for multidimensional chromatography	139
3.4.1 Concentration effects	139
3.4.2 Off-line multidimensional chromatography	139
3.5 Analysis of polymers by on-line multidimensional chromatography	153
3.5.1 Crosslinked polystyrene column packing	159
3.5.2 Crosslinked polyacrylamide column packing	166

CHAPTER 4 - CONCLUSIONS AND RECOMMENDATIONS

172

CHAPTER 5 - REFERENCES

177



## 1. INTRODUCTION

### 1.1 DEVELOPMENT OF COLUMN PACKINGS FOR LIQUID CHROMATOGRAPHY

By 1970 two types of column packing materials were available for liquid chromatography ( LC ): totally porous and superficially porous particles. Totally porous particles with a diameter (  $d_p$  ) greater than 50  $\mu\text{m}$  were soon considered undesirable for high performance liquid chromatography ( HPLC ) because of the slow diffusion of sample components into and out of the deeper pores[1]. Superficially porous particles, known as porous layer beads ( PLB ), were the standard packing for HPLC at that time, with a  $d_p$  between 30 and 40  $\mu\text{m}$ . The PLB consists of a solid glass bead with a thin porous outer shell ( about 5  $\mu\text{m}$  ) which may be silica, alumina, or ion-exchange resin ( often referred to as pellicular ), or a silica layer to which a "liquid" phase has been chemically bonded[2].

However, PLB packings could not be used for size exclusion chromatography ( SEC ) because of their low sample capacities[3]. The packings available for SEC at that time were macroporous particles of

totally porous beads that could be rigid ( silica or glass ), semirigid ( polystyrene gels ), or soft. The soft gels, such as agarose, were used in gel filtration for the separation of water-soluble polymers such as proteins[4].

#### 1.1.1 Microparticulate Packings

The production of commercial quantities of microparticulate packings in the first years of the last decade brought considerable advances in all areas of LC[5]. These particles, with a  $d_p$  around 10  $\mu\text{m}$  or below, required the development of more sophisticated column packing techniques and chromatographic apparatus and, when these problems were overcome, microparticulate packings quickly replaced the PLB packings[2].

The great advantage of microparticulate packings over PLB (  $d_p \approx 30 \mu\text{m}$  ) is the reduction of the analysis time. Smaller columns produce identical or higher numbers of theoretical plates because the column efficiency is inversely proportional to the  $d_p$  squared[6].

Presently, rigid solid particles based on a silica matrix are the most widely used packing material for HPLC. These silica particles can be obtained in a variety of sizes, shapes and varying degrees of porosity. Various functional groups or polymeric layers can readily be attached to the silica surface, extending the utility of these particles for applications to any individual LC method[7]. Porous semirigid

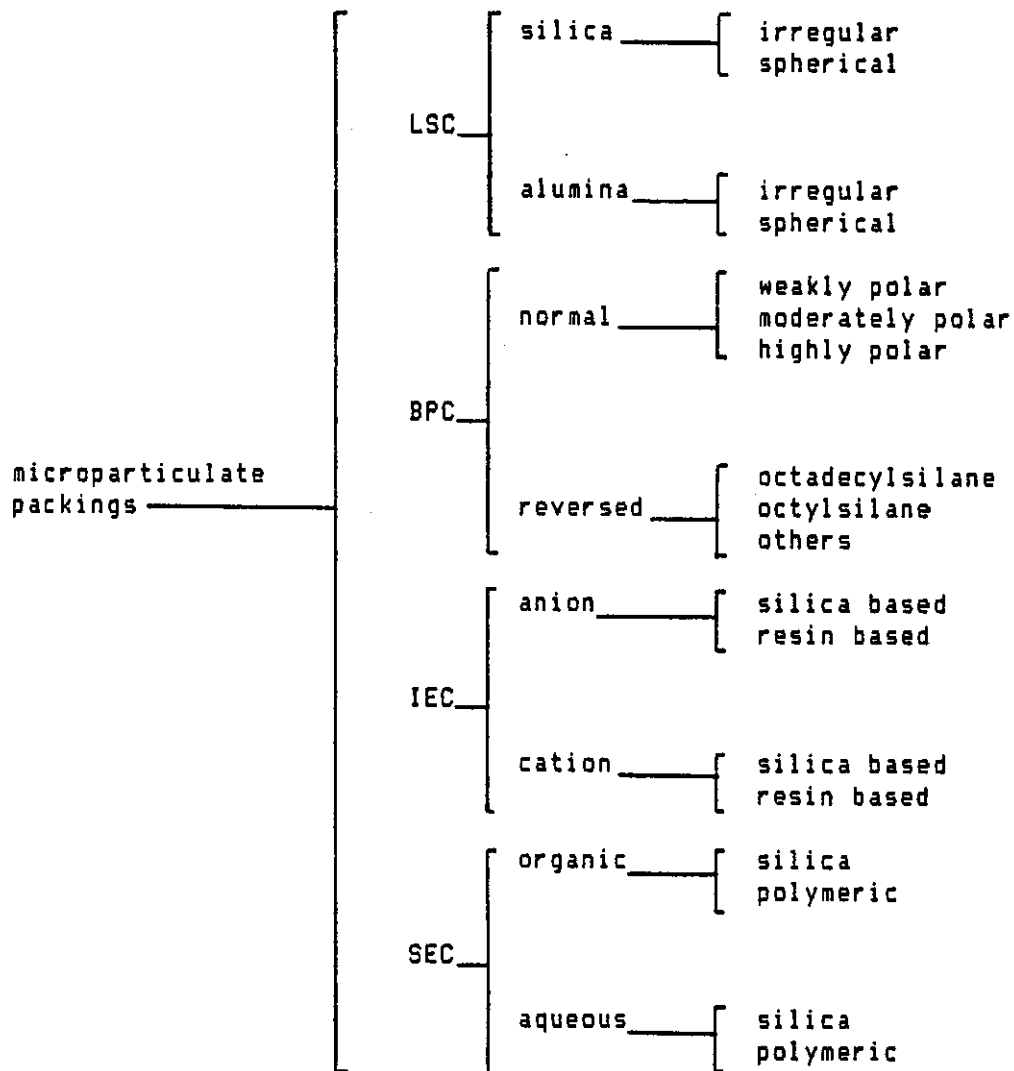
microparticles based on polystyrene cross-linked with divinylbenzene ( PS-DVB ) are the most common packing material for ion-exchange and size exclusion chromatography. Depending on how they are prepared, the resulting particles can vary in both rigidity and porosity over fairly wide limits[7]. A recent survey on trends in HPLC column usage shows a continuous increase on uses of polymeric packings, especially for reversed-phase work[8]. Figure 1.1 shows the most common types of microparticulate packings available for each chromatographic separation mode.

#### 1.1.2 Liquid-solid Chromatography

Liquid-solid or adsorption chromatography involves the retention of the solute by attraction to the surface of the packing particles[9]. Alumina and silica are the microparticulate packing traditionally used for LSC. Their use is now on the decline and many LSC applications are being performed by chemically bonded-phase chromatography[10].

#### 1.1.3 Bonded-phase Chromatography

FIGURE 1.1  
TYPES OF MICROPARTICULATE PACKINGS FOR HPLC



The separation mechanism in bonded-phase chromatography ( BPC ) can be regarded as a partition of solute molecules between the mobile and stationary phases[9]. Most of the applications in BPC use silica-based supports. The bonded-phase packings are generally obtained by reaction of organochlorosilane or organoalkoxysilane with the surface hydroxyl ( silanol ) groups of silica gel, producing the siloxane ( Si-O-Si-C ) type of bond, which is more stable and normally used in pH range 2 - 8. By varying the nature of the organic portion of the silane, the surface polarity of the bonded phase packing can be altered. Bonded-phases vary from the hydrophobic octadecylsilane group to the polar amino functionality and ionic phases for use in ion-exchange[2].

For purposes of comparison, the BPC packings can be divided into two types: reversed-phase and normal-phase. This simple division based on relative polarities of the mobile and stationary phases is somewhat arbitrary for under the appropriate chromatographic conditions a polar bonded-phase can function as a reversed-phase packing while packings having an octadecylsilane group can behave as modified adsorbents. The reversed-phase mode is referred to when the stationary phase, usually hydrophobic, is less polar than the mobile phase while normal-phase chromatography is the term used when the mobile phase is less polar than the stationary phase, often hydrophilic[2].

#### 1.1.3.1 REVERSED-PHASE

The reversed-phase technique in its various forms - regular partition ( or adsorption ), ion suppression, ion pair partition - is the most widely used mode in HPLC. There is a large number of reversed-phase packings commercially available. The bonded-phase packings are classified according to polarity, which is given by the length of the organic sidechain: long ( C18 ), medium ( C8 ) or short ( C2 ). PS-DVB packing material, which is non polar, is also used as a reversed-phase column packing. Since these resins can be used at virtually all pH values, they present advantages over bonded-phases for certain applications[2].

#### 1.1.3.2 NORMAL-PHASE

Polar bonded-phases used in the normal mode sometimes give separations similar to those obtained on silica or alumina but have the advantage of more rapid response to solvent compositional changes. Also, they give less tailing for polar compounds since the strong ( reactive ) silanols responsible for tailing are eliminated by the reaction with organosilane.

These phases are classified by the nature of the polar functional

group on the organic sidechain. The weakly polar packings are mainly diol, dimethylamino or nitro. Polymeric beads which display weakly polar functionality ( PS-DVB and acrylic ) are also included in this category.

Cyano bonded-phase column packings show medium polarity and have become quite popular in that they can be a useful alternative to silica . Compared to amino phases, when used in the normal-phase mode, cyano column packings show fewer side reactions and can also be used for reversed-phase work. The polar aminoalkyl functional group is particularly interesting in that being basic it imparts a quite different chromatographic selectivity when compared to the slightly acidic surface of silica gels[10].

#### 1.1.4 Ion-exchange Chromatography

Two types of microparticulate packings are used in ion-exchange chromatography: silica and crosslinked PS-DVB resins[10]. Silicas for ion-exchange may be used at room temperature and provide higher chromatographic efficiency. At room temperature, crosslinked porous resins exhibit lower rates of mass transfer and thus generally are used at elevated temperatures ( 50 - 80°C ) to reduce solvent viscosity and improve efficiency and peak shape. A great advantage of the ion-exchange resins is their pH stability, generally 1 - 14 for cation exchangers, 0 - 12 for anion exchangers. The silica-based exchangers have an upper pH limit of 7.7 - 9 depending on the manufactures specifications, because the siloxane

bonds are attacked by hydroxide in aqueous solution[10].

#### 1.1.5 Size Exclusion Chromatography

The mechanism of separation in SEC is based on the dimensions of molecules in solution and will be presented in more detail in section 1.2. Packings for high performance size exclusion chromatography ( HPSEC ) can be semirigid organic gels or rigid inorganic packings[11]. The rigid packing materials available for HPSEC is porous glass, silica or chemically modified silica. The great advantages of porous silica and glass over polymeric packings are their excellent thermal and mechanical stability, a well-defined pore size distribution[12] and the ability to be used with a wide variety of solvents, both aqueous and nonaqueous[11]. However, because of the active surface sites, adsorption or partition occurs very often producing tailed peaks, retarded peaks or peaks eluting beyond the column total permeation volume. Some of the adsorption effects can be eliminated or substantially reduced by modifying the siliceous particles[11]. Some bonded-phase packing material have been especially produced for HPSEC and are commercially available. One of these packing materials is a porous silica chemically modified with ether groups and can be used with both organic and aqueous mobile phases. Another silica packing was chemically modified with glyceryl groups and was developed to be used with aqueous and other highly polar mobile phases. However, as



with all silica based packing materials, they are stable only between pH 2 to 8[13].

#### 1.1.5.1 Organic Size Exclusion Chromatography

Most HPSEC analyses of synthetic organic polymers are performed with 10  $\mu\text{m}$  particles of PS-DVB with variable degrees of crosslinking. These gels are compatible with most common organic solvents, except acetone alcohols and some very polar solvents[11]. The PS-DVB gels show minimum interaction with solutes, and can be used to analyse a wide variety and size range of polymers, oligomers and low molecular weight samples[10].

Rigid packings are also used with organic solvents but, interactions between solute-packing are difficult to avoid, especially for polar molecules. These effects will be discussed in more detail in section 1.3.2.

#### 1.1.5.2 Aqueous Size Exclusion Chromatography

The soft gels traditionally used in gel filtration, such as

cross-linked dextrans, polyacrylamide gels and agarose, have low mechanical stability and cannot withstand the high pressures generated in HPSEC[14]. Porous glass and silica packings when used with aqueous eluents lead to adsorption of the solutes and even surface treated silicas show potential difficulties due to the presence of untreated ionic sites[15]. Therefore, the development of new packings for HPSEC analyses of water-soluble polymers, free of solute packing interactions, has been a field of intense activity in recent years[16,17].

Water-soluble polymers represent a large class of polymeric substances which range from biologically active compounds to synthetic polymers. Molecular weights (MW) can be several hundred to many millions. Some polymers are monodisperse such as biopolymers. Water-soluble polymers can be classified into nonionic polymers and polyelectrolytes. To be water-soluble, nonionic compounds must be hydrophilic and generally contain polar groups like hydroxyl, amino or ether. Polyelectrolytes can be anionic, cationic or ampholytic[16].

Because of the polar nature of water-soluble polymers, many types of interactions may occur in aqueous HPSEC. Besides all the interactive effects common to organic and aqueous HPSEC, there are two mechanisms that are unique to aqueous HPSEC: ionic interactions between polyelectrolytes and the packing and intramolecular electrostatic effects of the polyelectrolyte [16]. These effects will be discussed in section 1.3.3.

One way of reducing the interaction problems associated with polar silica and silica-based packings would be the use of less polar polymeric packings. Some of the commercially available polymeric packings for aqueous HPSEC are based on a crosslinked methacrylate glycerol copolymer, a sulfonated PS-DVB and a crosslinked hydroxylated polyether[16,17].

Several studies were made to evaluate the polyether-based column packing and there was no evidence of secondary effects in the analysis of oligomers and ionic and nonionic polymers[14,17-24] with aqueous eluents. It was also proved that under appropriate ionic strength conditions, the universal calibration reveals no adsorptive effects for strongly cationic polymers[24].

Recently, a new type of high resolution polymeric-based column packing for use in aqueous HPSEC has become commercially available[25]. These columns are packed with a very hydrophilic gel formed in the copolymerization of acrylamide and N, N'-methylene-bisacrylamide, where the crosslinking agent is the major component by weight[26]. These microparticulate packings have proved suitable for the analysis of poly ( ethylene glycol ) samples but there is no published data concerning their use for the analysis of other polymers[26].

## 1.2 CALIBRATION OF SEC SYSTEMS

SEC, when used with only a concentration detector, is a nonabsolute method for determining MW averages and molecular weight distributions ( MWD ) of polymers and so requires calibration[27]. The only way to avoid the use of a calibration curve, turning SEC into an absolute technique, is the use of dual detection with a concentration detector coupled to a MW detector ( low-angle laser light-scattering photogoniometer ) ( LALLS ) [12].

### 1.2.1 SEC Separation Mechanisms

The mechanism of retention in SEC can be explained as a network-limited separation with a distribution of the solute between the solvent outside the porous particles in the column and the solvent filling the pores. Therefore, the retention volume (  $V_R$  ) of a solute in a porous packing can be expressed in terms of a distribution coefficient for SEC (  $K_{SEC}$  ):[28]

$$V_R = V_0 + K_{SEC} \cdot V_i \quad (1.1)$$

where  $V_0$  is the total volume of mobile phase, i.e. interstitial or void volume, and  $V_1$  is the total volume of the stationary phase, i.e. solvent within the porous packing.  $K_{SEC}$  represents the ratio of the concentration of solute of given size in the stationary phase to that in the mobile phase. Very large molecules are confined to the mobile phase because their size in solution is greater than the size of the packing pores ( $K_{SEC} = 0$ ). Small molecules however have free access to both stationary and mobile phases ( $K_{SEC} = 1$ ). As solute molecules migrate through the chromatographic column, the large molecules are eluted first, followed by solute of decreasing size which penetrates an increasing fraction of the solvent within the particles ( $0 \leq K_{SEC} \leq 1$ ) [29]. To account for other possible retention mechanisms, Dawkins and Hemming [30] proposed that the distribution coefficient needs to be expanded so that

$$K_{SEC} = K_D K_P \quad (1.2)$$

where  $K_D$  is the distribution coefficient for size exclusion and  $K_P$  is the distribution coefficient for solute-packing interactions. Under normal chromatographic conditions the solute distribution between mobile and stationary phases achieves thermodynamic equilibrium. So, it is assumed that, at constant temperature, the relationship between the standard free energy change  $\Delta G^\circ$  for the transfer of solute molecules from the mobile to the stationary phase and  $K_{SEC}$  is given by [31]

$$\Delta G^\circ = -kT \ln K_{SEC} \quad (1.3)$$

where  $k$  is the Boltzmann constant and  $T$  is the absolute temperature. The

standard free energy change depends on the standard enthalpy change  $\Delta H^\circ$  and the standard entropy change  $\Delta S^\circ$ : [31]

$$\Delta G^\circ = \Delta H^\circ - T\Delta S^\circ \quad (1.4)$$

Combining equation 1.3 and 1.4 gives

$$K_{SEC} = \exp(-\Delta H/kT) \cdot \exp(\Delta S^\circ/k) \quad (1.5)$$

Based on the foregoing equations Dawkins[31] suggested that  $K_p$  is determined by an enthalpy contribution

$$K_p = \exp(-\Delta H^\circ/kT) \quad (1.6)$$

and  $K_D$  is determined by an entropy contribution

$$K_D = \exp(-\Delta S^\circ/T) \quad (1.7)$$

When size exclusion is the only type of mechanism in the separation,  $\Delta H^\circ = 0$  and  $K_p = 1$ . Since solute mobility becomes more limited inside the pores of the column packing, solute permeation in SEC is associated with a decrease in entropy.  $K_D$  is defined as the ratio of accessible solute arrangements within the porous packing to those in the mobile phase, acquiring values between zero and unity and, in accord with

experimental findings, is independent of temperature.

Solute-packing interactions involve the transfer of solutes between the phases and are associated with inter-molecular forces and substantial enthalpy changes. If adsorption and/or partition of the solute takes place,  $\Delta H^\circ$  is negative and  $K_p > 1$ . When there is incompatibility between the solute and packing  $\Delta H^\circ$  is positive and  $K_p$  values range between zero and unity.

Consequently, if  $K_p$  is different from unity, nonexclusion interactions operate in the separation. If  $K_p$  is equal to unity  $K_D = K_{SEC}$  and the separation is based on pure size exclusion effects and is temperature independent. However, a slight dependence of  $V_R$  on temperature, sometimes found experimentally, can be explained as being due to the dependence of the effective dimensions of the separated macromolecules or of the porous network on temperature; otherwise it indicates enthalpic solute-packing interactions[28].

### 1.2.2 Molecular Weight Determination

The position, width, and shape of the elution curve provide information on MW and MWD of the polymer being analysed[28], and so the elution curve is very useful for relative sample comparison. However, the profile of an elution curve is also a function of the specific columns and instrumentation used in the experiment. As a consequence, relative sample

comparison is valid only for data obtained under the same experimental conditions and the elution curve must be transformed into MWD curves to allow data from different instruments to be compared[32-34].

The relations between the normalized molecular weight distributions  $I(M)$  and  $W(M)$  and the normalized chromatogram are[12]:

$$W(M) = -(dI(M))/dM = -(dI(V))/dV \cdot dV/d \log M \cdot d \log M/dM \quad (1.8)$$

where,  $I(V)$  is the weight fraction of polymer eluted up to retention volume  $V$ . The ordinate of the chromatogram is  $dI(V)/dV$  and  $d \log M/dM$  is  $1/M$ . With the knowledge of the calibration function,

$$\log M = f(V) \quad (1.9)$$

the MWD can be calculated.

Polymers are characterized by the existence of a distribution of chain lengths and therefore a MWD. Because of the existence of this distribution, any experimental measurement of polymer MW can give only an average value. Depending on the property being measured, different types of MW averages can be obtained[35]. The average molecular weights can be calculated with the relations:[36]

$$\bar{M}_n = 1/\int (1/M)W(M)dM \quad (1.10)$$

$$\bar{M}_w = [\int M^2 W(M)dM]^{1/2} \quad (1.11)$$



$$\bar{M}_w = \int MW(M) dM \quad (1.12)$$

Where  $\bar{M}_n$ ,  $\bar{M}_v$  and  $\bar{M}_w$  are respectively the number-average molecular weight, the viscosity average molecular weight and the weight-average molecular weight. The parameter  $a$  is a Mark-Houwink constant defined in equation 1.17 and the other parameters are defined in equation 1.8.

Because larger molecules contribute more to  $\bar{M}_w$  than small ones,  $\bar{M}_w$  is always greater than  $\bar{M}_n$ , except for a monodisperse polymer.  $\bar{M}_n$  is more influenced by species at the low end of the MWD curve. Polydispersity ( $d$ ), defined as

$$d = \bar{M}_w / \bar{M}_n \quad (1.13)$$

is a useful measure of the breadth of the MWD curve[37].

### 1.2.3 Calibration with Narrow-MWD Standards

The simplest method of calibration for HPSEC columns is the relation of the peak retention volume to MW for a series of narrow-MWD standards[38]. The applicability of this method depends on the availability of narrow polymer standards identical to the polymer being analysed. A range of narrow polymer standards are commercially available

but, except for a few polymers, the number of standards for each polymer is not large, so difficulties may be encountered in attempting to construct a calibration curve over a wide retention range[12].

The peak retention volume is calculated from the point of injection to the appearance of the maximum value of the chromatogram. The MW of the standard at this point is defined as  $M_{peak}$ . Polymer fractions of narrow-MWD elute as sharp peaks and the experimental average molecular weights are considered to be very similar, so it is assumed that

$$M_{peak} \cong \bar{M}_n \cong \bar{M}_v \cong \bar{M}_w \quad (1.14)$$

It is generally accepted that when the reference standards have a polydispersity below 1.1, the error in making this assumption is smaller than the error in the measurement of MW by other techniques such as osmometry and light scattering[12].

#### 1.2.4 Calibration with Broad-MWD Standards

When the available reference material has a broad-MWD, equation 1.14 is no longer applicable because it is not known which average MW will be similar to  $M_{peak}$ [12].

There are two common methods of using broad-MWD standards for SEC calibration; the integral and linear methods. The integral method requires

the knowledge of the complete MWD curve of the polymer standard. The linear calibration methods use only the average MW values of the polymer standard but assume a linear approximation of the SEC calibration curve[39].

The approaches to all methods of calibration using broad-MWD standards are trial-and-error methods, differing in mathematical and numerical details and in the amount of computer time required to adjust the calibration curve until an acceptable fit of the calculated MW data with the experimental information on average molecular weights and/or MWD is obtained[12].

#### 1.2.5 Universal Calibration

As it can be seen in equation 1.9, the SEC calibration is a function of the MW rather than the size of polymer molecules. The MW is <sup>(a)</sup> X intrinsic property of the polymer while the actual size of polymer molecules in solution can change with temperature and solvent. As the separation mechanism in SEC is based on molecular size, the MW calibration holds only for the specified experimental conditions as well as only for a specific polymer solvent system[40].

Many attempts have been made to determine a universal calibration parameter which characterizes the effective dimensions of various polymers.

The universal calibration parameter should be independent of the structure

of the macromolecule and so, polymers as different as linear, branched and starshaped homopolymers, or block, random, alternating and graft copolymers, eluting at the same volume, would have the same universal calibration parameter[41].

Some of the parameters that were recommended for use in universal calibration were the hydrodynamic volume[42], the radius of an equivalent sphere[43], the radius of gyration[44,45] and the square root of the mean square end-to-end distance of an unperturbed molecule[46]. Experimental work that was performed in this field provided considerable support to the method based on the hydrodynamic volume, introduced by Benoit et al[42].

The hydrodynamic volume,  $V_h$ , of a sphere in solution is defined by the Einstein viscosity relation[47]:

$$V_h = ([\eta])M / 0.025N_A \quad (1.15)$$

where  $[\eta]$  ( dl/g ) is the intrinsic viscosity and  $N_A$  is Avogadro's number.

A polymer molecule in solution can be represented as an equivalent hydrodynamic sphere and when separation occurs strictly by SEC, the theory predicts that polymers of different chemical structures, whether branched or not, will elute at the same retention volume from SEC columns provided that the polymers have the same hydrodynamic volume[48]. The hydrodynamic volume can be defined in terms of the hydrodynamic radius  $R_h$ [12]

$$V_h = ( 4\pi R_h^3 ) / 3 \quad (1.16)$$

The validity of the universal calibration parameter was verified for a variety of chemically and structurally different polymers where a

plot of  $\log [\eta]M$  versus  $V_R$  was the same for all polymers[42].

Intrinsic viscosity  $[\eta]$  is an experimental quantity derived from the measured viscosity of the polymer solution. The value of  $[\eta]$  for a linear polymer in a specific solvent is related to the polymer molecular weight through the empirical Mark-Houwink equation[48].

$$[\eta] = K M^a \quad (1.17)$$

where the values for the Mark-Houwink constants  $K$  and  $a$  vary with polymer type, solvent and temperature. The Mark-Houwink constants are tabulated for a wide variety of polymer / solvent / temperature combinations[49]. It follows from equation 1.15 that at a given  $V_R$  the relation

$$[\eta]_p M_p = [\eta]_{ps} M_{ps} \quad (1.18)$$

will apply, where  $p$  refers to a polymer requiring analysis and  $ps$  to a polymer standard.

One limitation of this approach is that the universal calibration parameters, which in principle characterize the dimensions of macromolecules, hold only under the assumption that the size exclusion mechanism predominates. However, under real chromatographic conditions, many other interactions among the solvent, solute and packing may occur, causing departures from the universal calibration plot[50].

### 1.3 SECONDARY EFFECTS

The retention mechanism in SEC depends on solute size in solution. However, abnormal retention has been observed showing that the solutes are being separated by a mixed mechanism [51,52]. These non-exclusion or secondary effects involve solute-packing-solvent interactions and can be explained by partial adsorption and partition, incompatibility, solvation, and ionic exclusion and inclusion[52]. Also, some of the operational variables that can affect the results of SEC are the volume of sample injected and its concentration and the eluent character, temperature and flow rate[50,52]. The experimental conditions must be optimized in order to minimise, or estimate quantitatively, all the perturbing factors which affect  $V_R$ [50].

Several theories have been proposed for the thermodynamic treatments of non-exclusion interactions[30,53-55]. One of the theories, proposed by Dawkins et al.[30] has been previously discussed in section 1.2.1. The  $V_R$  in SEC, for a polymer when solute packing interactions are operative, is given by combining equations 1.1 and 1.2

$$V_R = V_0 + K_D K_P V_i \quad (1.19)$$

Generally speaking, when the eluent is a good solvent for the solute, polymer-solvent interactions are higher than polymer-packing interactions, the exclusion mechanism predominates and  $K_P = 1$  and

$0 < K_D < 1$ [56]. When the eluent tends to a theta solvent, solute-packing interactions increase in relative terms. For adsorption-partition interactions  $K_D$  will be greater than unity and for polymer incompatibility smaller than unity[57,58].

When preferential interactions occur between a polymer, eluent and packing, it is not possible to use the universal calibration curve as it was explained in section 1.2.5. However, secondary mechanisms are not always undesirable. In some cases, as in chromatographic analysis of low MW solutes, these interactions may be desirable in order to provide complementary resolution[51,59,60].

### 1.3.1 Mixed Eluents

Solvation of solutes is especially observed in SEC when mixed eluents are used.[51,56] In this case, there is a selective sorption of the components in the solvent mixture on the solute or on the packing. Preferential solvation of macromolecules dispersed in a mixed solvent brings about a change in the composition of solvent in the vicinity of the chain relative to the rest of the solution. This effect is due to the differences in interaction between polymer segments and particular components of the mixed solvents[61].

The selective sorption on the gel can greatly influence the composition of the quasistationary phase. The sorbed molecules of solvent

may reduce the adsorption of the solute on the packing by blocking the active sites on its surface. This will result in a decrease of the corresponding elution volume. The magnitude of this shift must be a function of the MW and concentration of the polymer and will probably influence not only the position but also the shape of the elution curve, especially in the region of low concentrations[62]. This effect has been used to suppress or avoid secondary mechanisms in SEC[63], when one of the components of the mixture has strong interactions with the packing and the other gives an adequate solubility to the sample[51].

### 1.3.2 Adsorption and Partition

Adsorption and partition mechanisms result from solute-packing interactions and both give  $K_p > 1$ . They occur whenever the polarity of the mobile phase is very different from that of the packing and/or the polymer solute[52].

When inert packings such as PS-DVB and a good solvent for the solute are used, partition and adsorption do not influence the solute size separation[42]. However, when poor or theta solvents are used, several deviations from the universal calibration have been observed. The  $V_R$  is shifted towards higher elution volumes showing that adsorption and/or partition are present[30,56,64,65]. Good solvents help to avoid possible packing surface adsorption. Near theta conditions, the solvent is less



effective in preventing polymer solute molecules from adsorbing on the packing surface. In a thermodynamically good solvent, where polymer/solvent interactions are favored, a polymer coil in solution is more extended than in a poor solvent, and the exponent  $a$  in equation 1.17 varies between 0.67 and 0.80. When the solvent becomes poorer, the exponent  $a$  decreases, reaching the minimum value of 0.5 for a theta solvent (poorer solvents would not dissolve the polymer) [12].

With active packings, like porous silica, glass and even some modified silicas, displacements of  $V_R$  to both higher and lower elution volumes have been reported, when the interactive behaviour of the packings were studied with pure or mixed solvents. In a polar packing when pure or mixed solvents are used, the extent of adsorption may be controlled by the polarity of the solvent used. In general, the more polar the solvent, the smaller is the adsorption [62]. It was suggested [66-69] that for eluents with high polarity, there is a thick quasistationary layer of eluent strongly interacting with the substrate, preventing the polymer approaching the gel surface. The solute will display affinity for a mobile phase and a liquid stationary phase, which can differ in composition. Therefore, the partition mechanism will predominate. When the eluent displays low polarity, the layer thickness decreases, allowing the polymer to approach the gel surface. Partition and adsorption occur simultaneously. As the polarity of the eluent decreases more, adsorption on the gel is so strong that there is no solute recovery. A similar trend was observed for polystyrene and its oligomers and a more polar solute poly (methyl methacrylate) where it was suggested that hydrogen-bonding was also contributing to solute-substrate interactions [67-69]. Identical results were found by another group [70], where in solvent mixtures of high

polarity, when partition and adsorption were occurring simultaneously, the increase of eluent polarity would decrease the retention volumes. In solvent mixtures of low polarity, when only adsorption was occurring the decrease of eluent polarity would increase the retention volumes.

When silica or glass packings are used, adsorption occurs very often due to interactions via hydrogen bonding between silanol groups of the packing and the polymer[16,68,69]. Hydrogen bonding has been detected when organic[68,69] or aqueous[16] mobile phases are used and the addition to the eluent of a compound which preferentially adsorbs onto silanol normalizes the polymer elution. Adsorption due to hydrogen bonding has also been found in organic gels based on cellulose[71], dextran[52] and polyether[17], using either organic or aqueous mobile phases.

### 1.3.3 Ionic Effects

SEC of ionic polymers are markedly influenced by charge effects. The most common non-exclusion effects in aqueous SEC of ionic polymers are ionic interactions between polyelectrolytes and packings due to ion-exchange, ion-exclusion and ion-inclusion effects. Ion-exchange effects occur when the packing contains ionizable groups. These effects can be reduced or eliminated by the addition of electrolytes to the mobile phase to compete for ionic sites[16].

Ion-exclusion refers to that phenomenon in which the diffusion of an ionic species into the interior of a porous packing is restricted by

electrostatic repulsion. This effect can be used to separate nonionic from ionic species but it is undesirable in SEC experiments[16,72].

Ion-inclusion effects occur when the porous support acts like a semipermeable membrane for the polydisperse polyelectrolytes, because the equilibrium of electrical charges on the column is disturbed by the size exclusion of part of the polymer from the pore. The Donnan effect resulting from the nonequilibrium of electrical charges on the column will cause an additional permeation of the low MW part of the polymer or salt ions into the gel pore beyond the size distribution equilibrium. This results in retardation of the low MW part of the polymer[16,52,72]. Ion-exclusion and ion-inclusion become less important when the ionic strength of the solvent is raised because the interactions between the charges on the surface of the column packing and ionic groups on the polyelectrolyte are reduced. Also, the addition of electrolytes to the eluent is advantageous because it lowers the electrostatic repulsions along the polyelectrolyte chain. As a result the hydrodynamic volume of the polymer is reduced allowing greater permeation into the pores of the packing and decreasing the incidence of polymer concentration effects, which can be more severe than for a hydrophobic polymer in organic media[12,16,72].

Anomalous retention volumes have been observed for some nonionic polar polymers in pure DMF both for inorganic and PS-DVB packings. In the same way as for polyelectrolytes, the addition of salts to the mobile phase, normalizes the elution behaviour of the polymer. It is assumed that in this case salt interacts with both polymer and solvent preventing the formation of aggregates of solute[12,52].

#### 1.3.4 Concentration Effect

The dependence of shape and maxima of the elution curve on concentration and overall amount of injected polymer solution is known as the concentration effect which is due to several contributing processes. These processes have been studied for a rigid column packing by Janca et al[73-79]. It was proposed that the three main contributions are the change in the effective dimensions of the permeating macromolecules, the viscosity phenomena in the interstitial volume and secondary exclusion due to occupancy of a pore by another polymer molecule. The first two processes lead to an increase in  $V_R$  while the last causes a reduction in elution volumes with increase in concentration. The concentration effect is more pronounced for high MW polymers[52] and in some cases cannot be avoided[80].

Several methods have been suggested to reduce the error caused by concentration effects. Some of the methods proposed are based on extrapolation of the solute concentration to infinite dilution[43,81], or the construction of multiple calibration curves at several concentrations[82] and the use of equations to estimate hydrodynamic volumes of polymers at finite concentration[83,84].

## 1.4 AXIAL DISPERSION

An SEC chromatogram does not represent exactly the distribution of molecular sizes of the solute in the sample injected. Axial dispersion ( instrumental spreading or band broadening ) causes the elution of solute molecules of the same size over a range of retention times. This gives a distribution of  $V_R$  for each group of solute molecules with identical size and the chromatogram is a superposition of all the distributions[85].

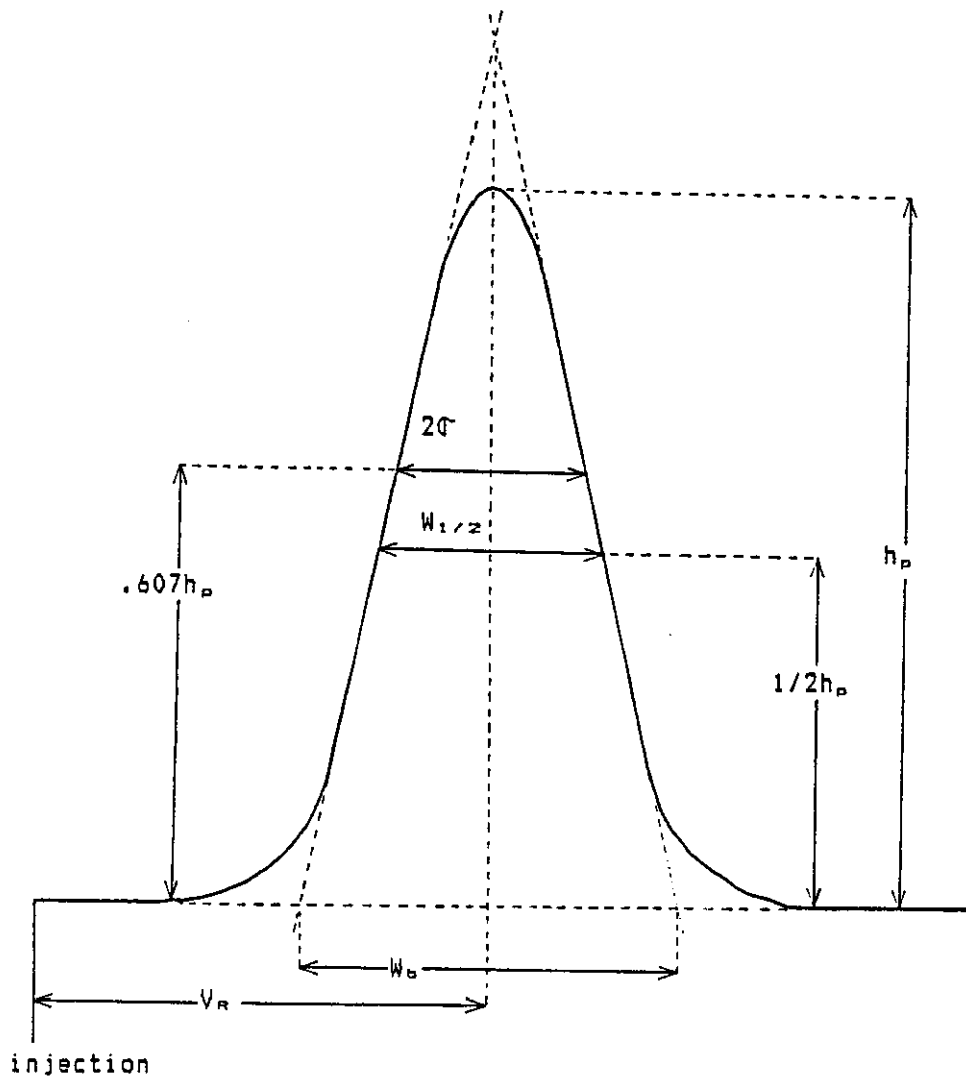
Axial dispersion can be separated into two distinct processes: extra column dispersion and column dispersion. Both types of dispersion are independent and additive. Extra column dispersion occurs in the injection valve, tubing and detector flow cell and is easily evaluated using the SEC instrument without the columns[85].

### 1.4.1 Plate Height

Chromatographic column performance can be expressed in terms of the number of theoretical plates (  $N$  ) or the plate height, i.e. the height equivalent to a theoretical plate (  $H$  ).

These variables can be related to the variance of a single

FIGURE 1.2  
GAUSSIAN PEAK MODEL



chromatographic peak (  $\sigma^2$  ) which is the fundamental parameter for evaluating column axial dispersion effects[86]. Assuming that the chromatogram has a Gaussian shape, as in figure 1.2, N and H are defined by:

$$N = V_R^2 / \sigma^2 \quad (1.20)$$

$$H = L/N = L( \sigma^2/V_R^2 ) \quad (1.21)$$

where L is the column length.

As the calculation of the peak variance is tedious, some approximations are made to express N and H as variables that are more easily measured experimentally. If the peak is symmetrical and close to a Gaussian shape, N can be defined by[87]:

$$N = 16( V_R/W_b )^2 \quad (1.22)$$

$$N = 5.54( V_R/W_{1/2} )^2 \quad (1.23)$$

where  $W_b$  and  $W_{1/2}$  are shown in figure 1.2. The method to calculate N using equation 1.22 is called the tangent method and using equation 1.23 is called the half-height method.

#### 1.4.2 Column Dispersion Processes

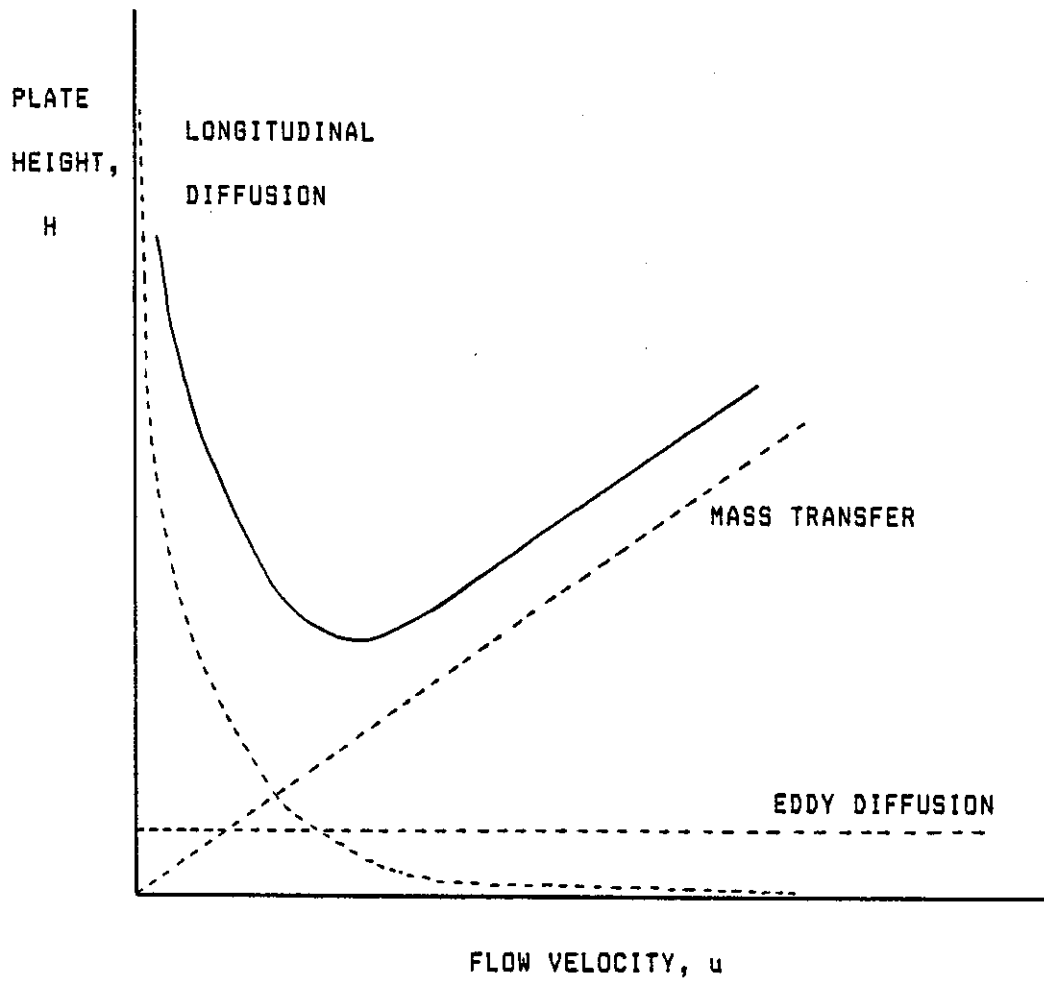
The column dispersion processes can occur inside the pore of a packing particle, defined as pore dispersion, or in the column interstitial volume, defined as interstitial dispersion[85]. Experimental data for  $H$  for a solute having constant retention volume  $V_R$  over the range of linear flow rate  $u$  of the eluent may be interpreted in terms of pore and interstitial dispersion mechanisms. The equation developed by van Deemter for gas chromatography is one of the most widely used methods for determining the solute dispersion mechanisms contributing to axial dispersion[88]. The equation is defined by[86]

$$H = A + ( B / u ) + Cu \quad (1.24)$$

where  $u$  is the eluent flow velocity and  $A$ ,  $B$  and  $C$  are constants associated with the plate height terms due to eddy diffusion, longitudinal diffusion, and mass transfer, respectively. A graphical representation of the parameters in equation 1.24 is shown in figure 1.3 [86]. Eddy diffusion is caused because sample molecules take different routes in the mobile phase through the packed bed and is not expected to vary with flow velocity. Longitudinal diffusion in the mobile phase is caused by molecular diffusion of the solute along the column's axis parallel to the flow direction. This term decreases with increasing flow rate since a



FIGURE 1.3  
THEORETICAL VAN DEEMTER PLOT.



shorter time is available for longitudinal diffusion in a faster chromatographic separation. The third term in equation 1.24 is the sum of the contributions from different mass transfer processes. Two mechanisms can be identified as giving major contributions to dispersion: the  $C_m$  term, due to resistance to mass transfer in the mobile phase and the  $C_s$  term due to resistance to mass transfer in the stationary phase. So, equation 1.24 can be rewritten in the form[29]:

$$H = A + (B / u) + C_m u + C_s u \quad (1.25)$$

Dispersion due to mass transfer in the mobile phase is caused by streamlines with different velocities so that solute molecules in different streamlines will move with different relative velocities. Dispersion due to mass transfer in the stationary phase happens because at any instance, a fraction of the molecules in the stationary phase is left behind by the remaining fraction in the mobile phase. So, in both cases, the dispersion due to mass transfer is increased by increasing the flow velocity. The solid line in figure 1.3 is the sum of all dispersion processes. This line shows a minimum in plate height which corresponds to a flow rate where the column has maximum efficiency.

However, studies of column efficiency in HPLC showed that equation 1.25 did not correlate well with experimental results. Giddings[89] recognized that radial movements of molecules will give a rapid interchange of solute molecules between streamlines, so that the molecules will have a range of velocities and will move from an unobstructed streamline between particles to a streamline moving round a particle. Consequently, mass

transfer in the mobile phase and eddy diffusion are interdependent. This is the basis of the coupling theory, developed by Giddings, and for a monodisperse solute the coupling equation is[29]:

$$H = (B/u) + C_m u + 1/[ (1/A) + (1/C_m u) ] \quad (1.26)$$

Dawkins and Yeadon[90] suggested that the first term in equation 1.26 may be neglected for high polymers at flow rates higher than  $1 \text{ mm.s}^{-1}$ .

Also, theoretical calculations showed that the term  $(1/A)$  is considerably larger than the term  $(1/C_m u)$  for high polymers[91]. Consequently, only two dispersion terms, namely eddy diffusion in the mobile phase and mass transfer in the stationary phase, have to be considered in the expression for  $H$  for a monodisperse high polymer. Simplifying and making the appropriate substitutions, the final form of equation 1.26 for a monodisperse high polymer is[91]:

$$H = 2\lambda dp^2 + R(1-R)dp^2u / 30D_s \quad (1.27)$$

where  $\lambda$  is a constant characteristic of the packing (close to unity),  $D_s$  is the diffusion coefficient of the solute in the stationary phase and  $R$  is the retention ratio defined for each solute by  $V_0 / V_R$  where  $V_0$  is the interstitial (or void) volume of the column.

For a polydisperse solute, equation 1.27 must be extended to include the true polydispersity  $[\bar{M}_w/\bar{M}_n]_T$ . The contribution of the true polydispersity to the plate height had been previously determined for a polymer which may be represented by a logarithmic normal distribution[90,92] and equation 1.27 takes the following form for a polydisperse polymer:

$$H = 2\lambda dp + R(1-R)dp^2u/30D_m + (L \ln [M_w/M_n]_T) / D_z^2 V_R^2 \quad (1.28)$$

where  $D_z$  is the slope of the calibration curve of  $\ln M$  against  $V_R$  in the partial permeation range.

#### 1.4.3 Correction for Axial Dispersion

The relation between the experimental chromatogram,  $F(v)$ , and the chromatogram after the correction for axial dispersion,  $W(y)$ , is given by Tung's integral equation[93]:

$$F(v) = \int W(y)G(v,y)dy \quad (1.29)$$

where both  $v$  and  $y$  represent retention volume and the function  $G(v,y)$  represents the overall instrumental spreading. Equation 1.29 reflects the fact that the chromatogram of a given sample is always broader than its component distribution. Several attempts have been made to solve this equation, either by numerical or analytical methods, and were thoroughly reviewed by Hamielec et al[85,94].

One of these attempts[95] provides the MW averages corrected for axial dispersion as a function of the slope of the calibration curve and

the dispersion factor:

$$M_K(t) / M_K(\infty) = \exp [ \{ (3-2K) D_z^2 \} / 4h ] \quad (1.30)$$

where  $K = 1, 2, 3, 4$  correspond to number-, weight-,  $z$ -, and  $(z+1)$ -average molecular weights, respectively,

$M_K(t)$  =  $k$ th. molecular weight average corrected for axial dispersion,

$M_K(\infty)$  =  $k$ th. molecular weight average uncorrected for axial dispersion,

$D_z$  = slope of a linear calibration curve ( or the slope of linear segments of the calibration curve ),

$h$  = dispersion factor.

The dispersion factor ( originally called resolution factor ) was defined by Tung[93]. The parameter  $h$  describes the width of the spreading and is related to the variance of the peak by:

$$h = 1 / 2\sigma^2 \quad (1.31)$$

It has been determined[96-98] that  $h$  varies with  $V_R$  and shows a minimum in the vicinity of the exclusion limit of the column[99]. It was also concluded that the dispersion factor is essentially independent of the chemical structure of the polymer[96]. It is very difficult to obtain the precise data for the variance of a SEC peak. Several techniques have been used, like recycling or reverse flow experiments and by chromatographic analysis of polymers which are chromatographically monodisperse or with precisely known MWD, and the choice between them will depend on availability of equipment or well-characterized material[99,100].

## 1.5. MULTIDIMENSIONAL CHROMATOGRAPHY

Multidimensional chromatography is also called column switching, multiphase, multicolumn, orthogonal or coupled column chromatography among other terms. It is a technique where fractions from one chromatographic column are transferred to one or more chromatographic columns for additional separation. Its most common uses are for better resolution of complex samples or for sample clean up prior to analysis. The technique can be carried out off-line or on-line[101]. The advantages and disadvantages of each technique are summarized in figure 1.4 and will be discussed in more detail in the following sections.

### 1.5.1 Separation Methods

The multidimensional technique has been applied for many years in thin-layer chromatography ( TLC ), where the same TLC plate is used but a secondary development is carried out, with a different mobile phase, by rotating the plate 90°. Column switching in gas chromatography ( GC ) has been performed with the use of different stationary phases in each column providing therefore different selectivity and retention. So, solute

FIGURE 1.4

COMPARISON BETWEEN OFF-LINE AND ON-LINE MULTIDIMENSIONAL TECHNIQUES.

OFF-LINE	ON-LINE
difficult to automate	easy to automate especially with modern chromatographs
greater chance of sample loss	less chance of sample loss since experiments are carried out in a closed system
can concentrate trace solutes from large volumes	difficult to handle trace compounds since very dilute in large volumes
can work with two LC modes which use incompatible solvents.	solvents from primary and secondary modes must be compatible, both from miscibility and strength requirements.
more time consuming	decreased total analysis time
more difficult to quantify and reproduce	more reproducible and easy to quantify
no need of expensive equipment	requires more complex equipment, more expensive.

unseparated in the primary column can be further resolved with the secondary column[101].

Modern LC also becomes more interesting and more powerful as the number of columns is increased. Usually, an LC system contains a simple flow through sequence but, if this sequence is branched, it becomes possible to exert more control on the quality of and the basis for the separation. This involves variable combinations of column, carrier and detector which co-operatively contribute to the overall system selectivity[102]. Therefore, the great potential of multidimensional techniques lies not only in the selection of different modes for the primary and secondary steps but also in the ability to use different mobile phases to provide the needed separation[101].

Multidimensional systems can consist of a single mobile phase and different columns in the first and second step. The major disadvantage of this case is that only a small number of components can be handled due to the limited range of capacity factors generated in isocratic elution. Or, they can consist of the same type of column in both systems but using different mobile phases in each step[101]. In this case, the separation mode could be different in the first and second step despite the fact that the chromatographic mode is generally considered to be based on the nature of the column stationary phase. However, it is well known that under certain conditions the operative mode is unrelated to the designed purpose of the stationary phase material and that the mobile phase can change the nature of the separation. So, mode shifting can be obtained by changing either the mobile phase or the column packing, or both[102].



### 1.5.2 Off-line Multidimensional Chromatography

Off-line multidimensional LC is carried out by collection of solutes at the detector exit from the first column and re-injection of the collected fraction into the secondary column. It is often employed when the solvents of the two columns are not compatible or when the concentration of the components of interest are too low and require concentration prior to injection into the second column.

Sample collection is carried out by sampling the eluent from the column ( usually after the detector ), either manually or by means of a fraction collector. The collected sample can be directly re-injected into a second liquid chromatograph, if the solvents used in both systems are compatible, both from miscibility and strength requirements. When solvents from both systems are immiscible, the sample can be carried down through the second column by the solvent of the first system, which may cause band spreading. Also, the collected solvent from column one must not be a strong solvent in the mobile phase of the second column, especially if large volumes are to be injected. The strongest solvent will preferentially move the solute down the column until the concentration of this strong solvent is diluted sufficiently that solutes begin to be retained. This will cause band spreading and the resolution of the overall system will be impaired. So, when the solvents of both systems are incompatible, the first column solvent should be removed from the sample, after collection. This can be done by evaporation and further dissolution

of the sample with a solvent compatible with the second system or by extraction with an immiscible solvent[101]. Another problem that will require the use of off-line technique is low solute concentration after elution from the primary column. In this case, the sample has to be concentrated by some means first and then re-injected in the second system.

All this sample handling makes sample losses probable. These losses can occur by means of volatilization, incomplete extraction, adsorption on glassware or even by chemical reactions like polymerization, oxidation or degradation[101].

The problems mentioned above show that off-line techniques are time consuming, difficult to quantify and to reproduce. They are preferable mainly when solvent incompatibility or low sample concentration make the use of on-line techniques impossible or when the minimum necessary equipment needed for on-line chromatography is not available.

### 1.5.3 On-line Multidimensional Chromatography

On-line multidimensional HPLC is achieved through coupling the outlet of one chromatographic system to a second one, by means of a high pressure switching valve which traps the desired solute and directs it to the second column. From a convenience and automation viewpoint, the on-line coupling of two ( or more ) chromatographic techniques is preferred. The process can be completely automated through the use of an pneumatically operated automatic switching valve actuated by timers or by time programmable events of a microprocessor-based chromatograph. An

important experimental criterion for on-line coupling is the exact timing requirements for valve switching. Since microparticulate columns produce very sharp peaks, it is very important to control switching time since errors will affect quantitative measurements. However, it is not only time errors that will affect the results, as small variations in flow will also have a marked effect on reproducibility.

A prime requisite in on-line chromatography is mobile phase compatibility, both from the standpoint of miscibility and strength, as was discussed in the previous section. Large injection volumes of a strong solvent would cause partial migration of injected fractions down the second column, thereby limiting resolution. On the other side, injection volumes that are too small tend to limit the sensitivity of the multidimensional technique. A compromise injection volume must be achieved. Sometimes, large amounts of sample can be injected onto the primary column, especially in the size exclusion mode which tends to have a higher sample capacity than other LC modes. Thus, a large sample can be fractionated and the individual fractions still contain an appreciable amount of material for detection during the second chromatographic step. Nevertheless, in those instances where the sample is too dilute for direct coupling, off-line techniques must be employed.

#### 1.5.4 Applications for Copolymer Characterization

Copolymers usually exhibit a complex structure because they have a molecular weight distribution ( MWD ), a chemical composition distribution ( CCD ), a sequence length distribution and the other kinds of structural inhomogeneities which are also present in homopolymers[103]. The complete characterization of a copolymer requires the determination of all distributions, since they highly influence the copolymer bulk properties[27].

The traditional method to evaluate copolymer properties is cross-fractionation, where the chemical composition is determined as a function of MW. It is a very time consuming method where the polymer is first fractionated with respect to MW by solubility based techniques. The fractions obtained are then fractionated again according to composition using a different solvent-nonsolvent system[104]. Thin-layer chromatography is also successfully used for the determination of CCD of copolymers but it is a time consuming technique and it cannot be automated[105]. HPSEC is a rapid and automatic method widely used for the determination of average molecular weights and MWD of copolymers. With the use of dual detection, it has been proved that HPSEC can also determine the CCD of copolymers[27]. To calibrate and interpret copolymer fractionation results by HPSEC it is necessary to determine the experimental conditions that ensure either size or composition fractionation. However, the relationship between molecular size and molecular weight is difficult to predict because changes in the microstructure are known to influence

solubility strongly and presumably adsorption, as well as the size of the macromolecules in solution. Three different approaches have been suggested for the MW calibration of SEC columns, since copolymer standards of varying MW, composition and microstructure are not available[106]:

- 1 - Polystyrene equivalent calibration and interpretation
- 2 - Dual calibration
- 3 - Universal calibration

The first approach, although useful for comparative purposes, does not yield the true MW of the copolymer. Dual calibrations require standards for both homopolymers and some interpolation. The universal calibration requires only standards for one homopolymer and the calibration is based on the assumption that the separation mechanism is strictly by molecular size. It has been shown that the dual calibration and the universal calibration are equivalent, and should yield similar results provided there are no interactions between the packing material and the functional group present in the copolymer molecule[106].

The use of the appropriate dual detection system in SEC of copolymers provides means of selectively detecting the concentration of the copolymer components from the eluting solution and obtain MW dependence of the composition if a suitable calibration is available. The nature of the additional detection obviously depends on the copolymer structures to be analysed, but the two specific detectors widely used, in addition to the universal refractometer, are the ultraviolet (UV) and, to a lesser extent, the infrared (IR) detector. The feasibility of LALLS detection for the quantitative characterization of chemical heterogeneities in copolymers has recently been demonstrated[27].

The selection of solvent systems for copolymer analysis is dictated

primarily by two factors: solvent transparency in the regions of polymer absorption, and solubility considerations that determine the coil size and the direction of the interactions with the packing material. The choice or availability of a detection system greatly limits the number of solvents that can be employed. In the case of styrene copolymers, solvents transparent in the region 230 to 270 nm are highly desirable ( strong absorption of the styryl group ). Solubility parameters and considerations of intermolecular forces can be used to estimate the solubility characteristics of the copolymers and indicate the direction of the interactions, i.e. polymer-solvent or polymer-packing. The quasistationary phase concepts discussed previously can also be used to guide the solvent selection. If polymer-packing interactions are to be diminished ( size separation ), a nonsolvent that preferentially wets the packing is to be selected. If interactions are to be enhanced ( composition fractionation ), a nonsolvent highly miscible in the solvent is to be preferred[106].

HPLC with dual detection has been used for the analysis of CCD of copolymers, where styrene-acrylonitrile[107] and styrene-acrylic[108,105] copolymers were separated by adsorption on silica-based columns. Teramachi et al[109,110] using PS-DVB column packings coupled to ultraviolet and refractive index detectors determined MWD and MW for styrene-methacrylate copolymers. The results obtained by them were in good agreement with those calculated theoretically.

In order to obtain information about MWD and CCD simultaneously, two detectors must be used. One detector should measure the total amount of copolymer and the other its composition. However, only the average composition of a certain eluate is known.

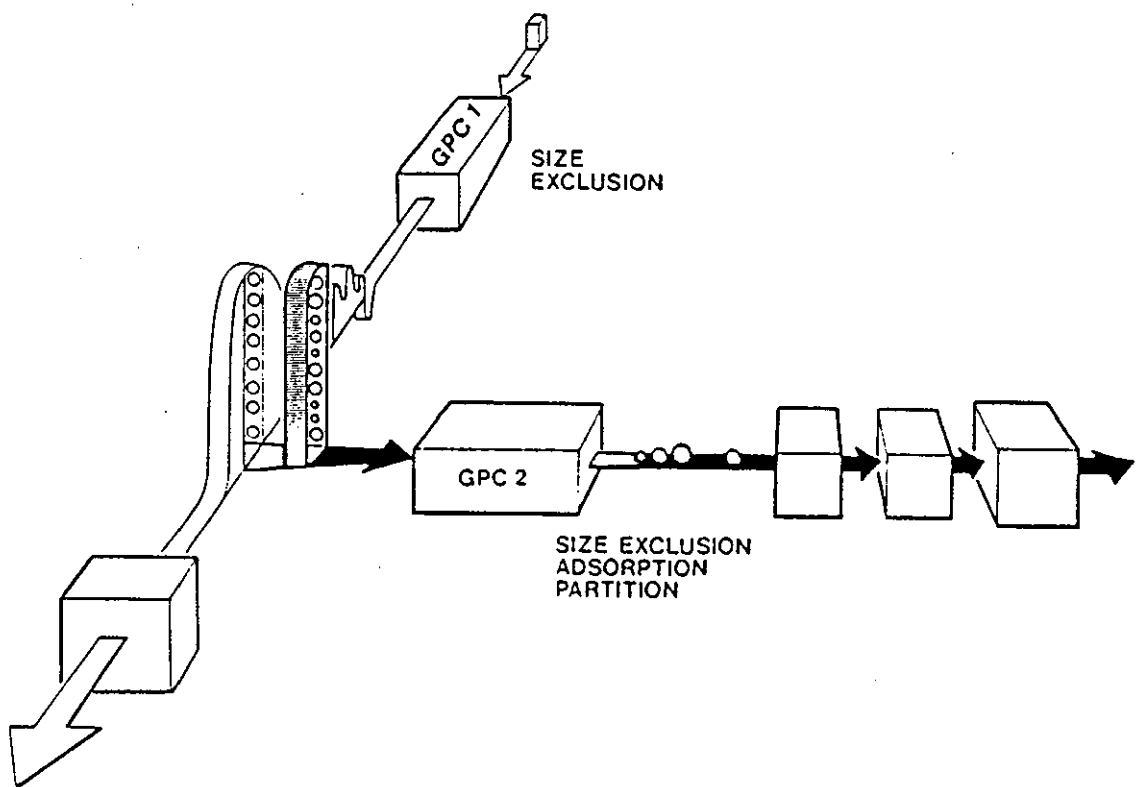
To know more about CCD and MWD of copolymers the principles of cross fractionation must be applied. This can be performed more efficiently by multidimensional chromatography. SEC can be used for the first fractionation and adsorption-partition chromatography for the second separation[103,104,111-115]. Or, inversely, the copolymer can be first analysed by composition and then the MWD of each fraction can be determined[116].

A schematic diagram of an on-line multidimensional system used by Balke et al[104,114]. is shown in figure 1.5. A mixture of poly(styrene-co-n-butyl methacrylate) (PSBA) polystyrene (PS) and poly(n-butyl methacrylate) (PBMA) was first analysed by MW with PS-DVB column packings and tetrahydrofuran (THF) as eluent. A slice of this polymeric mixture was then injected into the second system, which contained a polyether bonded-phase porous silica packings and a mixture of THF and n-heptane as eluent. It was shown that the effect of the solvent composition in the second system, where separation between the three polymers is obtained, depended on the n-heptane concentration.

As is shown in figure 1.5, when molecules of the same size are injected into the second system, they change in size in the new solvent and create a size distribution which also influences the separation in the second system. Then, molecular size exclusion, adsorption and partition are assumed to be present in this system. The styrene rich molecules will shrink from their original size in pure THF while n-butyl methacrylate rich molecules will be relatively unaffected. Furthermore, if the THF preferentially tends to fill pores in the packing and to coat surface area used for adsorption, then styrene rich molecules would be more attracted to the stationary phase than would n-butyl methacrylate rich

FIGURE 1.5

SCHEMATIC DIAGRAM OF AN ON-LINE MULTIDIMENSIONAL SYSTEM FOR COPOLYMER ANALYSIS[104,114]





molecules[104,114].

However, despite the fact that a qualitative CCD was achieved for the PSBA copolymer, the quantitative interpretation of data did not agree with the kinetic model prediction. The use of different detection systems, allowing the measurement of the sequence length effects on the fractionation, was suggested to overcome this problem[114,115].

Glockner et al[103,111] used an off-line multidimensional system for the fractionation of poly(styrene-co-acrylonitrile). The first fractionation was obtained by SEC with a PS-DVB column packing and THF as eluent and the second one by high-performance precipitation liquid chromatography (HPPLC) with a reversed-phase column and gradient elution using THF and isooctane as eluents. HPPLC is a technique based on the solubility of the polymer and it is well known that solubility methods cannot separate without an effect of MW. However, it is considered that the MW effect in a small slice uniform in hydrodynamic volume is negligible, especially at higher MW values. It is also pointed out that the separation by composition must not be superimposed by any size exclusion effect. For this reason the packing material used should have pores which are either large in comparison with the solute molecules or so small that none of the solute molecules can enter. Only under this condition can all components of a sample (irrespective of their size) interact with exactly the same stationary phase. The reversed-phase packing material used in this work was a small-pore packing (100 Å), and it is recognized that this material has an external surface which is still about 20% of the total surface area of a packing material with pores large enough for all solute molecules. Small pores are accessible to the eluent only and the macromolecular solute is restricted to the interstitial volume

of the packing. One consequence of this fact is that the sample solvent is stripped from the polymer injected right at the top of the column. The higher the THF content of the eluent, the later the precipitation composition is reached because the polymer bypasses the pores and thus overtakes the eluent having sufficient solvent power to keep the polymer in solution. The solute rushes into the poorer solvent running in front and consequently precipitates. In this way it is transformed onto a part of the stationary phase. When precipitated, it is retained in that zone of the column until an eluent of sufficient solvent power reaches this position. Then, the polymer is redissolved and transferred back to the mobile phase. One drawback of this technique is that solubility fractionation of copolymers is always linked to a separation by MW. It is however possible to choose conditions so well that the sensitivity to composition overrides the sensitivity to MW.

Mori et al[116] fractionated poly( styrene-co-methyl methacrylate ) copolymers according to chemical composition first and then by MW. The first separation was achieved by liquid adsorption chromatography with a silica column packing ( 30Å ), a gradient elution of chloroform and 1,2-dichloroethane, and the detection was by ultraviolet absorption. The second separation was performed with PS-DVB column packings and chloroform as eluent. The silica packing was chosen in a way that the copolymers were completely excluded from all pores and the results obtained were in agreement with those obtained previously by Danielewics[108].

### 1.6 Aims of the Present Work

The main aim of this work was to study the chromatographic behaviour of polymers with a new column packing based on crosslinked polyacrylamide. The preparation of these microspherical particles which are rigid and macroporous had been reported previously[26]. Two major types of chromatographic separation have been considered.

First, aqueous HPSEC has been performed in order to examine the validity of the universal calibration method based on hydrodynamic volume for non-ionic water-soluble polymers such as poly(ethylene oxide) and polysaccharides. Column efficiency data have also been obtained for poly(ethylene glycol) standards in order to interpret plate height data in terms of solute diffusion coefficients. An important objective was to compare the mass transfer characteristics of polymeric solutes into the crosslinked polyacrylamide packing with the diffusion data reported previously for separations of polystyrene standards in THF in packings based on silica and crosslinked polystyrene.

Second, although separations in SEC are dominated by the size exclusion mechanism, secondary interactive mechanisms by adsorption and/or partition may occur for polymers in poor solvents[30]. For statistical copolymers, copolymer solubility in the mobile phase and therefore the degree of interaction of copolymer with the stationary phase will be influenced by the type and concentration of comonomer. In multidimensional chromatography SEC with an eluent which is a good solvent for the copolymer is first performed followed by injecting the eluting

solution into a second column with a mobile phase which is a poor solvent for the copolymer, permitting the separation of copolymers according to composition[104,114-116]. In this research a comparison has been made of the behaviour of crosslinked polystyrene and crosslinked polyacrylamide gels as interactive packings in multidimensional chromatography. In order to facilitate the establishment of the optimum experimental conditions and also to compare data for the interactive chromatography of copolymers in poor solvents with the results reported by Balke[104,114-116], copolymers of styrene and n-butyl methacrylate have been used in this study. Multidimensional chromatography with the interactive column both off-line and on-line to SEC was attempted.

## 2. EXPERIMENTAL

### 2.1 MATERIALS

#### 2.1.1 Solvents

Unless otherwise stated, all eluents for chromatographic experiments were filtered through a glass sintered funnel and degassed for 30 minutes in an ultrasonic bath prior to use. When mixed solvents were used, each solvent was first filtered and then mixed. The composition of the mixtures was established in terms of volume. Then, the mixture was degassed for 30 minutes in an ultrasonic bath prior to use.

Water was doubly distilled from glass and 0.02% of  $\text{NaN}_3$  was added to prevent bacterial developments[117]. Methanol (MeOH) supplied by Tennants Lancashire Ltd., dimethylformamide (DMF), isopropanol (IP) and n-heptane (HEP) all supplied by Fisons plc were SLR grade.

Tetrahydrofuran ( THF ) supplied by BDH Chemical Ltd. was AR grade and this was supplied with an inhibitor ( 0.1% quinol ) which is a strong ultraviolet ( UV ) absorber. So, when UV detection was employed, unstabilised HPLC grade THF ( Fisons plc ) was used. However, unstabilised THF is easily oxidized forming peroxides which raise the UV absorbance of THF and also present a risk of explosion[118]. To reduce contact with oxygen from the air and therefore improve UV transmittance, this unstabilised THF was not filtered and was stored in small dark bottles. Every time the bottles were opened, oxygen free nitrogen was purged through for a few minutes. Just before use unstabilised THF was degassed and handled in the same way as the other solvents.

### 2.1.2 Solutes

#### 2.1.2.1 Polymer standards and low molecular weight solutes

Polystyrene standards, poly( ethylene glycol ), poly( ethylene oxide ), polysaccharide, were designated PS, PEG, PEO and PSA respectively, followed by a number corresponding to the MW (  $\text{g.mol}^{-1}$  ). All the polymeric standards used in this work were supplied by Polymer Laboratories Ltd and the characteristics of these standards are listed in table 2.1. Pentadecaethylene glycol[119,120] ( PDEG having MW 678  $\text{g/mol}$  ) was kindly provided by Dr. C. Booth, University of Manchester, Manchester, U.K.

The polymers were dissolved in the SEC eluent at least 6 hours in advance in order to allow complete sample dissolution. To increase the reliability of the retention time values, an internal standard ( IS ) was added to each solution[121,122]. Absolute ethanol ( James Burrough plc. )

TABLE 2.1

CHARACTERISTICS OF THE POLYMERIC STANDARDS

Polymer	$\bar{M}_w / \bar{M}_n$
PEG106	dimer
PEG200	1.09
PEG415	1.10
PEG630	1.08
PEG1000	1.06
PEG1580	1.06
PEG4250	1.03
PEG4820	1.04
PEG9200	1.08
PEG11250	1.07
PE018000	1.10
PE039000	1.07
PE086000	1.02
PE0140000	1.03
PE0250000	1.04
PE0590000	1.04
PE0990000	1.05
PSA5800	1.14
PSA12200	1.12
PSA23700	1.13
PSA48000	1.10
PSA100000	1.09
PSA186000	1.07
PSA380000	1.06
PSA853000	1.07

was the IS when water was used as eluent and toluene ( Carless Solvents Ltd. ) was the IS when THF or DMF were used as eluent.

When THF was used as eluent, the PEG and PEO samples were heated at 50°C for 20 minutes to promote complete sample dissolution and allowed to cool before injecting.

Sucrose and raffinose ( Sigma Lab ) were used as received.

#### 2.1.2.2 Styrene-n-butylmethacrylate copolymers

The poly( styrene-n-butylmethacrylate ) copolymers ( PSBA ) were prepared by Gibson[123] in the Polymer Science Laboratories, Chemistry Department, Loughborough University, U.K. The monomers were previously washed several times with dilute sodium hydroxide solution, followed by repeated water washing, and then dried over magnesium sulphate and calcium hydride. The monomers were distilled under reduced nitrogen atmosphere just before use. The PSBMA copolymers were prepared by bulk copolymerization of mixtures of styrene ( ST ) and n-butylmethacrylate ( BMA ) monomers in the ratios shown in table 2.2 at 70°C under nitrogen atmosphere using 0.1 g of azobisisobutyronitrile as initiator. The copolymerizations were stopped within 40 min ( 20% conversion ) by pouring the reaction mixtures into MeOH. The copolymer samples obtained were dried in a vacuum oven at 60 °C.

The ST content of the copolymers was determined by UV spectrometry ( see section 2.7 ) and their molecular weights by SEC with PS calibration. Table 2.2 gives a survey of the characteristics of the samples obtained.



TABLE 2.2

Polymerization Conditions and Characteristics of  
Polystyrene ( PSS ), Poly( n-butylmethacrylate ) ( PBMA ),  
and Poly( styrene-n-butylmethacrylate ) ( PSBA )

sample	POLYMERIZATION MIXTURE		POLYMERS			
	[ST] mol*10 <sup>2</sup>	[BMA] mol*10 <sup>2</sup>	styrene content mol/%	$\bar{M}_n$	$\bar{M}_w$	$\bar{M}_w/\bar{M}_n$
PSS	8.72	0.00	100	24800	47000	1.90
PSBA8/2	6.98	1.26	65.1	28400	51600	1.82
PSBA6/4	5.23	2.52	51.5	29700	51600	1.74
PSBA4/6	3.49	3.78	36.0	34500	59800	1.73
PSBA2/8	1.74	5.04	19.5	45200	78500	1.74
PBMA	0.00	6.29	0.00	87600	192000	2.19

## 2.2 CHROMATOGRAPHIC INSTRUMENTATION.

Three chromatographic instruments were used in this study and are described below. As many different columns were used with each instrument, they are described in a separate section. Therefore, when a set of results is presented in the text, it is accompanied with a reference to the chromatographic system used ( i.e. chromatographic instrument and column ).

### 2.2.1 Instrument 1.

This apparatus consisted of an Altex pump model 110A ( Altex Scientific Inc. ), a Rheodyne injection valve model 7125 with a 50  $\mu$ l loop, a Waters differential refractometer model R-401 and a Vitron chart recorder type UR40.

### 2.2.2 Instrument 2.

This apparatus consisted of a Knauer pump model 64, a Rheodyne injection valve model 7125 with a 100 $\mu$ l loop, a Knauer differential refractometer type no. 98.00 and a Trivector multi-channel chromatography data system Trilab 2000.

### 2.2.3 Instrument 3

This apparatus was set up in order to give an instrument specifically designed for the study of multidimensional chromatography. Figure 2.1 shows a schematic diagram of the system. The apparatus consisted of two independent chromatographic systems joined together via a switching valve. The system 1 consisted of an Altex pump model 110A, a Rheodyne injection valve model 7125 with a 100  $\mu$ l loop, a six port switching valve Rheodyne model 7010 with a 200  $\mu$ l loop and a Knauer differential refractometer detector type no. 98.00

The system 2 consisted of a Knauer pump model 64, a Rheodyne six port switching valve model 7010 with a 200  $\mu$ l loop, which allows the transfer of solute from the first to the second system, a Pye Unicam LC-UV detector and a Knauer differential refractometer detector type no. 98.00

All these three detectors were connected to a Trivector multi-channel chromatography data system Trilab 2000.

The configuration of the six port switching valve that allowed the solute to be injected into the second system is shown in figure 2.2. In the loading position, the loop is part of system 1 and all the sample injected is passing through it. When the valve is turned to the inject position, the loop is part of system 2, and the solute that was trapped in the loop is carried to column 2 by the solvent being used in system 2.

FIGURE 2.1

Schematic Diagram of the Multidimensional System

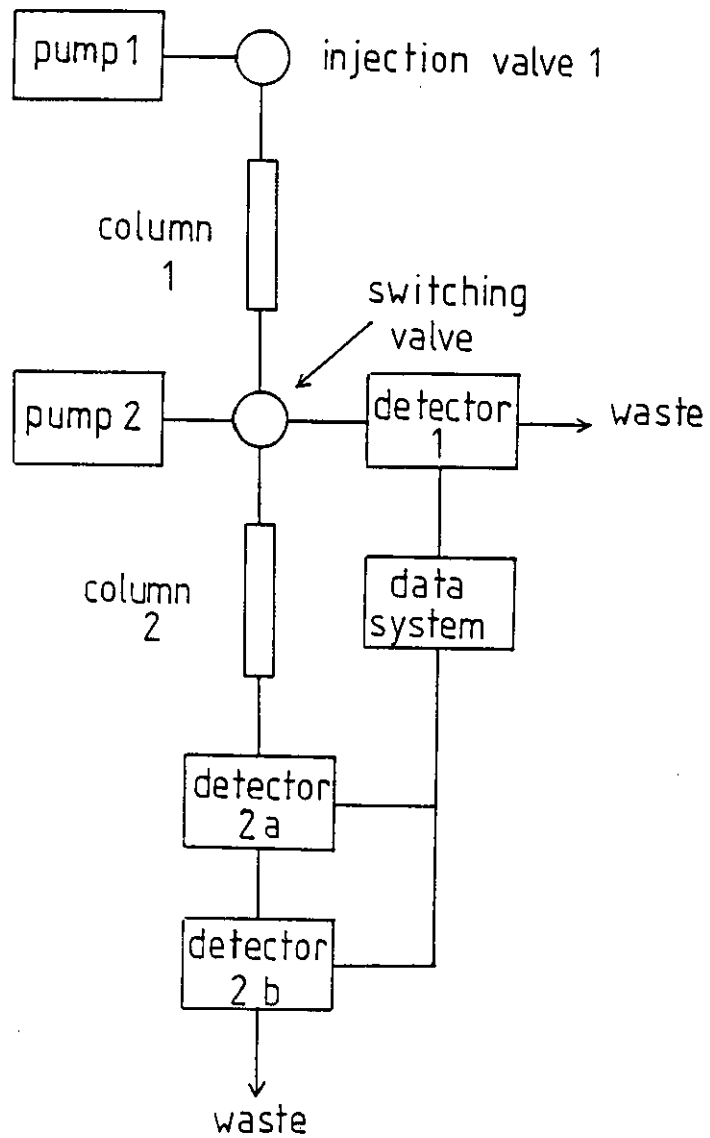
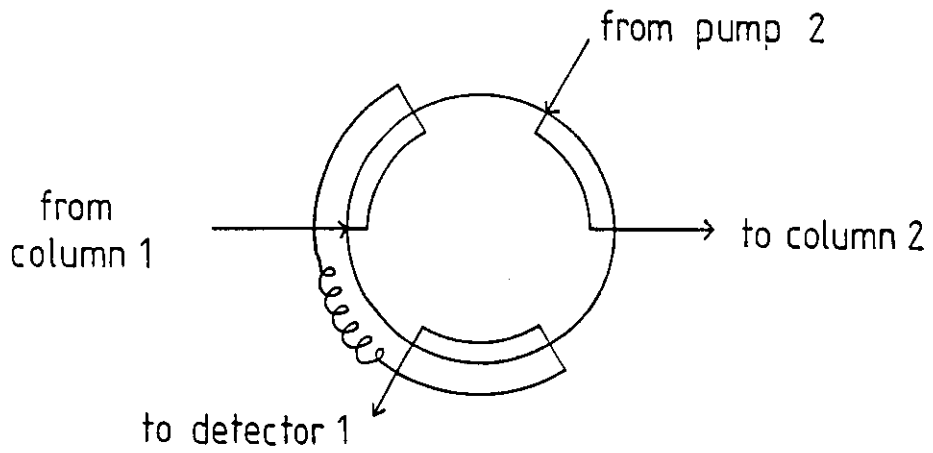
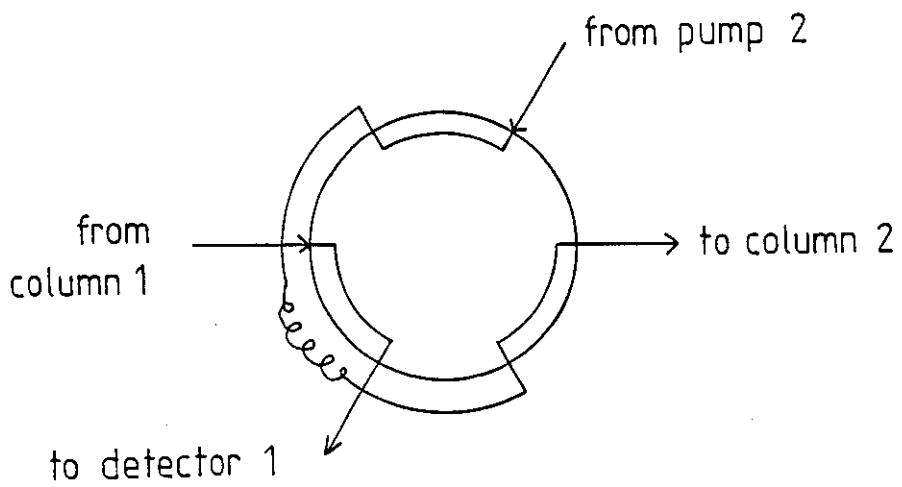


FIGURE 2.2

Schematic Diagram of a Six Port Switching Valve



position load



position inject

#### 2.2.4 High temperature SEC

Some SEC experiments were run at temperatures higher than ambient. In order to perform this experiment, the column was enclosed by a water jacket, with water circulating at the desired temperature.

## 2.3 CHROMATOGRAPHIC OPERATING PROCEDURES

### 2.3.1 Size exclusion chromatography

Either instrument 1 or 2 was used in SEC experiments. When a steady base line was shown in the chart recorder, the loop in the injection valve was filled by means of a glass syringe. The sample concentration was normally 0.1% unless otherwise stated and the amount injected was that necessary to fill at least twice the loop volume. The injection valve was switched to the inject position and the time measurement was started, either by producing a mark on the chart paper or by starting the timer on the computer. The injection valve was maintained in the inject position throughout the experiment. All the samples were injected three times and the results shown in this work are an average of these three values.

### 2.3.2 Multidimensional chromatography

#### 2.3.2.1 Off-line technique

Instrument 2 was used for off-line multidimensional chromatography experiments. The initial concentration of polymer was increased to 0.6% in order to allow the detection of the collected fractions. The injection and

time measurements were made in the same way as in the SEC experiments. ( See section 2.3.1 ) The tubing at the detector outlet was shortened and the fractions were collected as soon as they exited from the detector. Four or eight repeated injections were made with the same conditions. The time intervals in which the fractions were collected are specified in table 2.3. Identical fractions from the different injections were collected in the same vial. The sample solutions were then allowed to evaporate overnight in an open flask in the fume cupboard. When the solvent had totally evaporated, each fraction was re-dissolved in a small amount of the solvent to be used in the second system. The amount of solvent used was about 80  $\mu$ l which was a little less than the loop volume, in order to make sure that all the sample collected was retained in the loop. Interactive chromatography was then performed by replacing the SEC column with an interactive column which was then equilibrated with the mixed solvent mobile phase. The samples were then re-injected with a micro-syringe. The operating procedure was the same as in the SEC experiments ( see section 2.3.1 ).

#### 2.3.2.2 On-line technique

Instrument 3 was used for on-line multidimensional chromatography. The sample concentration was 0.4% and the injecting procedure was the same as for the SEC experiments. When the solute of interest was passing through the loop in the switching valve, the valve was turned to the inject position and the solute trapped in the loop was injected into the second



TABLE 2.3

Fractions Collected by Off-line Multidimensional Chromatography

Fraction number	Collection time ( s )
1	650-660
2	700-710
3	750-760
4	800-810
5	850-860
6	900-910
7	950-960
8	1000-1010
9	1050-1060
10	1100-1110

system. At the same time the switching valve was turned to the inject position, the time measurement for the second system was started on the computer. The valve was returned to the loading position after 20 s, when most of the solution on the loop had been removed.

## 2.4 COLUMNS

The technical data for all types of columns employed in this research are given in table 2.4. As usually more than one column of each type was used in this work, the serial number of the column used will be specified in each set of data.

TABLE 2.4

SPECIFICATIONS OF COLUMNS

Tradename and supplier	dimensions length ID (mm) (mm)	particle size ( $\mu$ m)	exclusion limit (for PEG)	theoretical plate number ( $m^{-1}$ )
PL aquagel <sup>a</sup> (Polymer Lab. Ltd.)	300 7	$10 \pm 2$	$1 \times 10^5$	20000
G3000-PW <sup>b</sup> (Toyo Soda Manufacturing Co.,Ltd.)	300 7.5	$13 \pm 2$	$2 \times 10^4$	16000
PL gel <sup>c</sup> (Polymer Lab. Ltd.)	300 7	$9 \pm 1$	----- d	30000

- a - Highly crosslinked polyacrylamide based macroporous particles.
- b - Crosslinked polyether gel, exact structure unknown.
- c - PS-DVB macroporous particles.
- d - Exclusion limit for PEG not available, exclusion limit for  
PS  $4 \times 10^5$ .

## 2.5 DATA ANALYSIS

Both manual and automatic procedures were used for data analysis. When instrument 1 was used, all the analysis was manual. The arrival of apparatus 2, with an accompanying computer, allowed automatic data acquisition and the calculation of calibration functions and average molecular weights.

### 2.5.1 Retention volumes

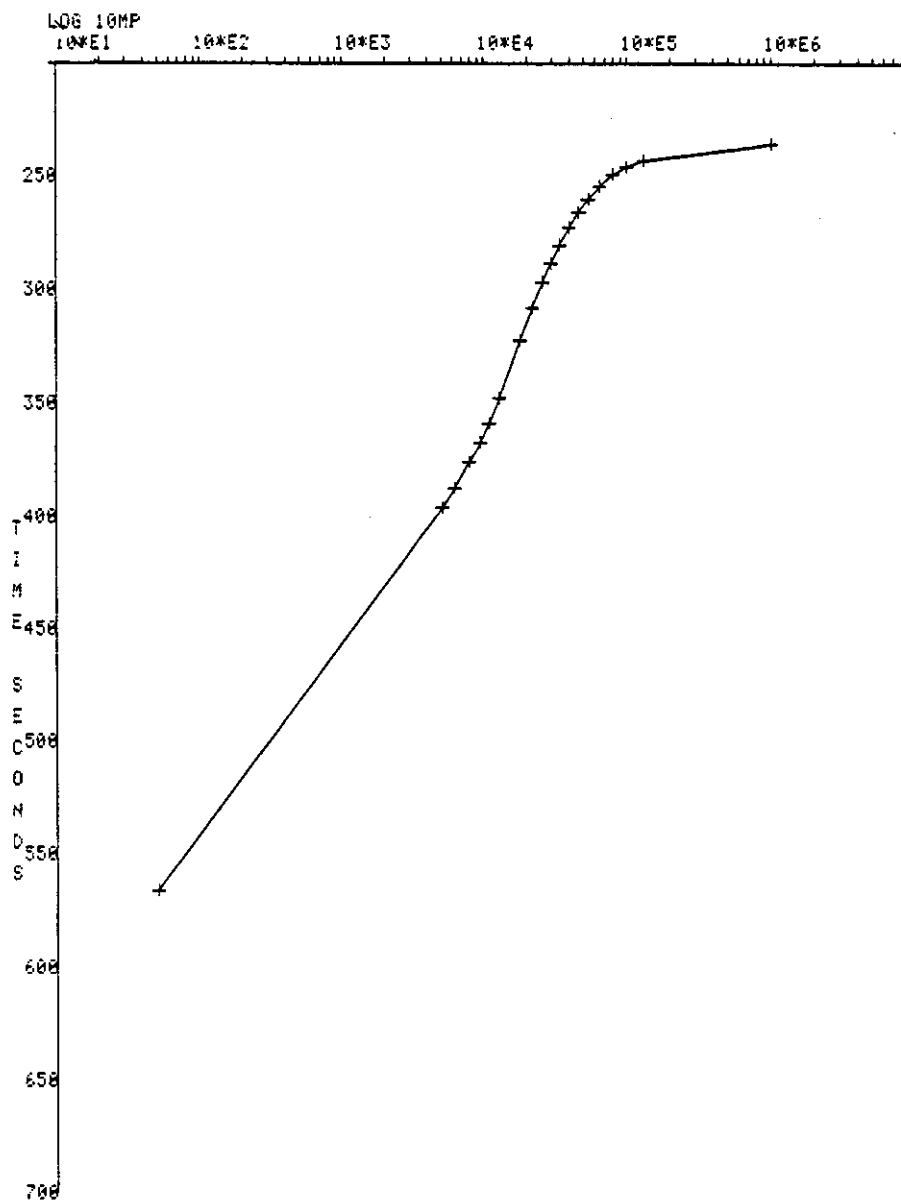
Retention volumes  $V_R$  were expressed in terms of a percentage of the retention time of an internal standard. When the mixture water - MeOH ( 80/20 ) was used as eluent, there was a solvent negative peak[61] eluting at the same time as the internal standard peak thus forbidding the use of an IS. So, when mixtures of water-MeOH were used, or when other eluents were compared with water-MeOH,  $V_R$  was expressed in min or s. In multidimensional chromatography, the use of a totally permeating IS was meaningless, due to the variation of the system pressure when the switching valve is turned to inject position and so,  $V_R$  are expressed in s.

### 2.5.2 Calibration curves

SEC provides a measure of molecular size as a function of elution volume which must be calibrated for MW using standard samples of known MW. Thus, the construction of a precise calibration curve is one of the most important factors in SEC[124]. When apparatus 1 was used, the molecular weights and the elution volumes for the standard samples were plotted on semilogarithmic graph paper followed by drawing the best smooth line through the calibration data. When apparatus 2 was employed, a calibration program was available. This program enabled the fitting of a first, second or third order polynomial to the calibration points. It also allowed the fitting of several straight lines between the calibration points by a procedure called multiple straight line. It was known that for PL aquagel columns, due to the shape of the calibration curve, neither of these approaches were satisfactory[125]. The recommended procedure for PL aquagel columns was to obtain a calibration curve in the same way as in the manual method. In this calibration curve the necessary number of straight lines were drawn in such a way that the final appearance was a smooth curve. Therefore, the points that were fed to the computer were the points between the straight lines and not the points obtained by injecting the standards on the equipment. A typical calibration curve obtained by this method can be seen in figure 2.3 and it is thought to give the most accurate MW values[125].

FIGURE 2.3

Calibration Curve Obtained by the Multi-straight Lines Method



### 2.5.3 Molecular weights

The average molecular weights were calculated by the Curve Summation Method[126]. When the manual approach was used, 20 or more heights were read per peak, and when the computer was used, data was taken every 2 seconds. The average molecular weights were not corrected for band broadening and the start and end points for the baseline were chosen by visual inspection[126].

### 2.5.4 Column efficiency

The column efficiency was estimated by measuring the height equivalent to a theoretical plate or plate height. The plate height was determined using equation 1.23 for the width of the chromatogram at half its height. When the manual approach was used, the peak width was measured by means of a travelling microscope. Both retention time and peak width measurements were made in a way that would produce at least three significant figures.

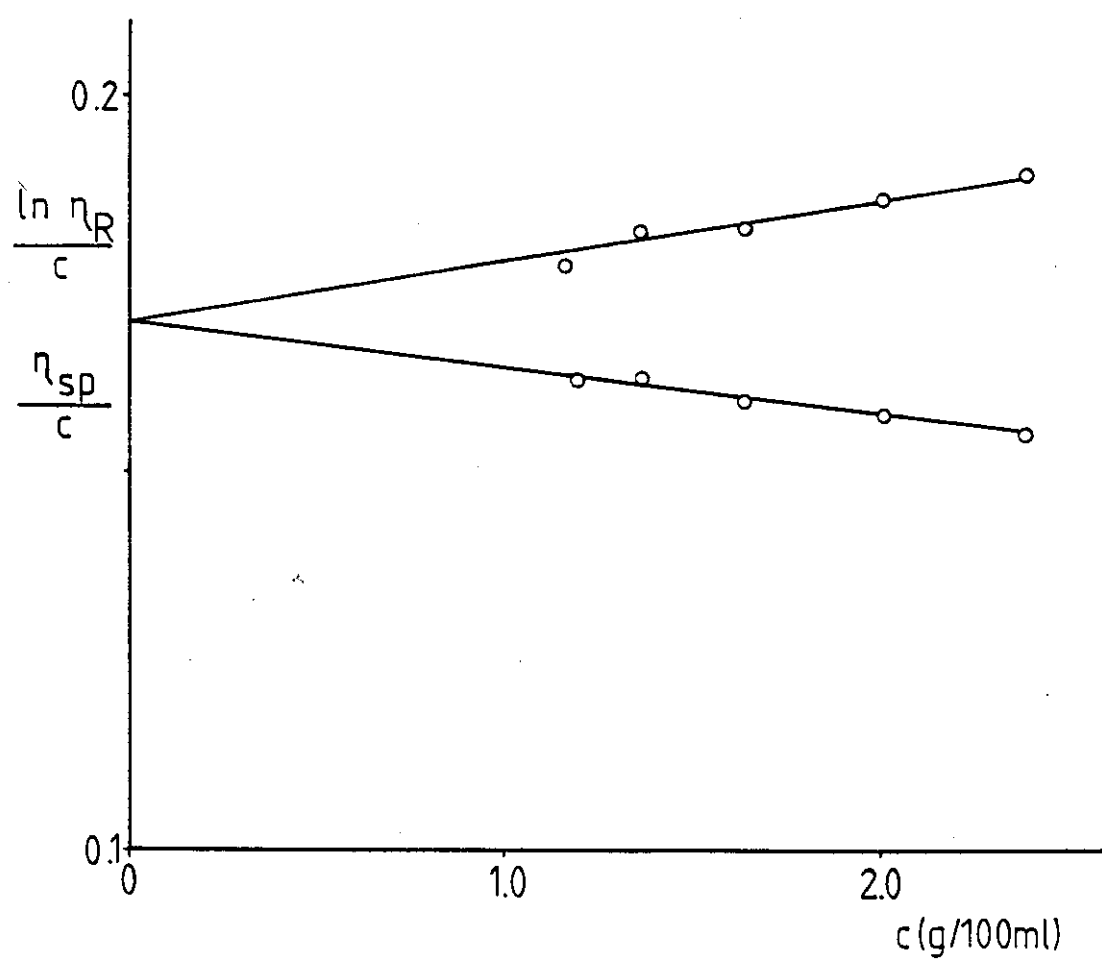


## 2.6 Solution viscosity measurements

The solution viscosity of the polymers was determined with an Ubbelohde miniature suspended level viscometer, type BS/IP/MSL, size number 2[127]. This viscometer was chosen in order to give an efflux time greater than 100 seconds for the solvents so that kinetic energy corrections were not significant[128]. Also, the miniature suspended level viscometer allows the use of small volumes, being the ideal choice when small samples are available. The viscometer was placed in a water bath maintained at  $25 \pm 0.1^\circ\text{C}$ , with the upright tubes exactly vertical. Without changing the concentration of the solution in the viscometer, the efflux time was measured until two successive times of flow agreed to within 0.2%. For each polymer, determinations were made at five different concentrations. Solution viscosity data were extrapolated linearly by the Huggins and Kraemer plots to infinite dilution in order to find the intrinsic viscosity  $[\eta]$  ( $\text{dl g}^{-1}$ ). For accuracy in extrapolating to infinite dilution, the solution concentration was restricted to the range that produced relative viscosities between 1.1 and 1.5[129]. A typical plot of  $\eta_{sp}/c$  and  $\ln \eta_r/c$  versus concentration obtained in this work is shown in figure 2.4.

FIGURE 2.4

Solution viscosity of PSA23700 measured in water at 25°C



## 2.7 ULTRAVIOLET ANALYSIS

UV measurements were carried out at room temperature in a Shimadzu UV-visible Recording Spectrometer model UV-160, equipped with quartz cells.

The absorbance range of 5 solutions of PSS in THF (concentration range from 0.2 to  $1 \times 10^{-2}$  mol/l) was measured at 260 nm to obtain a calibration curve. The copolymer samples were then analyzed, at a concentration of  $1 \times 10^{-2}$  mol/l, and their absorbance measured at 260 nm. With the use of the PSS calibration curve, the concentration of styrene in the copolymer was determined[130].

## RESULTS AND DISCUSSION

### 3.1 SAMPLE PREPARATION

#### 3.1.1 Concentration effect

Two samples, a polymer which elutes completely before  $V_0+V_i$  and a high molecular weight totally excluded polymer, were chosen to study the optimum concentration of injected polymer. To select these polymers a calibration curve ( Log MW versus  $V_R$  ) was obtained for the PEG/PEO standards, using a low concentration of the polymers ( 0.1% ) and this calibration graph is presented in figure 3.1. The selected polymers were PEG9230 as a permeating polymer and PEO660000 as a totally excluded polymer. The results obtained for  $V_R$  by changing the concentration of the injected standard can be seen in table 3.1. For the standard PEG9230

TABLE 3.1

Effect of the concentration of the injected polymer on  $V_R$  in  
polyacrylamide column packing, serial number JS6-3, water as  
eluent, instrument 1

PEG/PEO concentration ( g / 100 cm <sup>3</sup> )	$V_R$ ( % ethanol )	
	PEG9230	PEO-660000
0.05	60.5	46.7
0.1	60.4	47.4
0.15	60.9	47.2
0.2	60.5	47.2
0.25	60.3	47.5
0.5	60.4	48.3

there is no variation in  $V_R$  throughout the concentration range studied. Also, there was no distortion of the peak shape, confirming the fact that concentration effects are usually negligible for MW below  $10^6 \text{ g mol}^{-1}$  [80]. For the high MW PEO there is a peak shift towards high elution volume at a concentration of 0.5%. This shift should be due to the viscosity phenomena in the interstitial volume which is the only effect operative when the MW of the polymer being investigated is above the exclusion limit of the column [74]. To avoid this problem, it was decided to work at PEG/PEO concentrations of 0.1% as this was the lowest concentration at which a reasonable detector response was achieved.

### 3.1.2 Sample dissolution

Standard PEG9230 was chosen for the study of the optimum conditions of sample preparation as it was the highest MW standard available that was totally permeating on the column used. The sample solutions were heated for 15 min at different temperatures to reduce the solvent viscosity and speed up solvent diffusion within the swollen polymer. Then, the solutions were allowed to cool for 30 min at room temperature. The results obtained are shown in Table 3.2 from which data it is verified that variations in the heating temperatures did not alter the chromatogram for the standard PEG9230. This effect could be more pronounced for high MW polymers, but as the columns available for this work had a low MW permeation range, no studies of long chain PEO were performed.

TABLE 3.2

Effect of heating temperature on average molecular weights from SEC of the PEG9230, in polyacrylamide column packing, serial number J56-3, water as eluent, instrument 1.

Heating temperature °C	$\bar{M}_n$	$\bar{M}_w$
20	3700	7200
40	3500	7200
60	3600	7300
80	3700	7300

## 3.2 CALIBRATION FOR POLYACRYLAMIDE COLUMNS

### 3.2.1 Calibration for different polymers

The calibration curves ( Log MW against  $V_R$  ) for PEG, PEO and PSA standards in water and water-MeOH ( 80/20 ) are shown in figure 3.1 and 3.2 respectively. The characteristics of the standards used are described in Table 2.1. As they all have polydispersities below 1.1, equation 1.14 is valid and the placement of the calibration curve using  $V_R$  at the peak height maximum of a chromatogram will therefore be accurate[12]. The experimental results in figure 3.1 show that the PSA calibration curve is displaced to high  $V_R$  compared with the curve for PEG and PEO. The same effect is observed when the polarity of the mobile phase is decreased by the addition of 20% MeOH, as can be seen in figure 3.2. In this last case, the difference between the calibration curves for PEG/PEO and PSA is even more pronounced than in pure water.

The polysaccharide used in this study, an extracellular  $\alpha$ -glucan of the fungus *Aureobasidium pullulans*, known as pullulan, is a linear polysaccharide polymerized from maltotriose as the repeating unit through the  $\alpha$ -1,6-glucosidic linkage and its structure is illustrated in figure 3.3[131]. However, most of the work already reported in aqueous SEC[17] was performed with dextrans, another neutral polysaccharide available as well characterized fractions and with which the results obtained here will be compared.



FIGURE 3.1

Log molecular weight versus  $V_R$  calibration curves for water as eluent, at room temperature, polyacrylamide column packing, serial number J56-3, flow rate 1 cm<sup>3</sup>/min, instrument 1. PEG, PEO (O); PSA ( $\Delta$ )

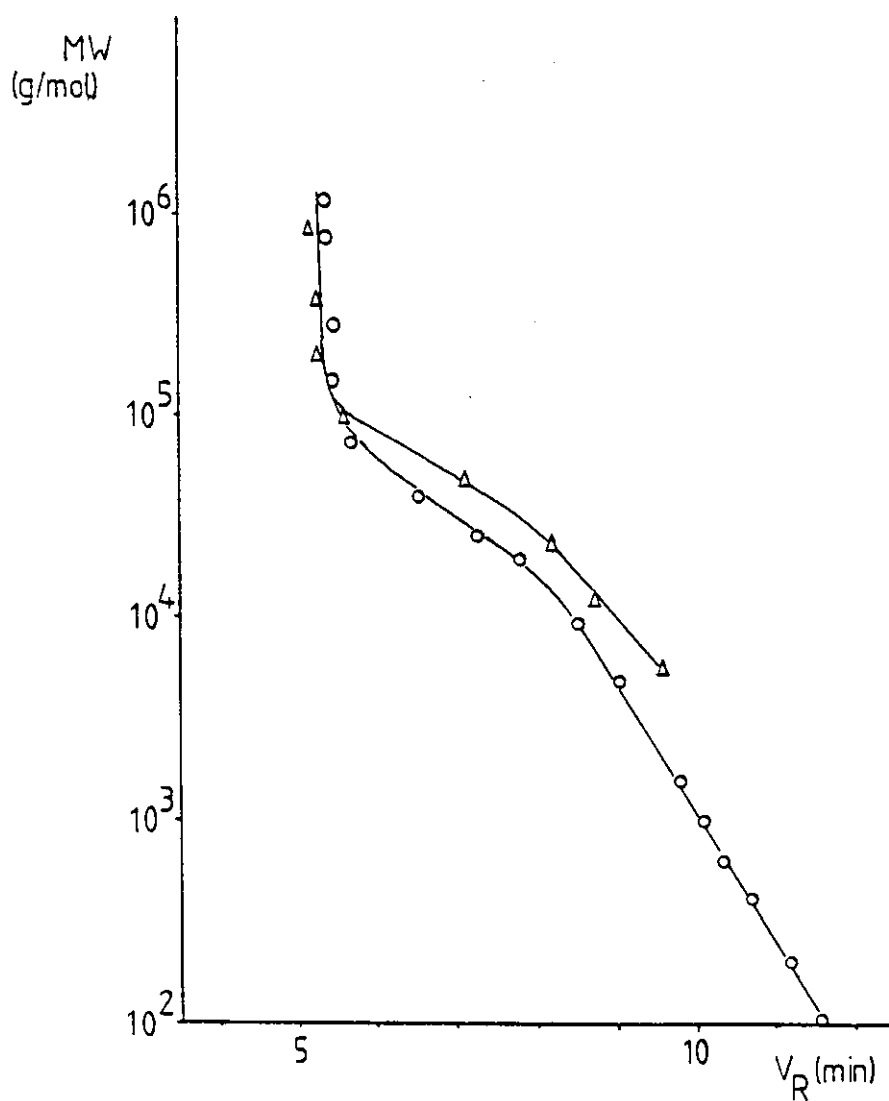


FIGURE 3.2

Log molecular weight versus  $V_R$  calibration curves for water-MeOH ( 80/20 ) mixture at room temperature, polyacrylamide column packing, serial number J56-3, flow rate 1 cm<sup>2</sup>/min, instrument 1. PEG, PEO ( O ); PSA (  $\Delta$  )

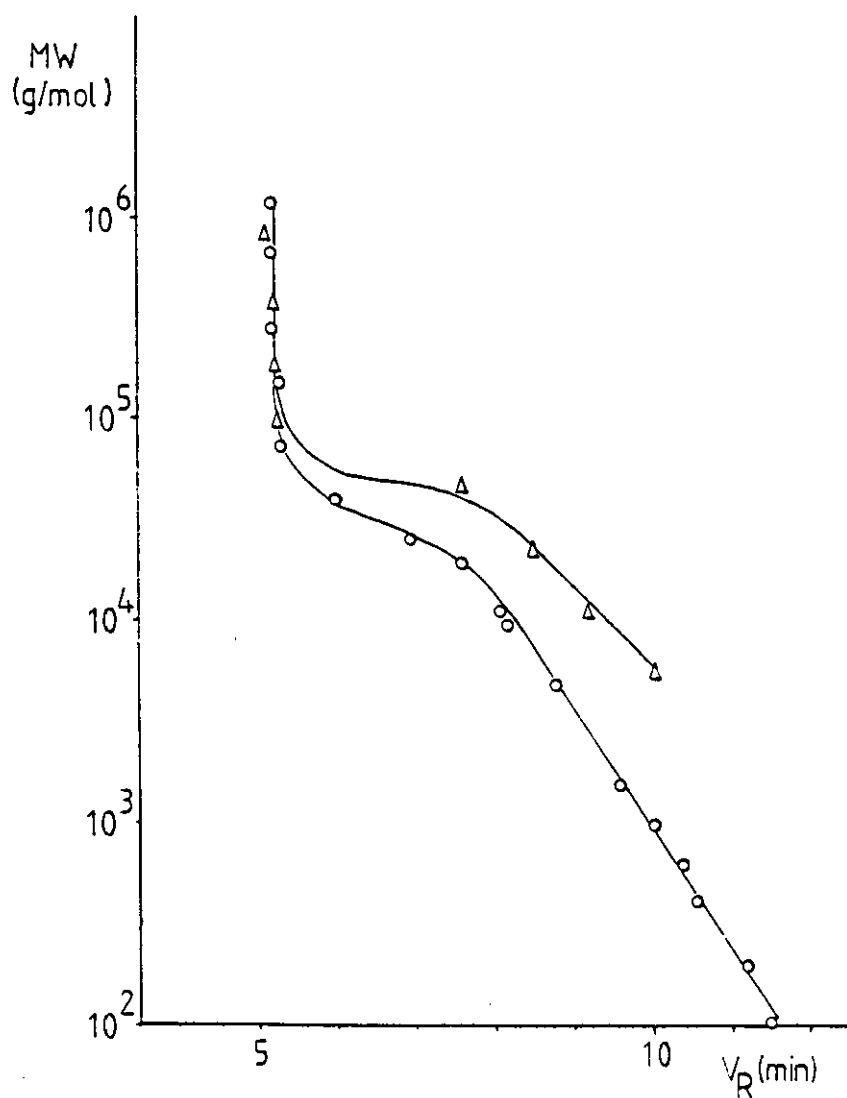
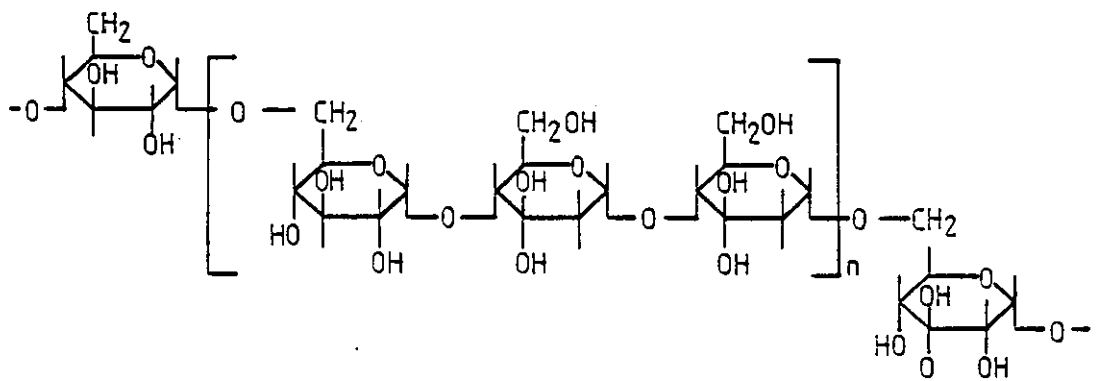


FIGURE 3.3

Structural Formula of Pullulan ( PSA ) [131]



It is well known that PEG/PEO samples strongly adsorb on untreated glass and silica column packings because of the multiple hydrogen bonds formed between these polymers and the silanol groups[15-17]. Dextrans however do not show specific interactions with glass[132] and most other aqueous SEC column packings[17,133]. Chemically bonded stationary phases based on a silica support offer the possibility of reducing or eliminating the interactive effects between silica packings and PEG/PEO. Stationary phases of the reversed-phase type may exhibit hydrophobic or solvophobic sorption properties with organic solutes if water or water mixtures are used as eluents. The introduction of polar functional groups into the organic moiety bonded on the silica surfaces can change the hydrophobic reversed-phases into hydrophilic phases. Engelhardt and Mathes[133,134] prepared bonded-phases with many different functional groups attached at the end of a silane  $[Si-(CH_2)_3-]$  bound to a silica surface. These phases have been evaluated for their use in SEC of synthetic water soluble polymers and were divided into three groups according to the type of interaction with PEG. The first group, called "non-polar" phases showed strong interactions with even small oligomers of PEG in water. The functional groups attached to silane were, in this case alkyl ( $C_3$ ), trifluoroacetyl, nitrile, mercaptane and diol. The second group of bonded phases, called "medium" polarity phases did not retain PEG oligomers but the PEG40000 was strongly retarded. These phases had a urea, an amide or a carbamate group attached to the silane. The third group of stationary phase, called "polar" phases did not interact at all with PEG oligomers. However, the degree of interaction with PEG40000 would depend not only on the nature of the functional group but also on the degree of surface coverage of the phases. So, among amine, sulfonamide, imidazoline,

triamine, glycinamide and diamine functional groups, only the last two bonded-phases showed no interactions with PEG40000, using water as eluent[133].

Hashimoto et al[14], using polyether column packings and a 0.08M tris-HCl buffer solution at pH 7.94 as the mobile phase, analyzed PEG and dextrans and found no evidence of adsorption. However, the calibration curve (Log MW versus  $V_R$ ) for dextrans was displaced to higher  $V_R$  in relation to PEG. The same effect was observed by Kato et al[22], using the same column packing type and 0.1M aqueous sodium chloride solution as eluent, where there was a displacement of the calibration curves, in order of increasing  $V_R$ , for PEO, PSA and dextrans. Both workers attributed the differences obtained between the calibration curves to differences in the hydrodynamic volume of the polymers. In order to study the changes in the hydrodynamic volume of the polymers, the intrinsic viscosity of some of the standards employed in figures 3.1 and 3.2 was measured. Figure 3.4 shows the MW dependence of  $[\eta]$  for PEG/PEO and PSA in water and water-MeOH (80/20) at 25°C. The Mark-Houwink equations were obtained by the linear regression of double-logarithmic plots of  $[\eta]$  against  $M_p$  and are:

For PEG/PEO:

$$[\eta]_{\text{PEG/PEO}} = 4.7 \times 10^{-4} M_p^{0.7} \quad (3.1)$$

$$[\eta]_{\text{PEG/PEO-MeOH(80/20)}} = 2.1 \times 10^{-4} M_p^{0.8} \quad (3.2)$$

For PSA:

$$[\eta]_{\text{PSA}} = 6.9 \times 10^{-4} M_p^{0.6} \quad (3.3)$$

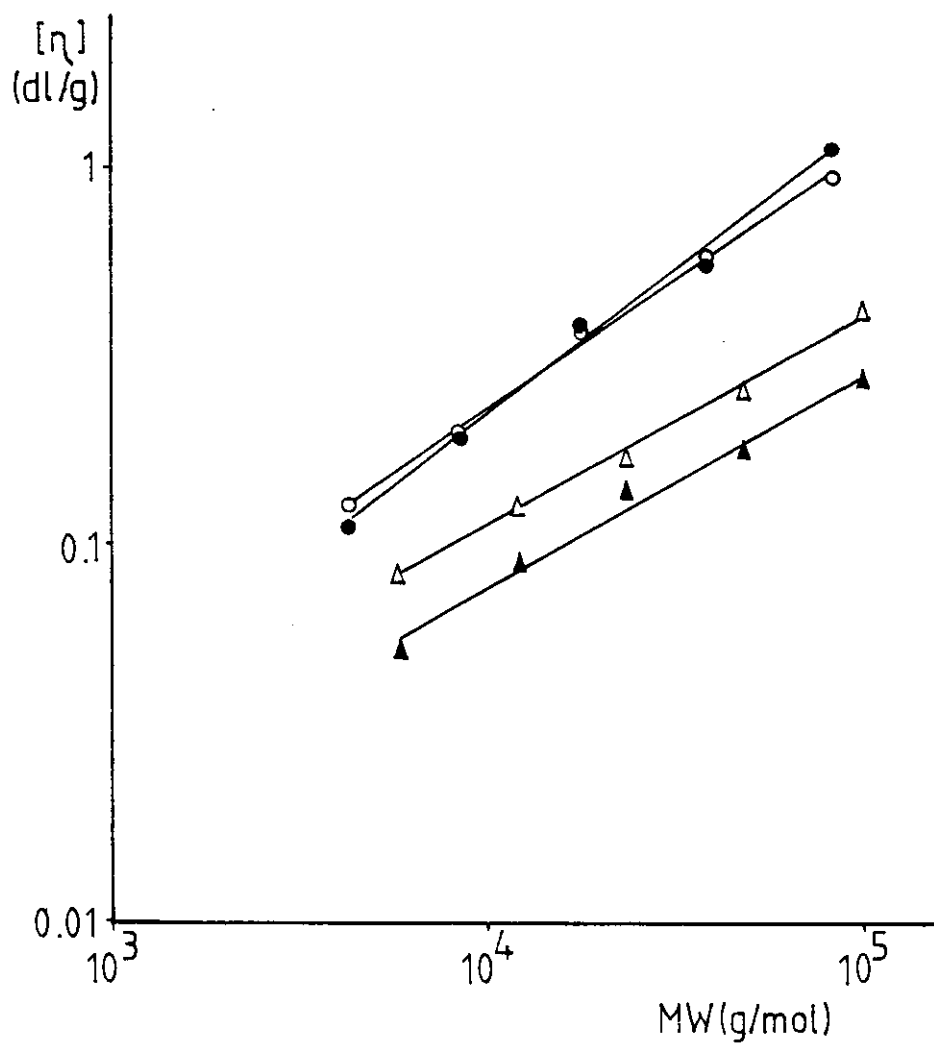
$$[\eta]_{\text{PSA-MeOH(80/20)}} = 4.4 \times 10^{-4} M_p^{0.6} \quad (3.4)$$

In all four cases, the error obtained in the slope of the regression lines in figure 3.4 was around 0.1. This rather large error is probably caused by two main factors: first the MW values attributed to the

FIGURE 3.4

Log Intrinsic viscosity versus log molecular weight at 25°C.

PEG/PEO-water (○); PEG/PEO-water-MeOH (80/20) (●);  
PSA-water (Δ); PSA-water-MeOH (80/20) (▲).



standards are not necessarily accurate and second the values for the exponent  $a$  is changing with MW in the range studied[135]. It has been demonstrated[135] and confirmed experimentally[136] for a number of polymers that  $a$  falls to 0.5 for short chains in good solvents. So, in the medium MW range, the values of  $K$  and  $a$  in equation 1.17 must change with MW[135]. It can be concluded from figure 3.4 that PEG/PEO have approximately the same intrinsic viscosities in both solvent systems and that from the exponent  $a$  in the Mark-Houwink equations 3.1 and 3.2, both solvent systems are good solvents for these polymers. There is no published data for the viscosity of PEG/PEO in water-MeOH systems, but the results obtained in water are in reasonable agreement with the existing literature. The intrinsic viscosity data obtained by Kato et al[137] for PEO samples with MW  $2 \times 10^4$  to  $1.3 \times 10^6$  was established as

$$[\eta]_{\text{PEG}} = 5.94 \times 10^{-4} \text{ ML}^2 \text{ g}^{-1} \quad (3.5)$$

However, for low MW PEO (  $< 1000$  ) the exponent  $a$  in equation 3.5 tends to the value 0.5[138]. It has been shown it is a characteristic property of low MW PEG to behave in a good solvent like PEO in a theta solvent although the thermodynamic conditions characteristic of this state are not realized.

This is apparently caused by a decrease or annulment of long range interactions ( excluded volume ) with decreasing MW[138]. So, the slope of the intrinsic viscosity versus MW curve should be 0.5 for MW below 1000 and gradually increases as the MW increases until it reaches a value around 0.7 as suggested by Kato et al[137] and found in equation 3.1.

Figure 3.4 also shows that PSA standards have different viscosities in water and water-MeOH. Studies performed with PSA showed that the

pullulan chain has significant flexibility as a consequence of the  $\alpha$ -1,6-glucosidic linkage, and in an aqueous solution the polymer behaves as an expanded flexible coil because of the excluded volume effect. The MW dependence of the intrinsic viscosity found by Kato et al[131] for PSA with MW greater than 48000 can be represented by

$$[\eta]_{\text{water}} = 1.91 \times 10^{-4} \text{ MW}^{0.47} \quad (3.6)$$

As the MW decreased, the slope of the Mark-Houwink equation decreased to 0.5, although data obtained for MW values below  $30 \times 10^3$  were considered somewhat unreliable. As equation 3.3 was obtained for MW values between  $5.8 \times 10^3$  and  $10^5$  and the values for  $a$  are changing from 0.5 to a higher value in this region, the low value obtained for  $a$  in this equation is then justified.

There is no data in the literature for intrinsic viscosities of PSA in water-MeOH mixtures. As the PSA standards used in this work did not dissolve in the mixture water-MeOH (60/40) and since the intrinsic viscosities of PSA are lower in water-MeOH (80/20) than in water (see figure 3.4), it can be concluded that the mixed solvent is a much poorer solvent for PSA than water.

The universal calibration plot  $\log [\eta]M$  versus  $V_R$  for PEG/PEO and PSA in water and water-MeOH (80/20) is shown in figure 3.5 and 3.6 respectively. With water as eluent, for values of  $[\eta]M$  above  $2 \times 10^3 \text{ dl mol}^{-1}$ , the hydrodynamic volume may be regarded as a reasonable representation of separation behaviour suggesting that separations of these polymers are dominated by a size exclusion mechanism. For the solvent mixture water-MeOH (80/20) this limit is higher, and it can be considered



FIGURE 3.5

Hydrodynamic volume calibration curves with water as eluent at room temperature, polyacrylamide column packing, serial number J56-3, flow rate  $1 \text{ cm}^3/\text{min}$ , instrument 1. PEG/PEO (  $\circ$  ); Polysaccharides (  $\Delta$  ).

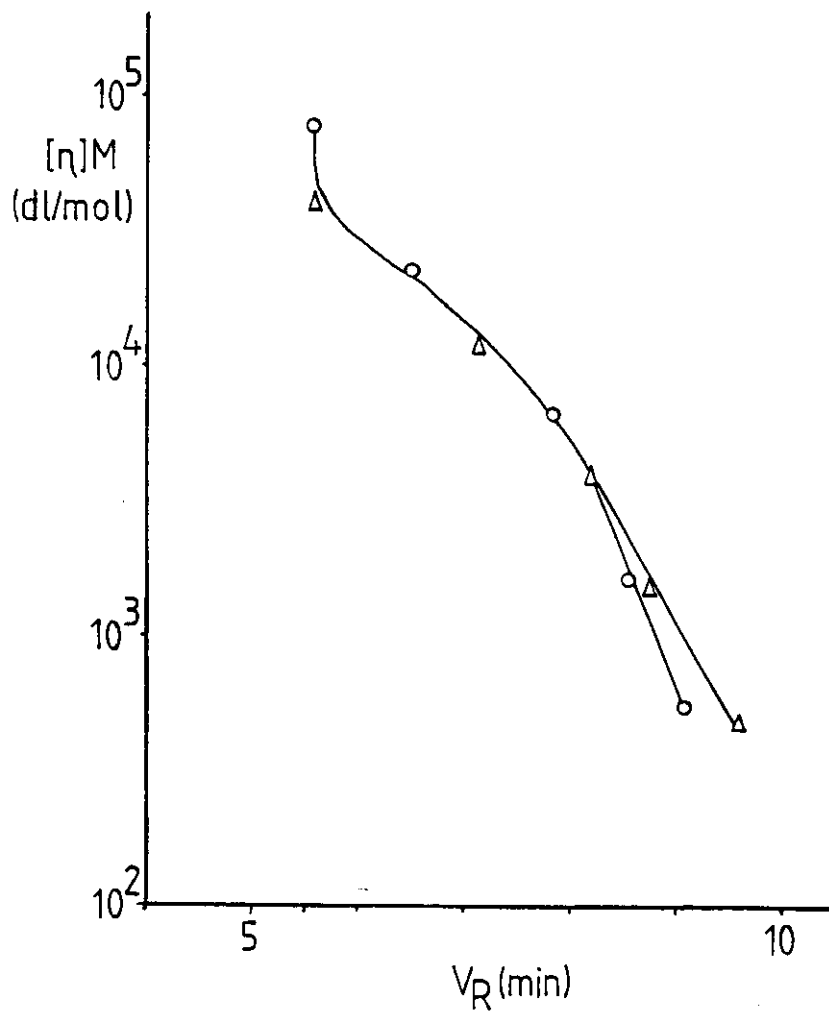
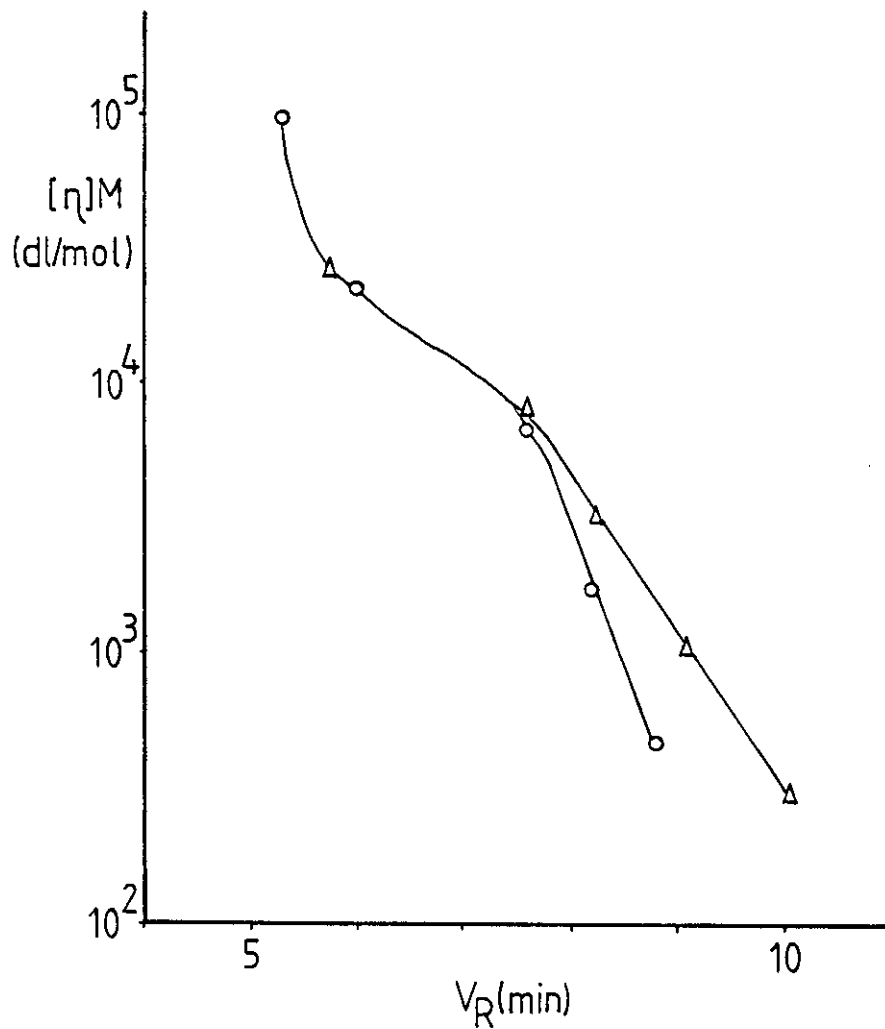


FIGURE 3.6

Hydrodynamic volume calibration curves with water-MeOH ( 80/20 ) mixture as eluent at room temperature, polyacrylamide column packing, serial number J56-3, flow rate 1 cm<sup>3</sup>/min, instrument 1. PEG/PEO ( O ); PSA ( Δ ).



that the universal calibration is valid for  $[\eta]M$  above  $9 \times 10^3$  dl mol<sup>-1</sup>.

Kato et al[22] using a polyether based gel and 0.1 M aqueous sodium chloride solution as eluent claimed that a line could be drawn through all points of the plot  $\log [\eta]M$  versus  $V_R$  for PEO, PSA and dextrans. However, Kato et al did not work with PSA in the MW range below  $2 \times 10^3$ , where the calibration curves diverge, as can be seen in figure 3.5.

At low hydrodynamic volumes, corresponding to MW below  $2 \times 10^3$  and  $4 \times 10^3$  for water and water-MeOH respectively, the PEG and PSA curves clearly diverge. Similar behaviour has been observed for short polycarbonate and polystyrene chains in chloroform[135] and two possible explanations were proposed which may apply to the behaviour of low polymers in figures 3.5 and 3.6. First, short PSA chains having a bulky repeating unit may adopt a different chain conformation from that of PEG, and so short PSA and PEG chains do not display the same hydrodynamic behaviour. Second, solute-gel interactions for small molecules have been observed to generate divergent calibrations[139].

### 3.2.2 Calibration in aqueous solvents

The effect of changing the solvent from water to water-MeOH mixtures on the separation properties of polyacrylamide packings is more easily seen in separate plots for each standard in different solvents. Figure 3.7 shows plots of  $\log MW$  versus  $V_R$  for PEG/PEO in water and in two mixtures of water-MeOH, ( 80/20 ) and ( 60/40 ). The plot of  $\log MW$  versus  $V_R$  for PSA is shown in figure 3.8 for water and water-MeOH ( 80/20 ) only,

FIGURE 3.7

Log molecular weight versus  $V_R$  calibration curves for PEG/PEO standards at room temperature, polyacrylamide column packing, serial number J56-3, flow rate 1 cm<sup>3</sup>/min, instrument 1. water (○); water-MeOH (80/20) (Δ); water-MeOH (60/40) (□)

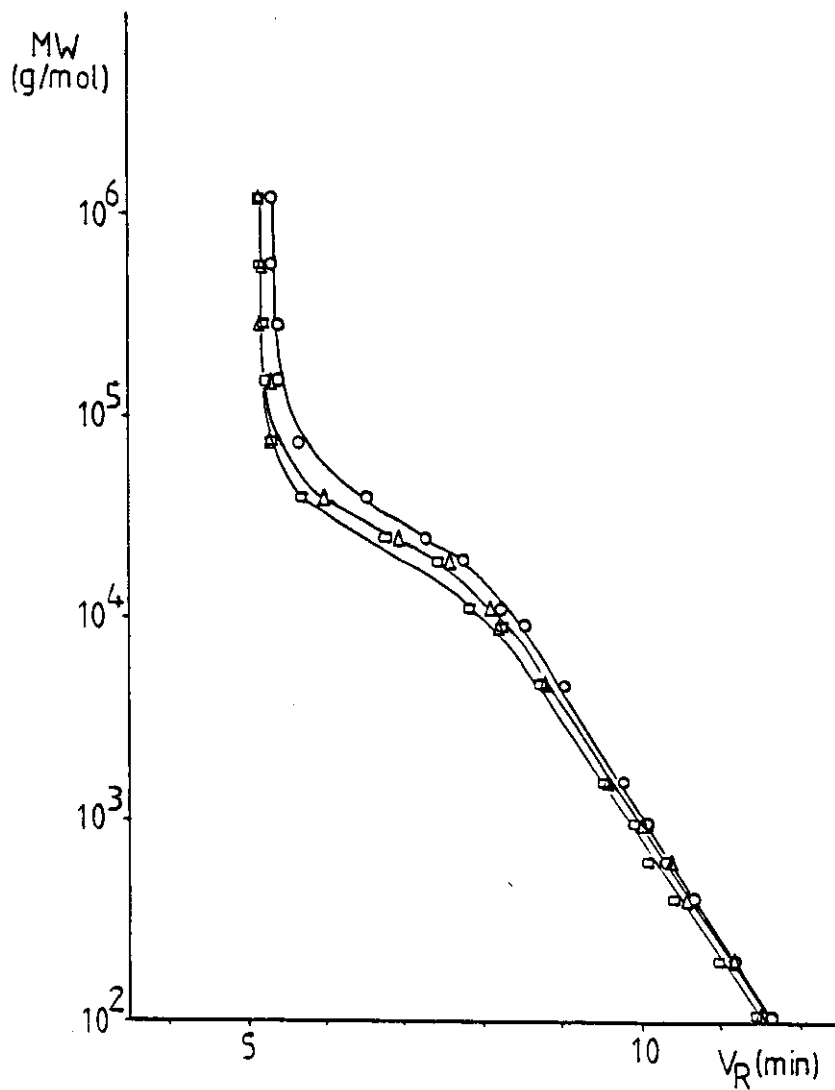
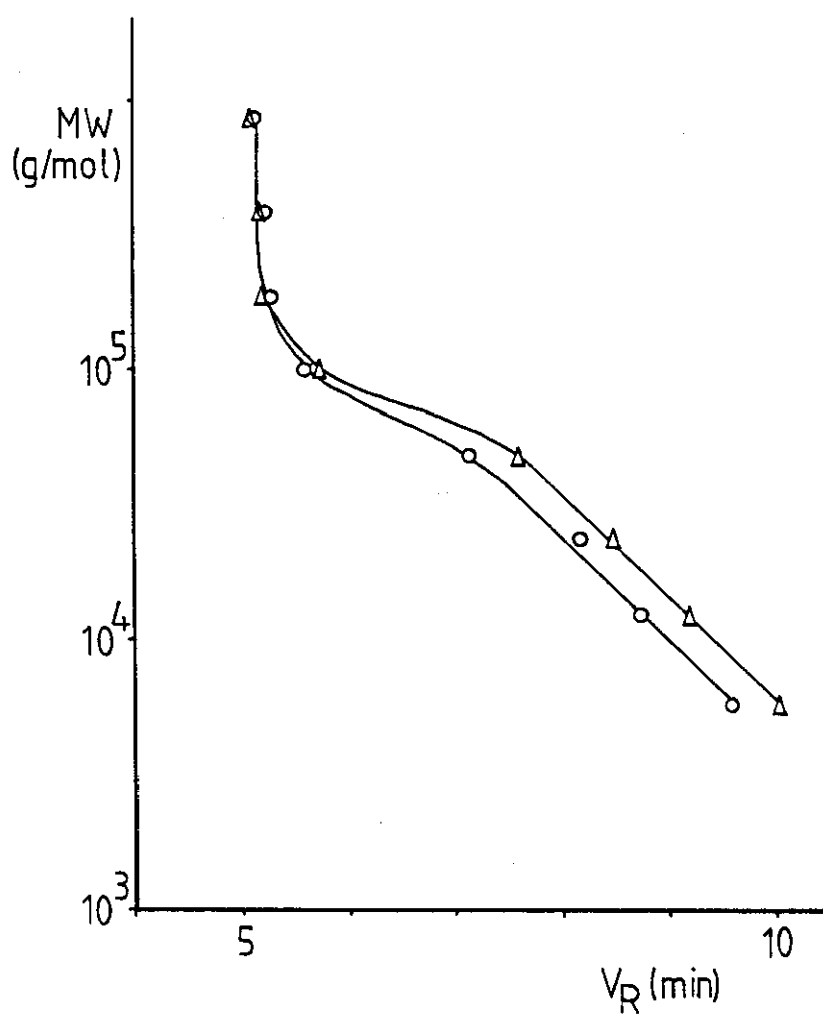


FIGURE 3.8

Log molecular weight versus  $V_R$  calibration curves for PSA standards at room temperature, polyacrylamide column packing, serial number J56-3, flow rate 1 cm<sup>3</sup>/min, instrument 1. water (○); water-MeOH (80/20) (Δ).



since PSA standards were not soluble in the mixture water-MeOH ( 60/40 ). It can be seen in figure 3.7 that for PEG/PEO standards all the calibration curve is displaced to lower  $V_R$  when the solvent is changed from water to water-MeOH mixtures and even the void volume of the column changes. However, a different effect is observed for PSA standards where the void volume of the column remains the same but the permeating part of the calibration curve is displaced to higher  $V_R$  when the solvent is changed from water to water-MeOH ( 80/20 ). Changing the solvent in a SEC experiment with semi-rigid polymeric column packing could cause, beside the effects on the hydrodynamic volume of the polymer and on the secondary mechanisms already mentioned in the previous section, a change in the volume of the column packing.

The semi-rigid polyacrylamide column packing material being used in this work is a very hydrophilic gel formed in the copolymerization of acrylamide and N,N' - methylene-bisacrylamide where the crosslinking agent is the major component in weight. It is claimed that these macroreticular gel particles can be used with most eluents of solubility parameter greater than 9.0, which include water, acetone and alcohols[25]. However, there is no published data concerning the effects of the use of solvents different from water in these packings.

Bio-Gel P is a well known soft column packing used for gel filtration chromatography of proteins and other biological compounds[140]. Bio-Gel P is a soft polyacrylamide gel and its chemical composition is very similar to the semi-rigid polyacrylamide gel used in this work. It is claimed that this soft polyacrylamide gel is very hydrophilic and does not swell in organic compounds. However, water-alcohol mixtures, up to ( 80/20 ) do not substantially alter the exclusion properties of the

gel[140]. Since both polyacrylamide gels ( soft and semi-rigid ) have a similar chemical composition, an analogous behaviour with regard to solvent compatibility can be expected of them. So, water should also be a better solvent for semi-rigid polyacrylamide gels than water-MeOH mixtures. In this case, the packing swells in water and so the pore volume increases, shifting  $V_R$  to higher values. This would explain the shift in the permeation part of the calibration curves obtained for PEG/PEO where, when the solvent is more compatible with the packing, the values of  $V_R$  are displaced to high elution volumes. The change in the degree of swelling of polymeric packings, caused by different eluents has been verified before[30,133,141]. In this work, this change can be confirmed by the increase of  $V_T$ , the total volume of eluent, given by the  $V_R$  of a totally permeating solute ( ethanol ), from 12.0 cm<sup>3</sup> in water-MeOH ( 60/40 ) to 12.3 cm<sup>3</sup> in pure water. However, the swelling of the packing does not explain the shift in the excluded volume part of the calibration curve. Actually, it is expected that when the pore volume increases, the void volume of the column decreases and so the excluded volume part of the calibration curve is shifted to smaller  $V_R$ . But, it is known that comparison of elution volumes obtained in various systems is complicated as  $V_R$  depends on the volume of solvent in which the chromatographic process takes place[60]. The total volume of gel bed (  $V_T$  ) has been defined for gel filtration as[142]

$$V_T = V_0 + V_R \quad (3.7)$$

and the fraction of the volume of gel that is available for each solute can be expressed by  $K_{av}$ , the distribution coefficient, defined by[142]

$$K_{av} = (V_R - V_0) / (V_T - V_0) \quad (3.8)$$

The coefficient  $K_{av}$  varies from zero, for molecules excluded from the gel pores, to one, for totally permeating molecules.  $K_{av}$  has been used to allow the comparison of SEC systems using different mobile phases, either for rigid[132] or for soft[60] column packings. For porous glass the changes in the effective pore volume of the packing with different eluents are attributed to differences in surface tension between the porous glass and the solvent media employed[132].

A plot of log MW versus  $K_{av}$  for PEG/PEO and PSA is shown in figures 3.9 and 3.10 respectively. It can be seen in figure 3.9 that the data for all the three solvent systems agree well once the correction for differences in the volumes accessible for separation is made. One possible explanation for the differences in void volume found in figure 3.7 is based on the effects of selective sorption in mixed eluents[62]. Water is more compatible with the packing material than MeOH, so when a water-MeOH mixture is used as mobile phase there is a quasistationary gel-phase rich in water, surrounding the gel. As PEG/PEO shows some hydrophobic interactions[16,133] it will not approach the water-rich quasistationary layer, staying more in the MeOH-rich mobile phase. This would cause an early elution of PEG/PEO throughout the elution range when water-MeOH mixtures are used as the mobile phase.



FIGURE 3.9

Log MW versus  $K_{av}$  calibration curve for PEG/PEO standards at room temperature. water (  $\circ$  ); water-MeOH ( 80/20 ) (  $\Delta$  ); water-MeOH ( 60/40 ) (  $\square$  ).

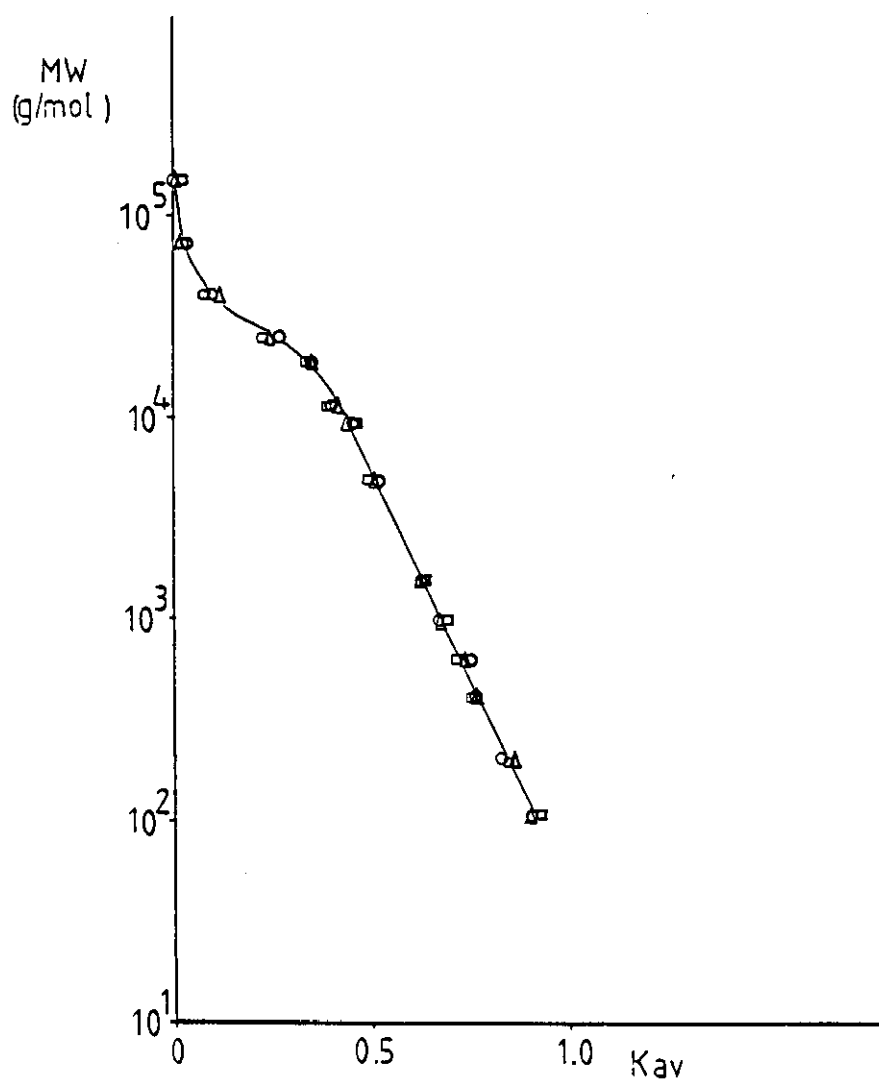
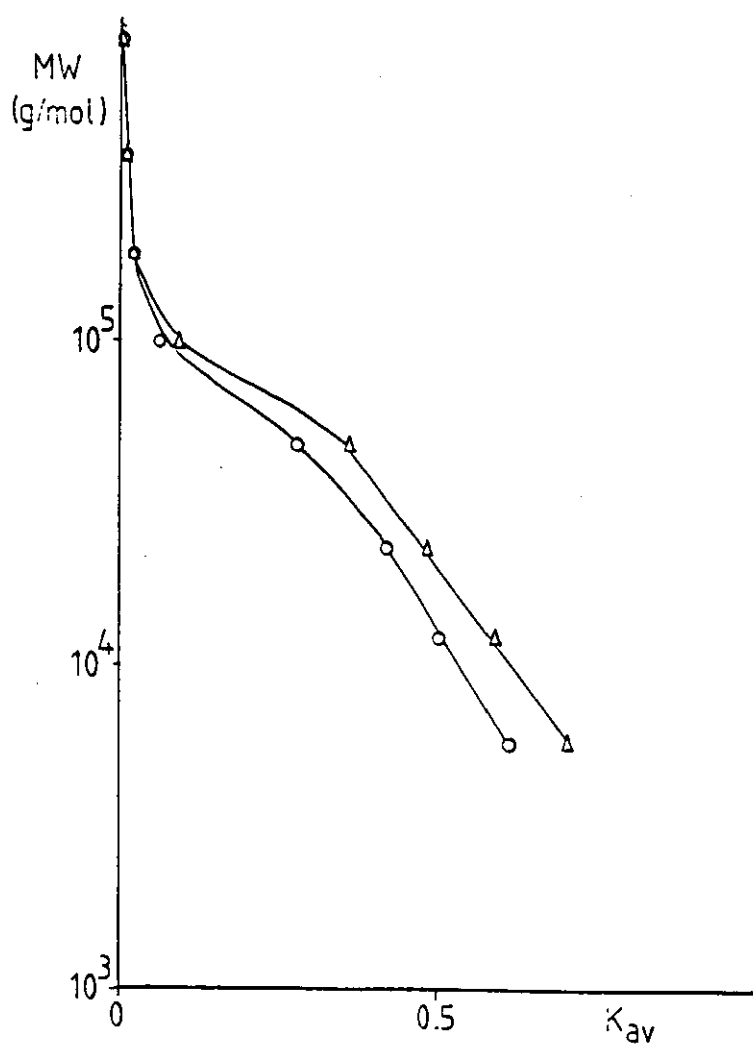


FIGURE 3.10

Log MW versus  $K_{av}$  calibration curve for PSA standards at room temperature, polyacrylamide column packing, serial number J56-3, flow rate 1 cm<sup>3</sup>/min, instrument 1. water (○); water-MeOH (80/20) (Δ)



For the PSA standards the shift in the calibration curves is caused by other factors than the change in the volume of liquid phase because the difference between the calibration curves in figure 3.8 is also found in figure 3.10 when the corrections for the volume accessible for the separation were made. As water is a better solvent for PSA than water-MeOH, the solute molecules would have access to the same volume of liquid phase in both solvent systems as water will strongly interact with the gel but the water-rich quasistationary phase formed when the eluent is water-MeOH would be more attractive to the PSA molecules. So,  $V_R$  of PSA in water-MeOH ( 80/20 ) should be larger than in pure water due to the increased interaction of the solute with the water-rich quasistationary phase layer. Beside this interactive effect, other effects could operate in the separation like adsorption on the gel and changes in the hydrodynamic volume of the polymer, which would also displace the calibration curve for water-MeOH to higher  $V_R$ . In order to analyse the influence of these two effects on the separation, plots of  $\log [R]M$  versus  $V_R$  and versus  $K_{av}$  are shown in figure 3.11 to 3.14 for PEG/PEO and PSA standards. The curves for PEG/PEO in figure 3.11 are displaced in the same direction as the MW calibration curves in figure 3.7 and are almost parallel throughout the studied range. The values obtained for the exponent  $a$  in equations 3.1 and 3.2 suggests that the eluents are good solvents for PEG/PEO and so, the separation in polymeric packings should be according to solute size[30]. Therefore, the only reason for the non-coincidence in the calibration curves in figure 3.11 should be the change of the eluent volume available for the separation, due to the swelling of the packing and to the non-interaction with the quasistationary layer. So, when the correction for the volumes is made, as in figure 3.13,

FIGURE 3.11

Hydrodynamic volume versus  $V_R$  calibration curves for PEG/PEO standards at room temperature, polyacrylamide column packing, serial number J56-3, flow rate 1 cm<sup>3</sup>/min, instrument 1. water ( O ); water-MeOH ( 80/20 ) (  $\Delta$  )

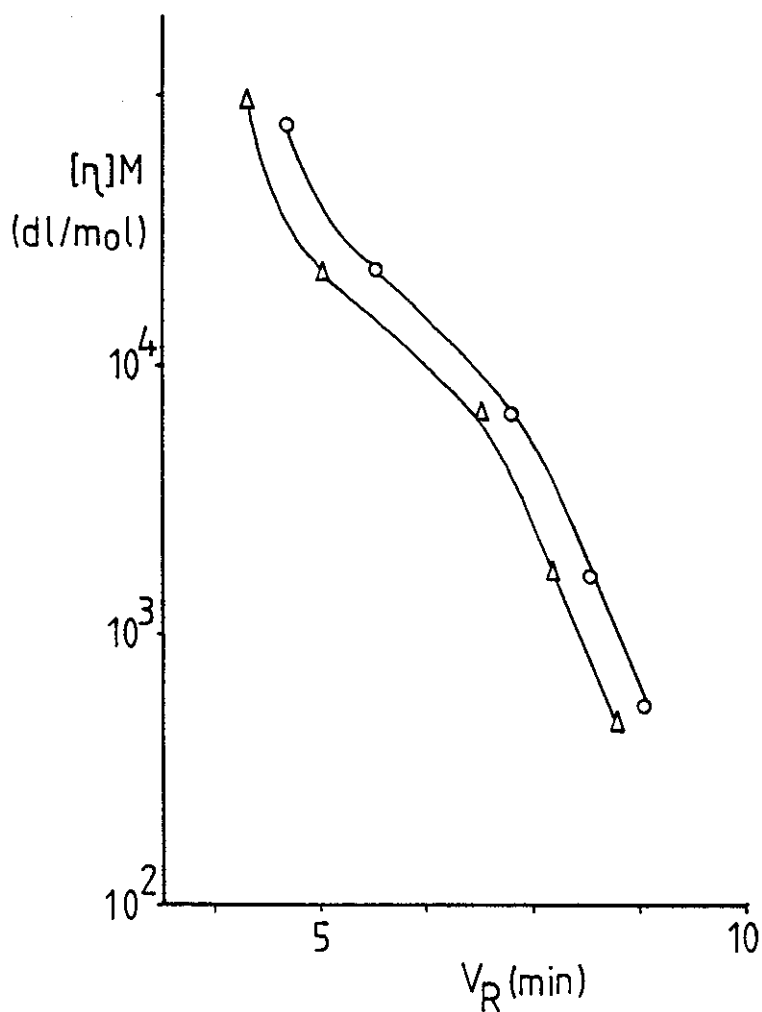


FIGURE 3.12

Hydrodynamic volume versus  $V_R$  calibration curves for PSA standards at room temperature, polyacrylamide column packing, serial number J56-3, flow rate 1 cm<sup>3</sup>/min, instrument 1. water (○); water-MeOH (80/20) (Δ)

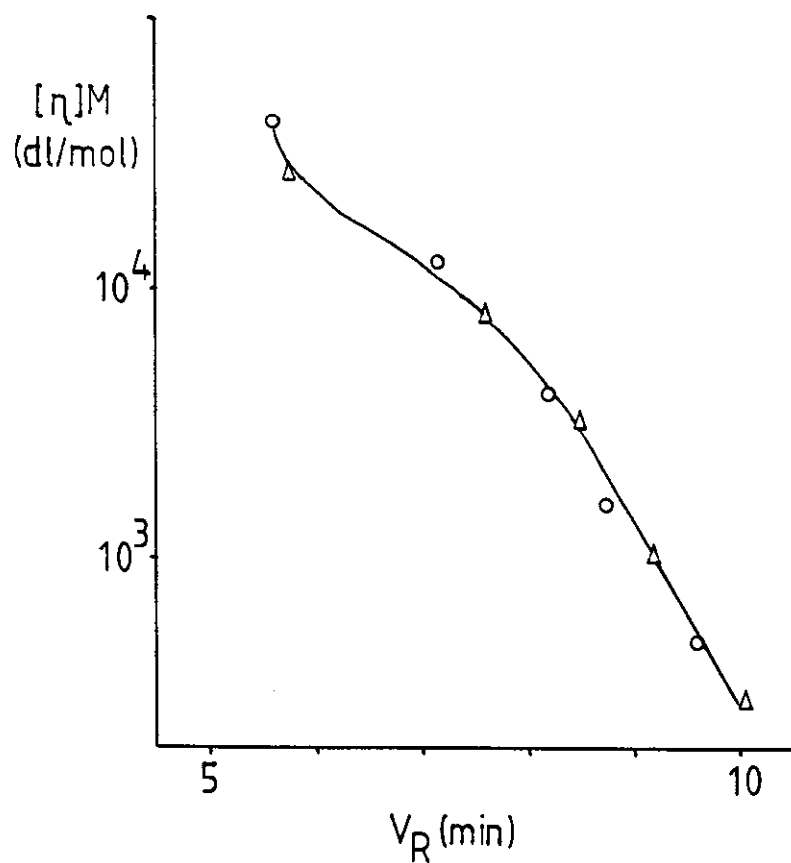


FIGURE 3.13

Hydrodynamic volume versus  $K_{av}$  calibration curves for PEG/PEO standards at room temperature, polyacrylamide column packing, serial number J56-3, flow rate 1 cm<sup>3</sup>/min, instrument 1. water (○); water-MeOH (80/20) (Δ)

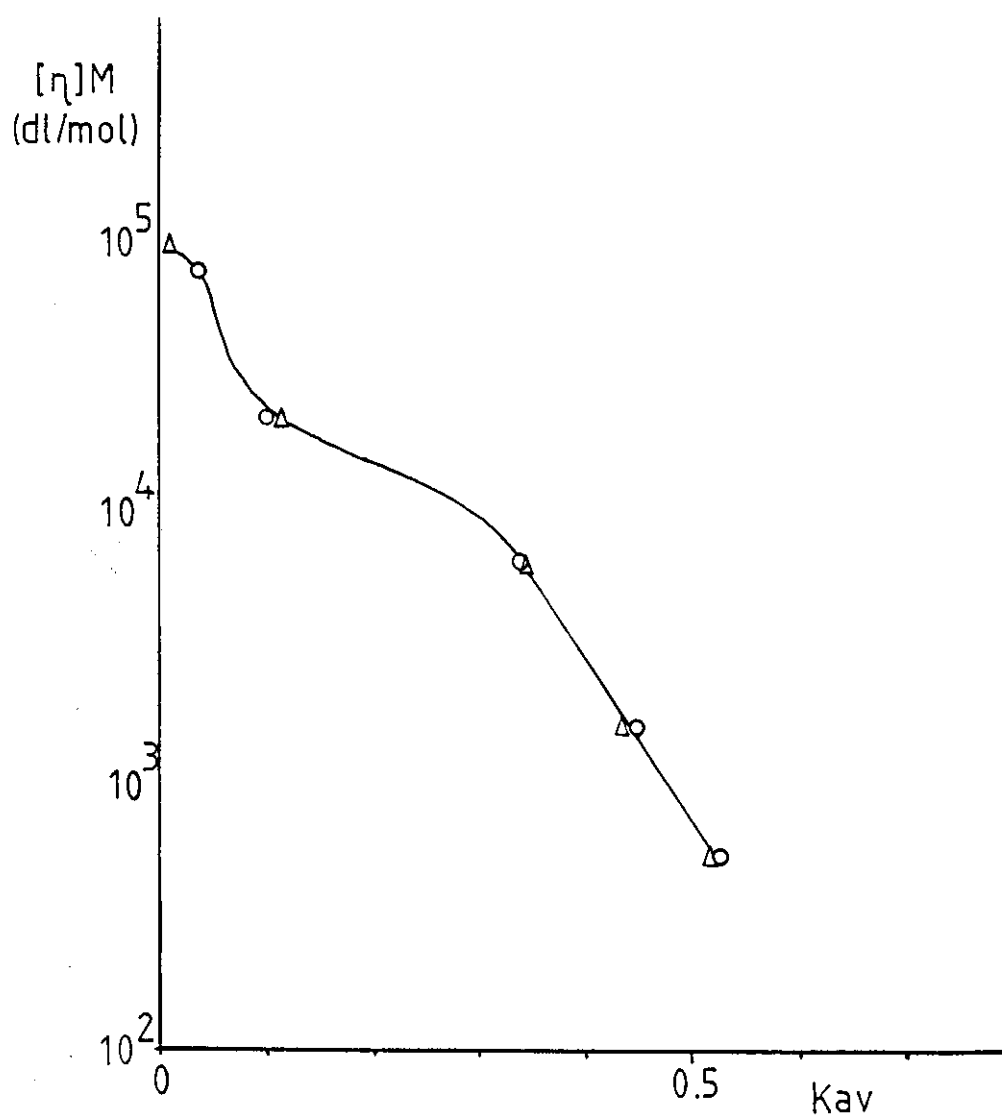
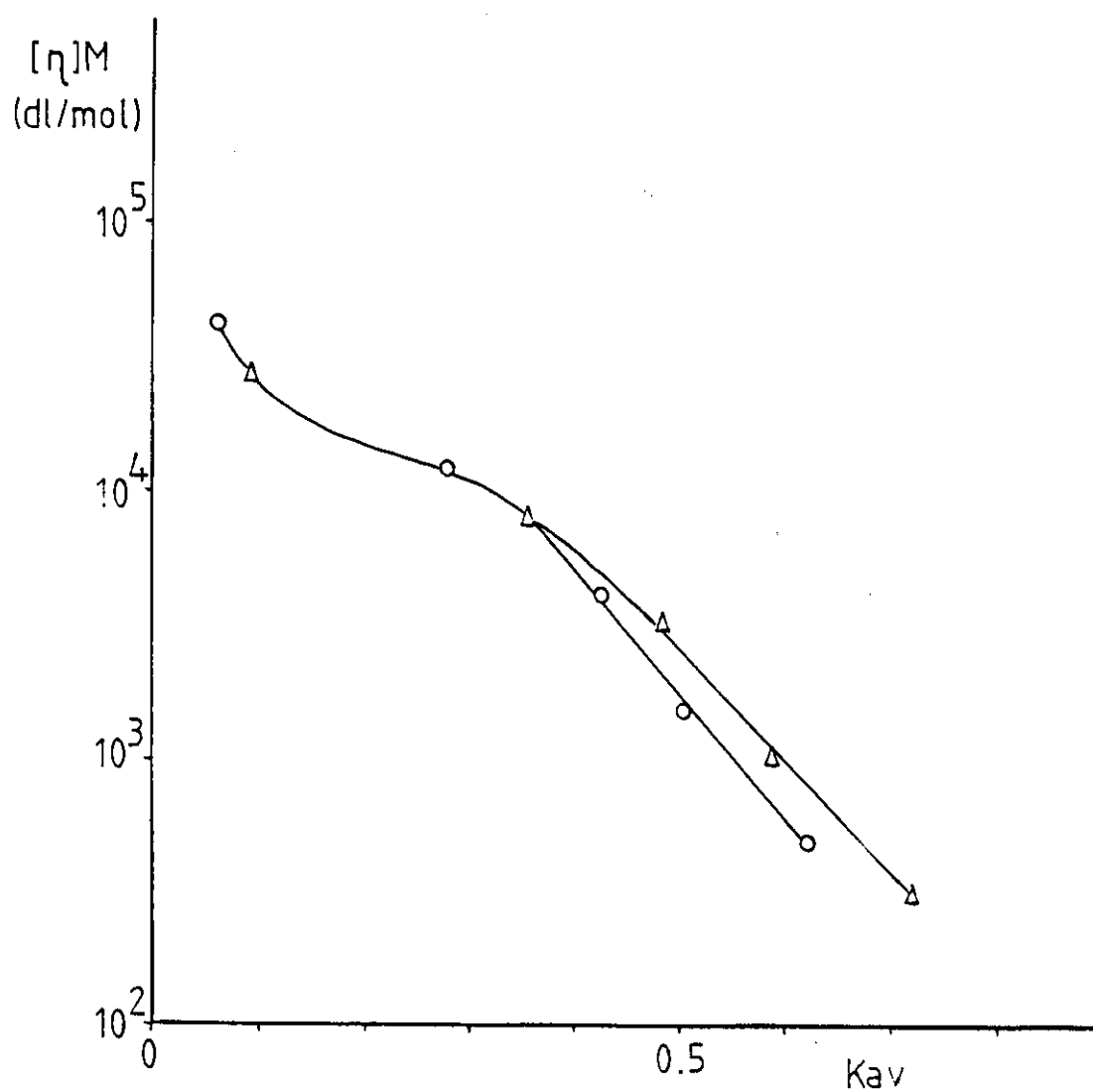


FIGURE 3.14

Hydrodynamic volume versus  $K_{av}$  calibration curves for PSA standards at room temperature, polyacrylamide column packing, serial number J56-3, flow rate 1 cm<sup>3</sup>/min, instrument 1. water ( O ); water-MeOH ( 80/20 ) (  $\Delta$  )



the curves are coincident, as expected, showing that polyacrylamide packings do not show interactive behaviour with PEG/PEO for the various water-MeOH solvent mixtures. The curve obtained for the PSA standards in figure 3.12 is coincident for both solvent systems. The increase in the pore volume of the column with water should shift the calibration for water to high elution volumes. Also, as water is a better solvent for PSA than water-MeOH mixtures the solute will display more affinity for the water-rich quasistationary phase, which would shift the calibration curve to high elution volumes. It can be deduced from figure 3.4 that PSA molecules in water will have a larger hydrodynamic volume than in water-MeOH and so the calibration curve for water will be displaced towards smaller  $V_R$ . Figure 3.14 shows the hydrodynamic volume calibration curve when the effects due to different volumes of liquid phase are corrected. It can be seen that for MW higher than  $4 \times 10^5$  a single line can be drawn through all points. As water-MeOH ( 80/20 ) is a poorer solvent for PSA than pure water, interactions with the packing are favoured[30,64,65] and for MW below  $4 \times 10^5$  in figure 3.14 the deviation between the curves indicates that secondary mechanisms appear to be taking part in the separation.

It can be concluded that both polyacrylamide and polyether based column packings are more suitable for aqueous SEC of non-ionic polymers than silica packings, showing no adsorptive behaviour, provided that the eluent is a good solvent for the polymer.



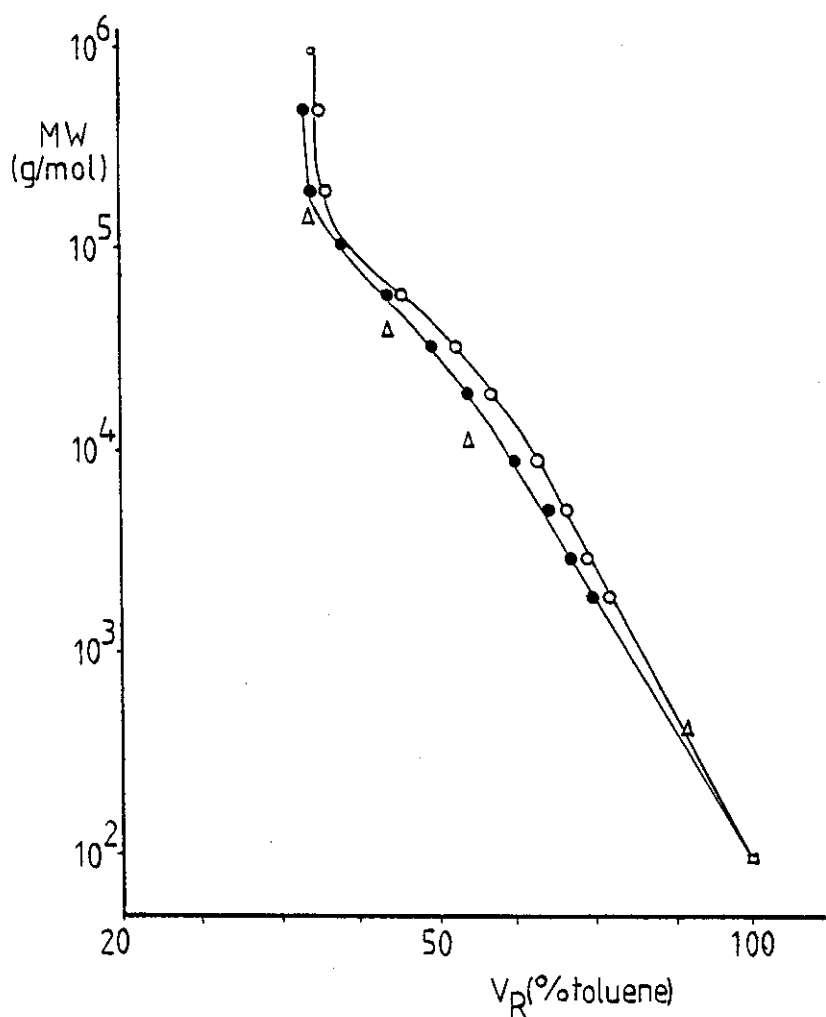
### 3.2.3 Calibration in organic solvents

Studies were performed with the solvents THF and DMF in order to examine whether polyacrylamide packings provided SEC separations with typical organic eluents. THF is a fairly polar solvent with a solubility parameter ( $\delta$ ) = 9.1 and neutralizes most of the active sites in inorganic column packings. Also, THF dissolves a large number of commercial synthetic polymers and has low viscosity permitting high SEC resolution and relatively low operating pressures[143]. DMF is a polar ( $\delta$  = 12.1) aprotic solvent which dissolves both polar and non-polar solutes[71]. The log MW versus  $V_R$  calibration curves obtained for PS standards and THF as eluent and PS and PEG/PEO standards in DMF are shown in figure 3.15. The PEG/PEO standards were strongly retained in this column with THF as eluent showing two peaks after  $V_0 + V_i$ . However, the adsorption of PEG/PEO is not a constant characteristic of polyacrylamide packings. The retention behaviour of PEG/PEO standards was not reproducible from one column to another, so that in some column packings PEG/PEO eluted within the permeation volume range whereas PEG/PEO was adsorbed with other columns. Further work is required to understand these variations which may depend on the fabrication method and/or changes to the pore surfaces during extensive use of the gels for chromatographic separations.

It can be seen in figure 3.15 that PS standards are eluted earlier in DMF than in THF. PEG standards with low MW (200 and 106) were adsorbed in the column with DMF as eluent and eluted after  $V_0 + V_i$ . High MW PS ( $9.55 \times 10^5$ ) and PEO ( $5.94 \times 10^5$  and  $9.96 \times 10^5$ ) could not be

FIGURE 3.15

Log MW Versus  $V_R$  calibration curves with THF and DMF as eluents for PS and PEG/PEO standards at room temperature, polyacrylamide column packing, serial number 8-29, flow rate 1 cm<sup>3</sup>/min, instrument 2. PS/THF (○); PS/DMF (●); PEG/PEO-DMF (Δ)



analysed with these solvents because they caused a great pressure increase in the system.

The Mark-Houwink equations for PS in THF and DMF are given by[144]:

$$[\eta] \text{ in THF} = 1.18 \cdot 10^{-4} M^{0.707} \quad (3.9)$$

$$[\eta] \text{ in DMF} = 4.65 \cdot 10^{-4} M^{0.607} \quad (3.10)$$

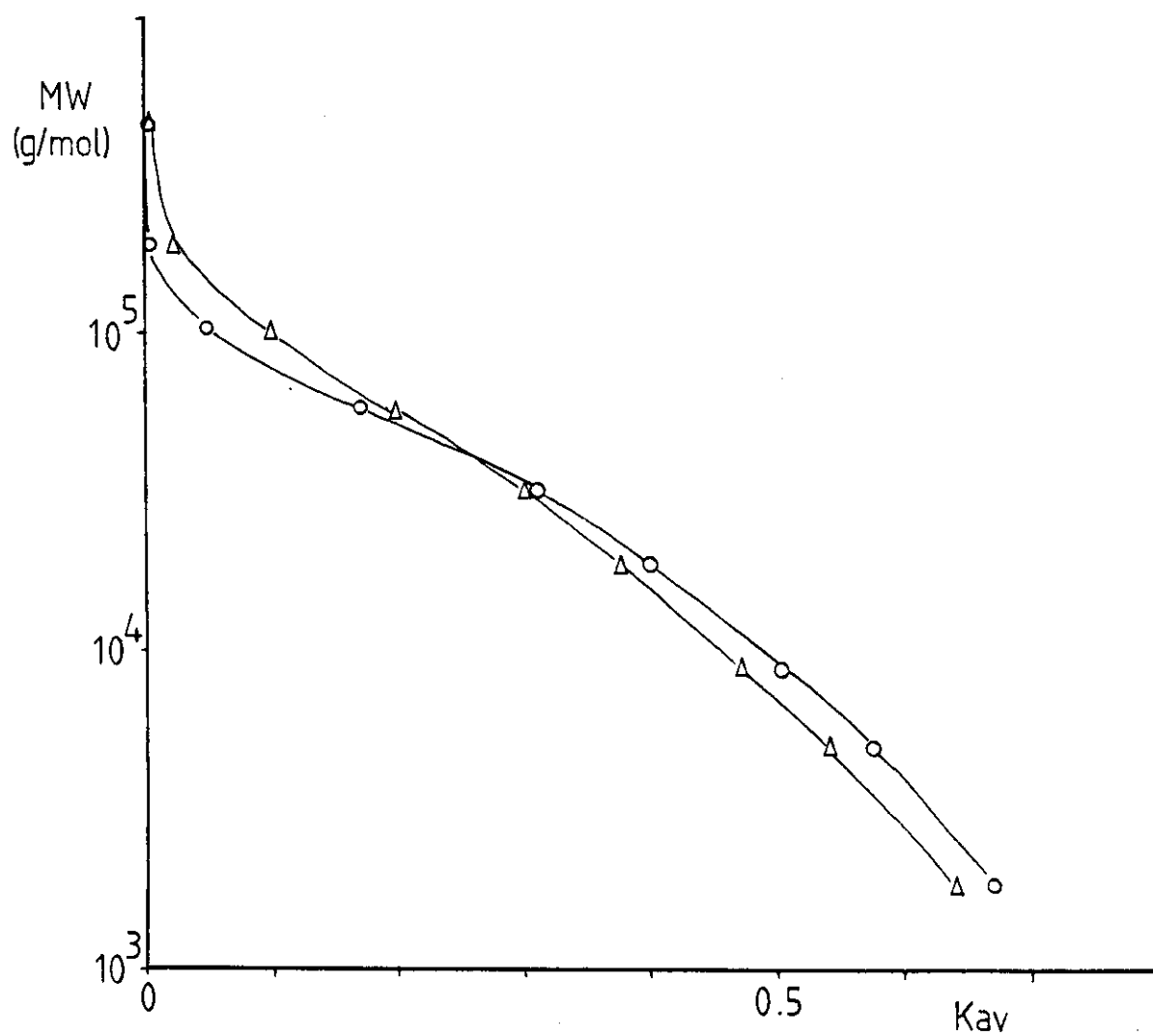
It can be seen from the exponent  $a$  in equations 3.9 and 3.10 that THF is a better solvent for PS than DMF. So, if the differences in the calibration curves for PS in figure 3.15 were only due to differences in the hydrodynamic volume of the solutes it would be expected that the  $V_R$  for PS in THF will be lower than in DMF.

There are no published data about the compatibility of polyacrylamide packings with THF and DMF, but from the results obtained in the system water-MeOH it can be supposed that DMF, being more polar, would interact better with the packing than THF. In order to compare the two different solvent systems, which might have different accessible eluent volumes, the calibration curve  $\log MW$  versus  $K_{av}$  was plotted for PS and can be seen in figure 3.16. The distribution coefficient was not calculated for PEG/PEO standards because of the uncertainty on the measurement of  $V_r$  and  $V_0$  due to adsorption of the solute and pressure increase of the system.

It can be seen in figure 3.16 that for  $MW$  below  $1.4 \cdot 10^4$   $V_R$  for PS in THF are larger than for DMF. However, for  $MW$  larger than  $1.4 \cdot 10^4$  the

FIGURE 3.16

Log MW versus  $K_{av}$  calibration curve for PS standards, at room temperature, polyacrylamide column packing, serial number 8-29, flow rate 1 cm<sup>3</sup>/min, instrument 2. PS/THF (○); PS/DMF (Δ)



opposite happens and PS in THF elutes before PS in DMF.

With PS-DVB column packings and DMF as eluent it is known that PS elutes at higher  $V_R$  than expected from a size exclusion mechanism. This behaviour is due to solute-gel interactions which influence the separation of PS in poor and theta solvents with PS-DVB gels[47]. Dubin et al[145,146] compared the elution behaviour of PS in PS-DVB packings using THF and DMF as eluents. It was found that PS elutes later in DMF than in THF and that the differences in  $V_R$  increases with decreasing MW. The divergences among the calibration curves were too great to be accounted for by differences in the dependence of molecular size on MW, especially at the lower MW range. So, the universal calibration concept was not valid and it was suggested that there was an adsorption or partitioning of the apolar PS to the apolar PS-DVB gel in a polar solvent. This effect shows an increase dependence on MW, so contact between solute and gel are expected to decrease as molecular size increases with polymer being excluded from more pores of the gel. The same group of workers[146] also studied the behaviour of three SEC systems in DMF for several polymers, including PS and PEO. It was verified that in PS-DVB column packings apolar interactions with the stationary phase lead to partitioning and retention of the solutes in order of decreasing polarity. So, PS was retained in relation to PEO. Similar effects, somewhat reduced in magnitude, were observed for the second system used, which consisted of a silanized glass column packing with DMF. For these systems the universal calibration concept was not valid. The third system, consisting of untreated glass with DMF, did not show interactive behaviour with either PEO or PS and a single curve could be drawn through the universal calibration data for PS and PEO.

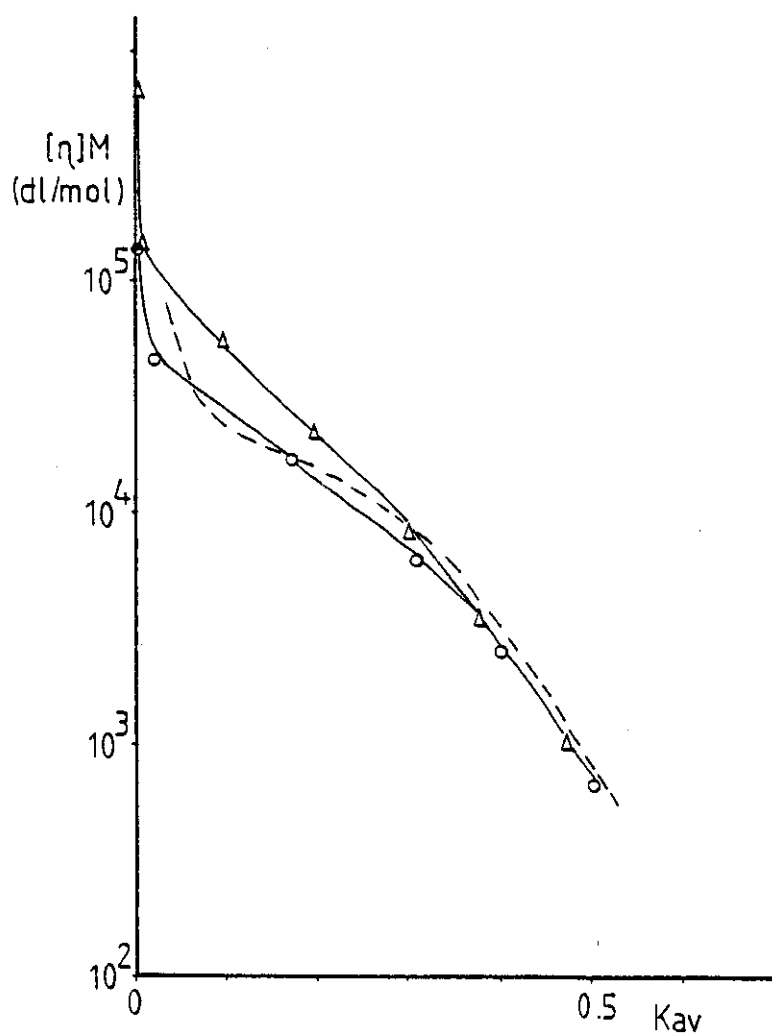
Mencer and Gallot[144] studied the elution of PS standards on column packings consisting of porous silica gel chemically modified with ether using DMF and THF as eluents. The results obtained were similar to those obtained for the polyacrylamide packing showing in figure 3.15, where PS in DMF elutes earlier than in THF. The universal calibration was not valid and it was suggested that DMF, as a very polar aprotic solvent, preferentially interacts with the gel, and so PS is "repulsed" from the gel.

The adsorption of PEG in active packings has been verified by Nakamura and Endo[147], using porous glass and THF or benzene as eluent. When PS-DVB was used as column packing, the universal calibration was valid for PS and PEG, in both THF and benzene. However, using columns packed with glass, the  $V_R$  for PS was smaller than that of PEG at the same hydrodynamic volume. The deviation of  $V_R$  from the universal calibration curve increased with increase in MW. These results were explained by the adsorption of PEG onto glass, not by end groups but mainly by adsorption sites on the polymer chain. Mori et al[148] studied PEG oligomers on PS-DVB and THF as eluent and found that  $V_R$  for PEG were smaller than for PS whilst there was no adsorptive behaviour.

Universal calibration plots  $\log [\eta]M$  versus  $K_{av}$  for PS in DMF and THF is shown in figure 3.17. The viscosity values for PS standards were calculated from equations 3.9 and 3.10 and the universal calibration curves for PS were compared with the curve obtained in figure 3.13 for PEG standards, water as eluent, where it was showed that no secondary mechanisms were influencing the separation. It can be concluded that in THF and DMF, polyacrylamide packings show some kind of interactive behaviour with PS and PEG and this kind of interaction is more similar to

FIGURE 3.17

Log  $[\eta]M$  versus  $K_{av}$  calibration curves for PS with THF (O) and DMF ( $\Delta$ ) as eluents at room temperature and 40°C respectively, polyacrylamide column packing, serial number 8-29, flow rate 1 cm<sup>3</sup>/min, instrument 2. (dotted line: water and PEG standards from figure 3.13)



the active chemically modified silica phases than to PS-DVB column packings.



### 3.3 COLUMN EFFICIENCY.

#### 3.3.1 Dispersion mechanisms

The dependence of column efficiency on the flow rate for water with polyacrylamide and polyether column packings was determined from chromatograms obtained at various different flow rates, with equations 1.20 and 1.21. The calibration curves for these columns are shown in figure 3.18. The positions of the curves were not altered by flow rate variations within the studied range.

The dependence of plate height on eluent flow rate for PEG/PEO standards with polyacrylamide and polyether columns is shown in figures 3.19 and 3.20 respectively. The results obtained for the PEG660000 standard are different from what was expected for totally excluded polymers, which are known to give little variation of  $H$  with flow rate[91].

The calculation of  $H$  via equation 1.23 demands the knowledge of  $h_p$  ( see figure 1.2 ) in order to measure  $w_{1/2}$ . However, as peaks obtained for excluded polymers are usually deformed, very often  $h_p$  does not correspond to the maximum of the peak, leading to some doubt on which value should be considered as  $h_p$ . It is probably this uncertainty on the measurement of  $h_p$ , and so on  $w_{1/2}$ , that causes unreliable  $H$  values for excluded polymers and therefore, the results for PEG660000 were not used in this work. The results obtained for ethanol and permeating polymers are consistent with those previously obtained for other types of packings[88,90,91]. Ethanol, which is a totally permeating solute gives little variation of  $H$  with the flow rate. For the standards PEG998, PEG4820 and PEG9230, the ability of the column to resolve the peaks is increased as the flow rate decreases.

FIGURE 3.18

Log MW versus  $V_R$  calibration curve for PEG/PEO standards in water as eluent at room temperature, flow rate 1 cm<sup>3</sup>/min, instrument 1. polyacrylamide column, serial number J10-3 (○); polyether column (Δ); ethanol in both columns (●)

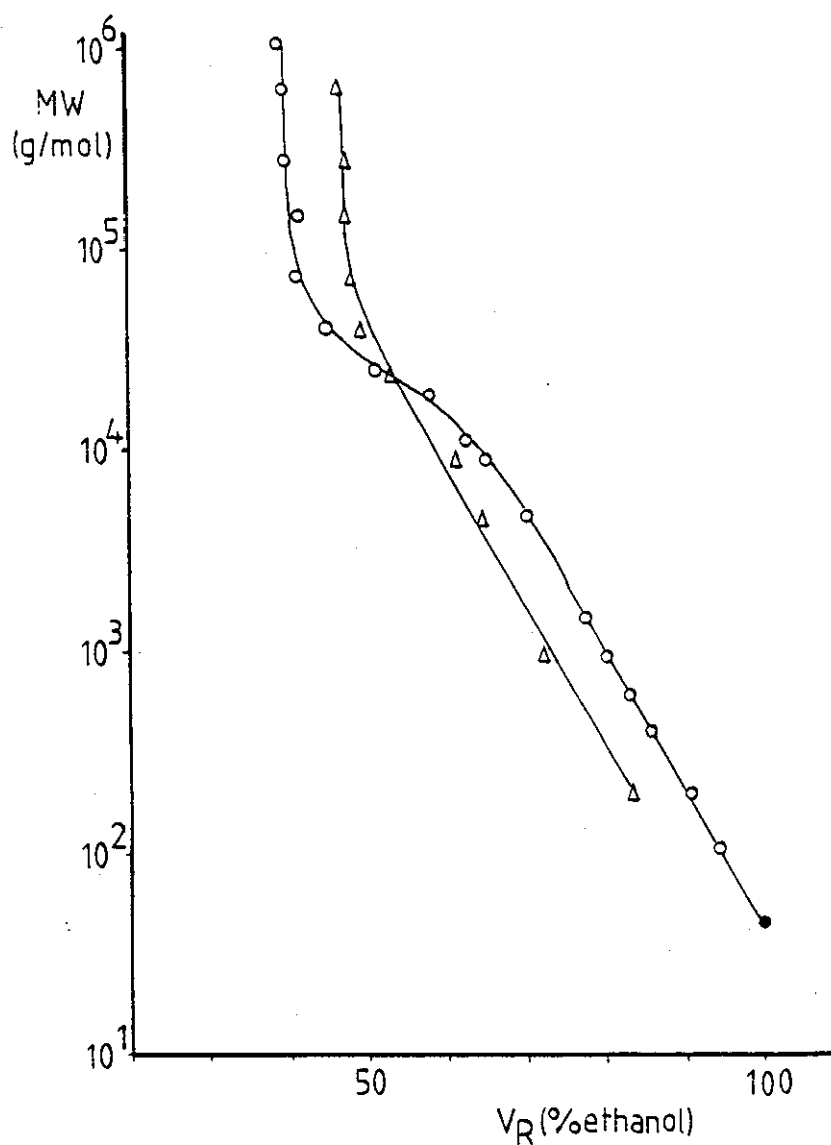


FIGURE 3.19

Dependence of plate height on eluent flow rate for PEG/PEO standards on polyacrylamide column packing, serial number J70-3, instrument 1. ethanol (○); PEG200 (Δ); PEG998 (□); PEG4820 (●); PEG9230 (▲); PEG660000 (■).

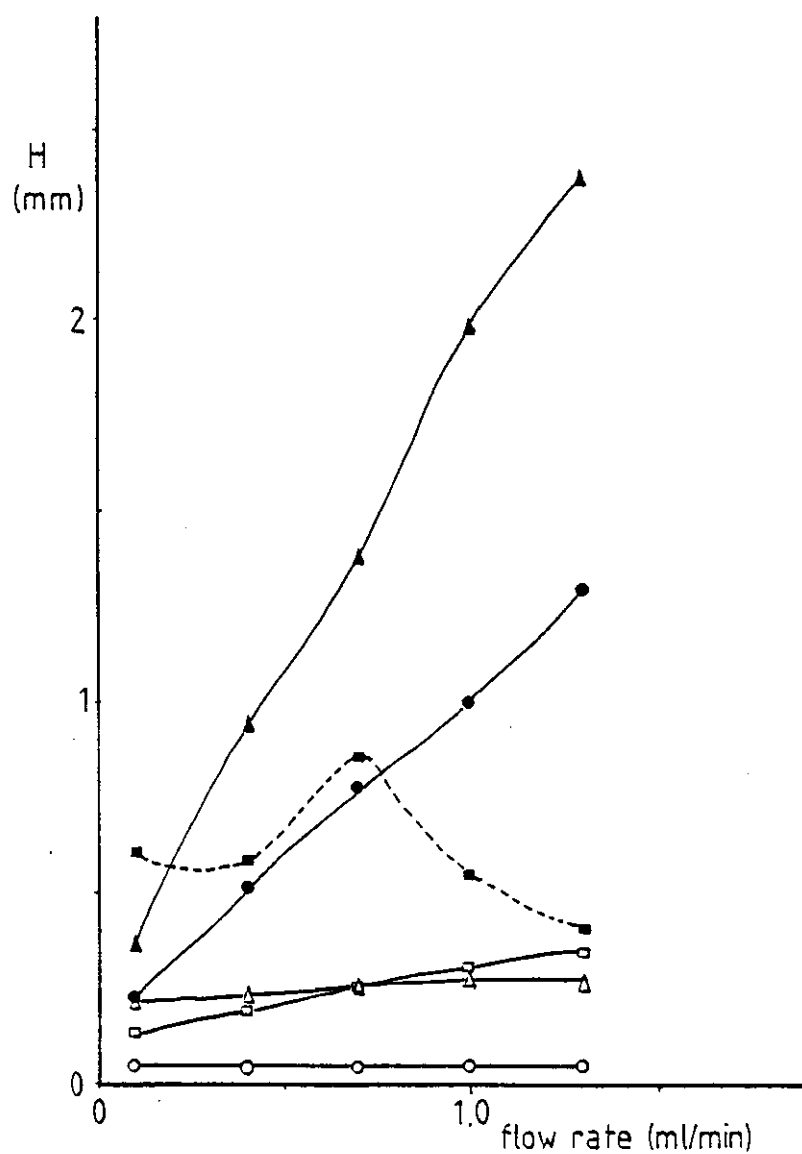
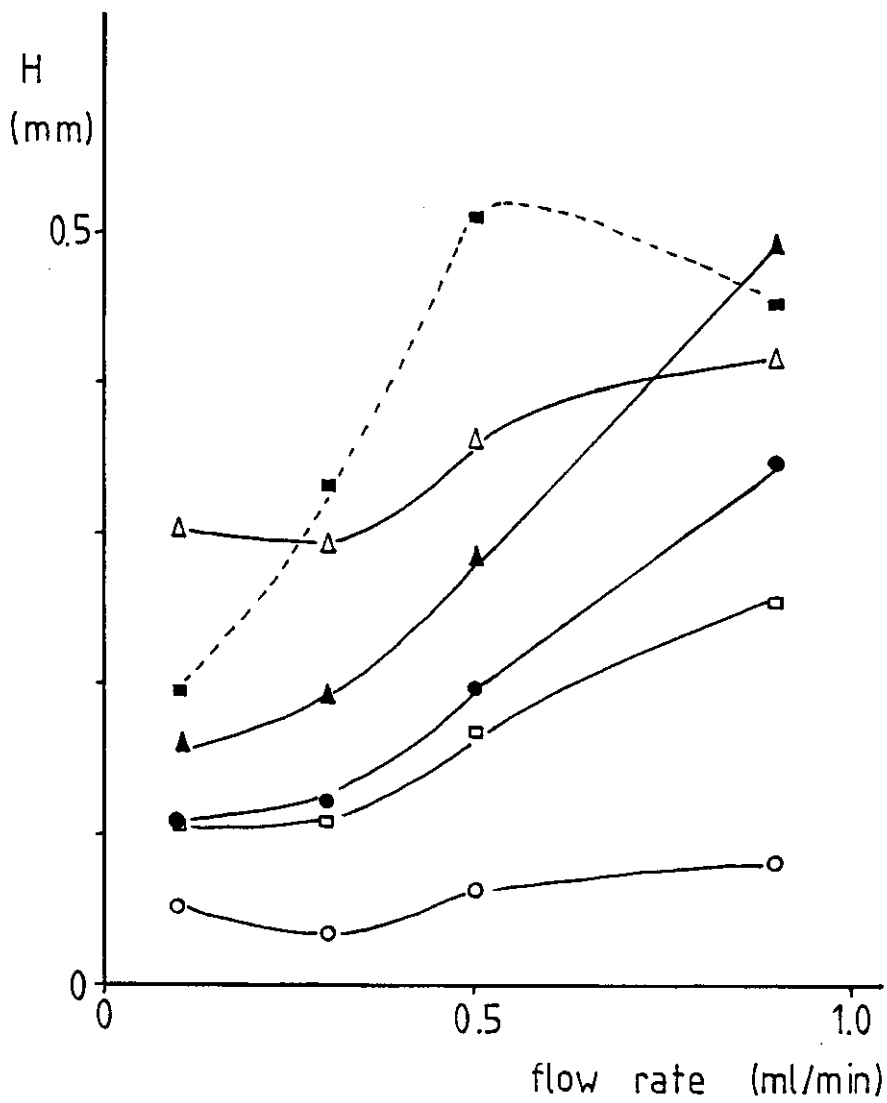


FIGURE 3.20

Dependence of plate height on eluent flow rate for PEG/PEO standards on a polyether column packing. ethanol (○); PEG200 (△); PEG998 (□); PEG4820 (●); PEG9230 (▲); PEG660000 (■)



This effect can be predicted by figure 3.19 and 3.20, where as  $H$  decreases the column efficiency increases and is further illustrated by the separation with the polyacrylamide column packing, at five different flow rates, of one PEO and four PEG standards in figure 3.21. The peak at the left, with the smallest  $V_R$  is due to the standard PEO660000 followed by the peak due to both PEG4820 and 9230 standards which elute together at all flow rates. Only at 0.1 cm<sup>3</sup>/min there is some resolution between the peaks and PEG9230 appears as a shoulder of the PEG4820 peak. As the flow rate increases, the peaks due to the PEG4820 and 9230 standards merge completely and the other standards appear in order of decreasing MW up to the high  $V_R$  peak which is ethanol, the internal standard.

The column efficiency can also be increased by increasing the column temperature[149]. This effect can be seen in figure 3.22 for the polyacrylamide column packing with a calibration curve  $\log MW$  versus  $V_R$  shown in figure 3.23 where the separation of a "cocktail" sample consisting of the PEO594000, PEO18000, PEG4820, PEG998 and PEG200 standards is displayed. The theoretical plate number obtained with ethanol was increased from 19900 to 22200 plates/m as the column was heated from 24 to 60°C. Improvements in column efficiency when the column is heated are usually caused by the decrease of solvent viscosity[149]. The void volume of the column remained the same as can be seen by the  $V_R$  of the excluded polymer PEO594000. The other solutes eluted in order of decreasing MW and the peaks were displaced towards higher  $V_R$  as the temperature was increased. As hot water is a nonsolvent for PEO/PEG[49], the displacement of  $V_R$  to larger values can be interpreted as the PEG/PEO decreasing in size as the solvent is poorer and so, penetrating more pores. However, as the  $V_R$  of ethanol is also increased, the pore volume of the column should also

FIGURE 3.21

Effect of flow rate on the ability of the polyacrylamide column packing, serial number J70-3, to separate a cocktail of PEG/PEO standards consisting of PEG200 ( e ) PEG998 ( d ), PEG4820 ( c ), PEG9230 ( b ), PEO660000 ( a ) and ethanol ( f ) ( 0.05% each ) in water, instrument 1.

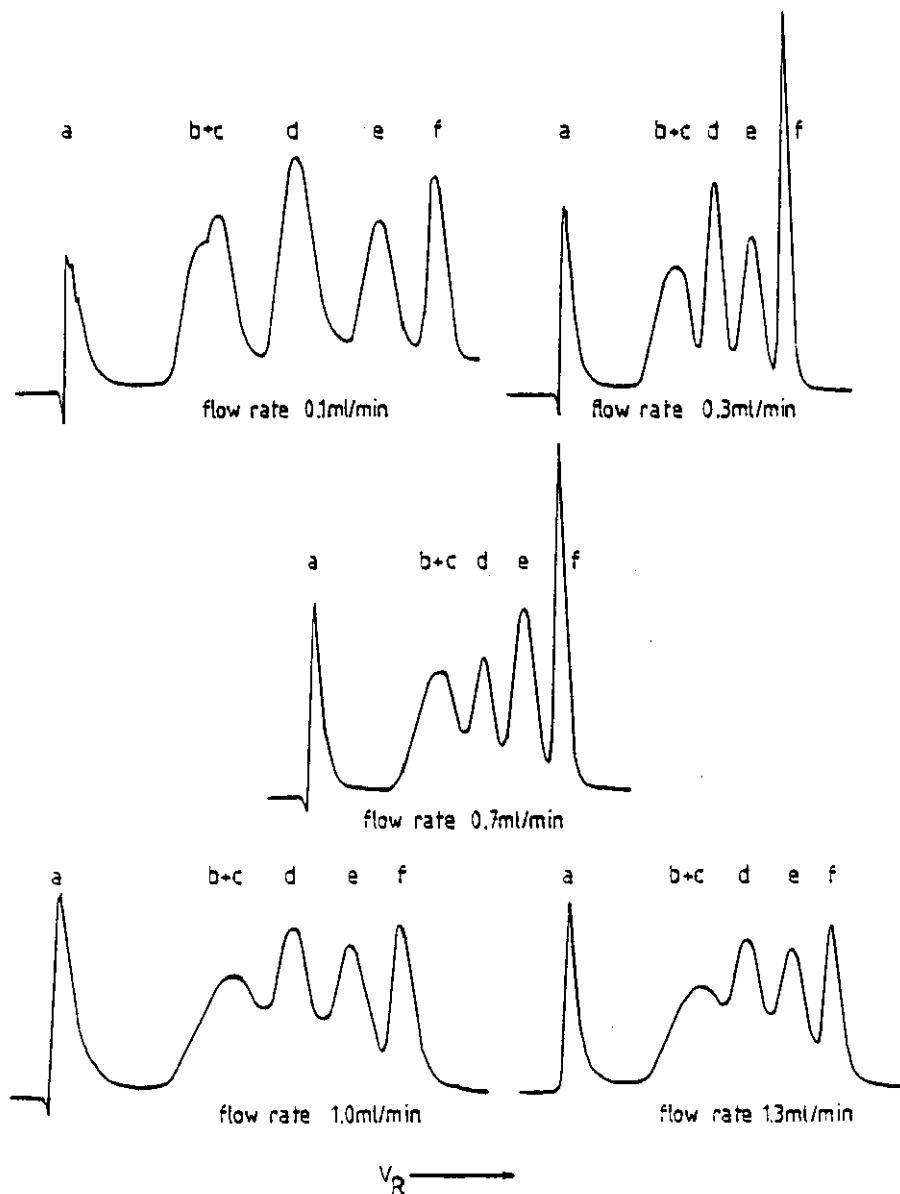


FIGURE 3.22

Effect of temperature on the separation of a cocktail sample of PEO594000, PEO18000, PEG4820, PEG998, PEG200 and ethanol in polyacrylamide column packing, serial number 6-7 and Water as eluent, flow rate 1 cm<sup>3</sup>/min, instrument 2.

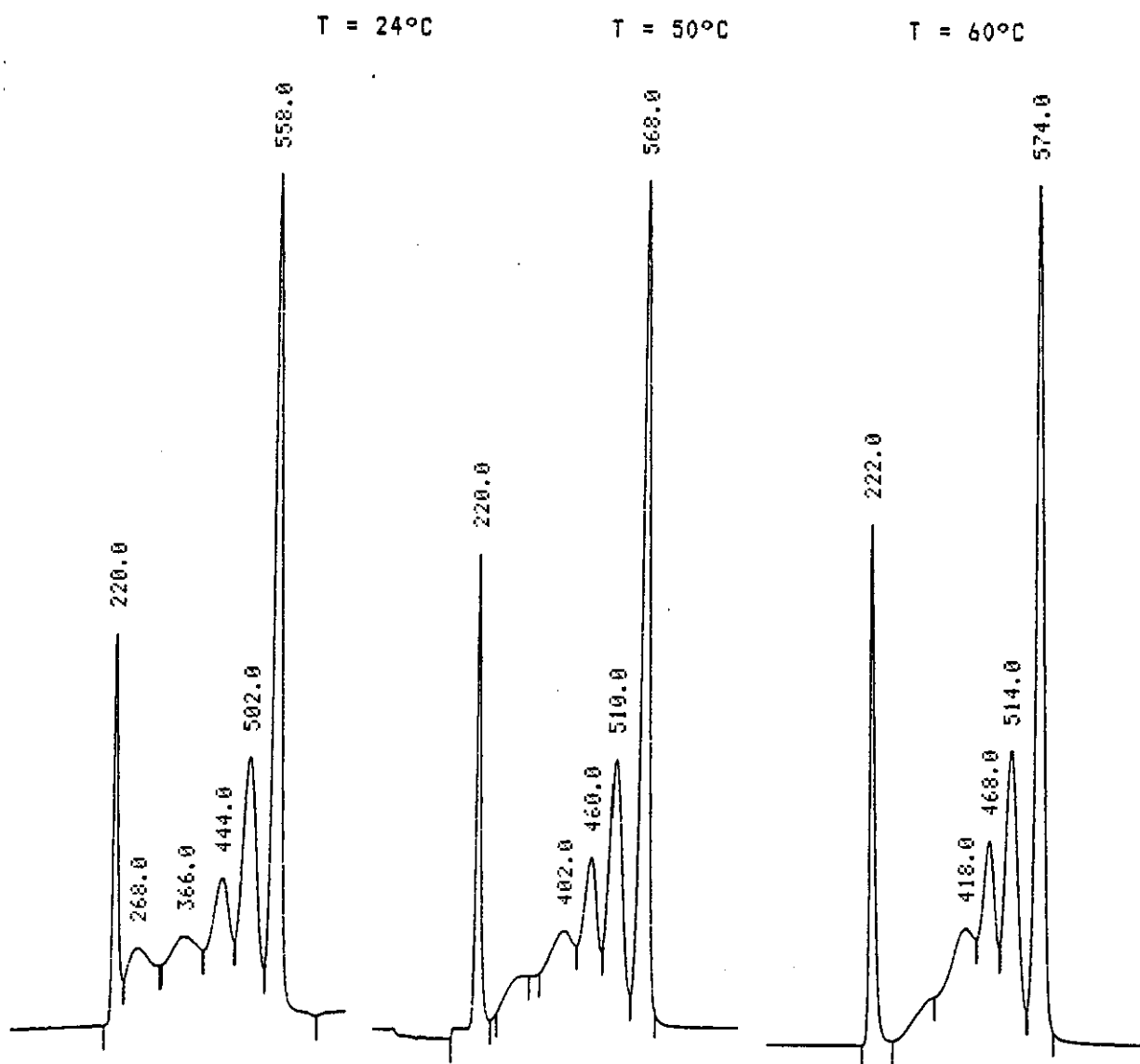
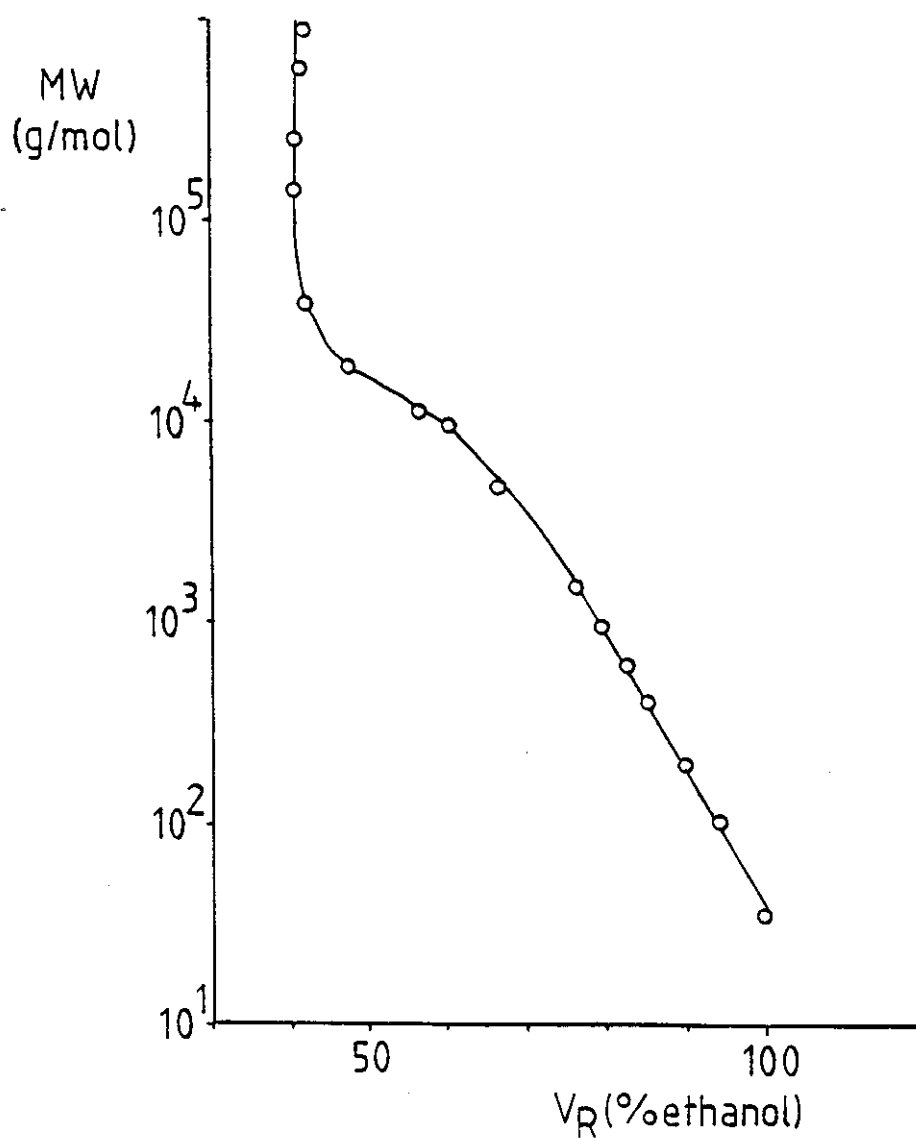


FIGURE 3.23

Calibration curve log MW versus  $V_R$  for PEG/PEO standards in water as eluent, at room temperature, for polyacrylamide column packing, serial number 6-7, flow rate 1 cm<sup>3</sup>/min, instrument 2.





be increasing as the column packing is heated. So, for the standards PEG18000, PEG4820, PEG998 and PEG200 the combination of two effects should be causing the displacement of the peaks towards high  $V_R$  as the column temperature is increased, i.e. the decrease in the hydrodynamic volume of the polymer and the increase of pore volume.

It follows from the theory of solute dispersion mechanisms discussed in section 1.4.2 that the value of  $H$  determined from an experimental chromatogram for a permeating polymer will contain a contribution from the polydispersity of the polymer. Dawkins et al[90,92] suggested that the true polydispersity of the polymers under investigation may be evaluated with equation 1.28. The first term in equation 1.28 arises from eddy diffusion due to solute dispersion in the mobile phase, the second term arises from solute dispersion owing to mass transfer in the stationary phase and the third term is the contribution of the polymer polydispersity. So, from a plot of  $H$  versus eluent flow velocity, the polymer polydispersity and the diffusion coefficient of the solute in the stationary phase can be evaluated as long as the eddy diffusion term is known from independent measurement. Figures 3.24 and 3.25 show the dependence of experimental plate height on eluent flow velocity for the polyacrylamide and polyether columns respectively. The plot for each solute in figures 3.24 and 3.25 exhibits reasonable linear behaviour, and it can be verified that the slopes of the curves depend on the MW of the solutes. In terms of equation 1.28, the explanation for this dependence of slope on MW is the decrease in diffusion coefficient for longer chains (which will have higher mass transfer dispersion)[150]. It can be seen in figures 3.24 and 3.25 that the regression lines for the standards PEG4820 and PEG9230 show a larger slope for polyacrylamide packings than

FIGURE 3.24

Dependence of experimental plate height on eluent flow velocity for polyacrylamide column packing, serial number J70-3, in water, instruments 1 and 2. ethanol ( O ); PEG200 (  $\Delta$  ); PEG630 (  $\square$  ); PDEG (  $\blacktriangle$  ); PEG998 (  $\nabla$  ); PEG 4820 (  $\bullet$  ); PEG9230 (  $\blacksquare$  )

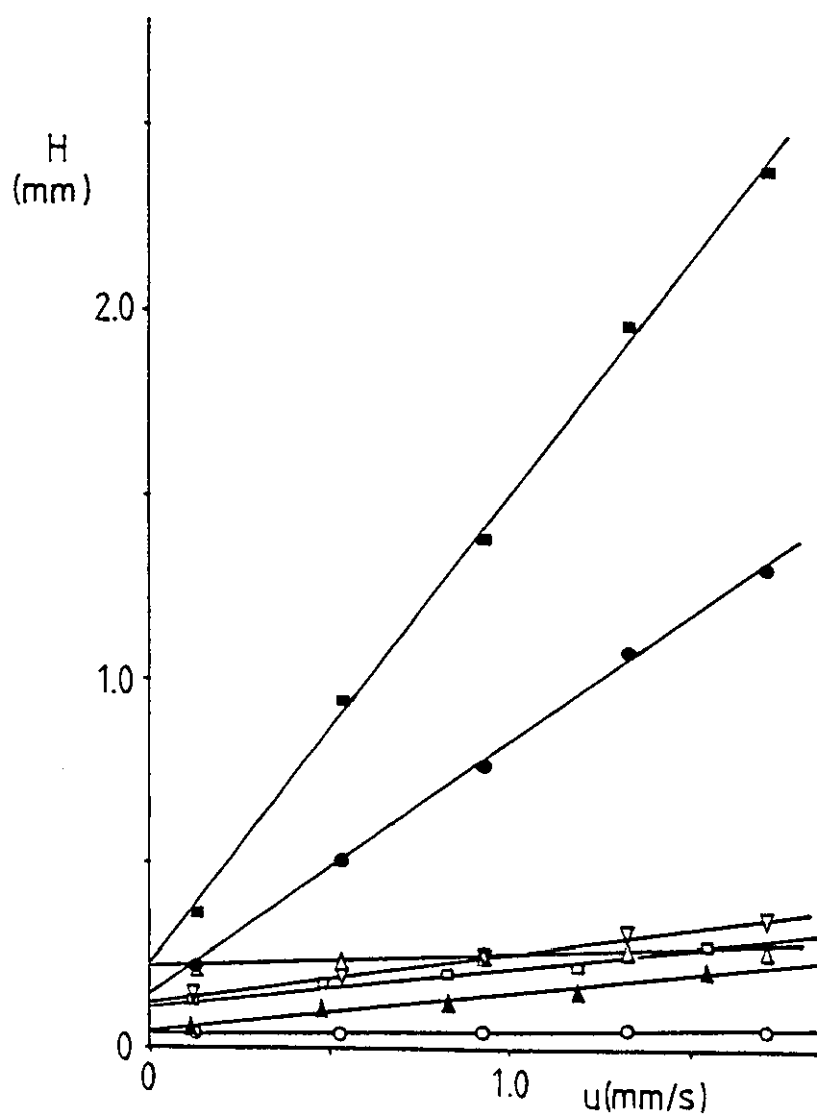
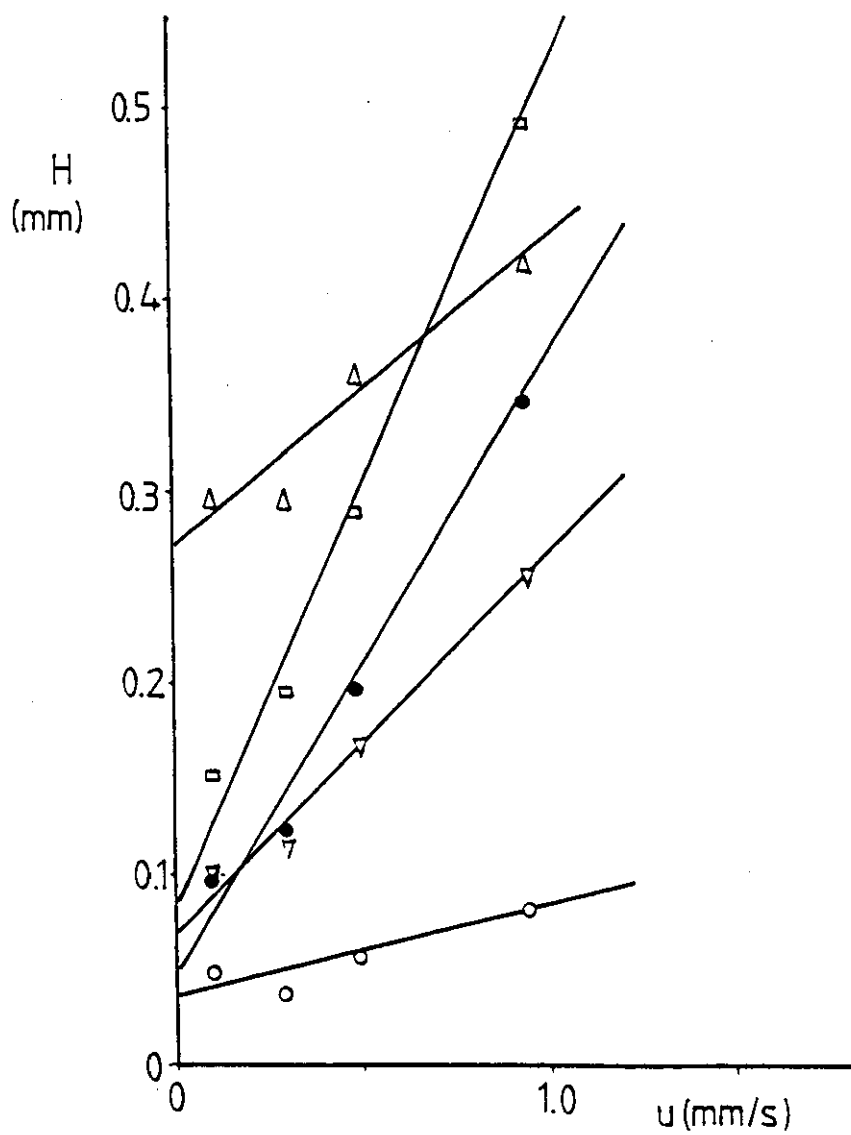


FIGURE 3.25

Dependence of experimental plate height on eluent flow velocity for polyether column packing, in water, instrument 1, Ethanol (○); PEG200 (△); PEG998 (▽); PEG 4820 (●); PEG9230 (□)



for polyether packings while for PEG998 and PEG200 the slope is larger for polyether packings. The results obtained for the slope of the regression lines of PEG4820 and PEG9230 can be interpreted in terms of the predominance of dispersion caused by mass transfer in the stationary phase for polyacrylamide packings, in relation to polyether packing. However, the results obtained for the PEG998 and 200 are not easily interpreted because, as Dawkins et al[91,150] pointed out, for small molecules the dispersion due to longitudinal diffusion ( see equation 1.26 ) is important and attempts to interpret the dispersion mechanisms for small molecules in terms of equation 1.28 are questionable.

### 3.3.2 Diffusion coefficient

Results for  $D_s$  calculated from figure 3.24 and 3.25 are given in table 3.3. The calculation with equation 1.28 involved the determination of the slope  $D_2$  for each solute from the calibration curves in figure 3.18.

The values for the diffusion coefficient (  $D_m$  ) shown in table 3.3 were obtained from figure 3.26 where literature values for the diffusion coefficient of PEG in water were plotted against MW. These literature values of the diffusion coefficient were assumed to be the diffusion coefficient of PEO in free solution at infinite dilution. The derived data for  $D_s$  in table 3.3 for both polyacrylamide and polyether column packings were much less than the literature values of  $D_m$ . Errors in the procedure for determining  $D_s$  may result from the choice of the value for  $d_p$ , since  $dp^2$  appears in the second term in equation 1.28. However, both column

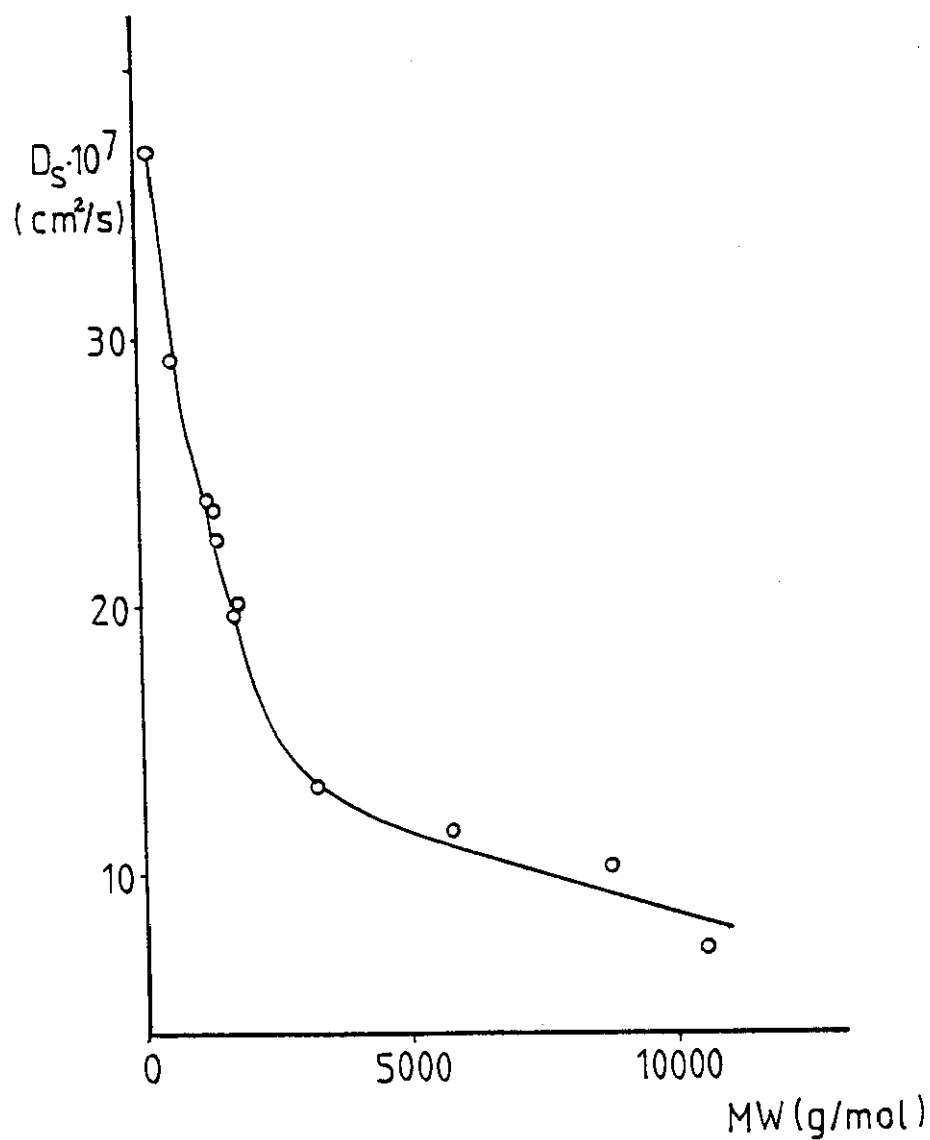
TABLE 3.3

Diffusion coefficients of PDEG and PEG standards for polyacrylamide ( PA ) and polyether ( PE ) column packings.

SOLUTE	$D_m \cdot 10^7$ ( $\text{cm}^2/\text{s}$ )	$D_s \cdot 10^7$ ( $\text{cm}^2/\text{s}$ )		$D_s/D_m$	
		PA	PE	PA	PE
PEG200	39.0	2.13	0.862	0.055	0.022
PEG630	31.4	0.891	-----	0.028	-----
PDEG	30.8	0.782	-----	0.025	-----
PEG998	26.5	0.517	0.650	0.020	0.024
PEG4820	11.9	0.119	0.356	0.010	0.030
PEG9230	8.9	0.063	0.232	0.007	0.026

FIGURE 3.26

Diffusion coefficients for PEO versus MW in water[49].



packing materials used in this work are claimed to have narrow particle size distribution:  $10 \pm 2 \mu\text{m}$  for the polyacrylamide[25] and  $13 \pm 2 \mu\text{m}$  for the polyether[151] column packing. For polyacrylamide packings as the MW of the polymer is reduced,  $D_s/D_m$  increases ( see table 3.3 ) in agreement with results found by Knox and McLennan[152], van Kreveld and van den Hoed[153] and Dawkins and Yeadon[91,150] for porous silica packings in conditions specified in table 3.4, where the values for  $D_s/D_m$  found in this work and the literature values are compared. For polyether packings, as it can be seen in table 3.3,  $D_s/D_m$  is almost constant throughout the investigated MW range. Giddings et al[154] found the same trend for porous glass packings, in conditions specified in table 3.4. Comparing the values for  $D_s/D_m$  obtained by other workers in table 3.4 with the values found in this work it can be seen that the latter values are lower than the literature values, suggesting that PEG in water in both polyacrylamide and polyether column packings is subject to restricted diffusion. From the literature data obtained with PS and proteins[91,150] it is expected that the mobile phase dispersion of PEG solutes having a value of  $D_m$  around  $10^{-6} \text{ cm}^2\text{s}^{-1}$  will be dominated by eddy diffusion because mobile phase dispersion mechanisms which depend on  $u$ , e.g. longitudinal molecular diffusion and mass transfer, may be neglected for polymeric solutes having low values of  $D_m$  with  $u$  in the range  $1-3 \text{ mm s}^{-1}$  ( see PEG4820 and PEG9230 in table 3.3 ).

Consequently, it appears that restricted diffusion of solutes during mass transfer into the stationary phase is higher for polyacrylamide and polyether packings than for silica based packings. Also, it can be deduced that this restricted diffusion of solutes during mass transfer is higher for polyacrylamide than for polyether column packings.

TABLE 3.4

Comparison of  $D_w/D_m$  values.

packing material	diameter ( $\mu\text{m}$ )	solute type	MW range	$D_w/D_m$	reference
porous silica	7.5	PS	2000-33000	0.059-0.167	[152]
porous glass	44-74	PS	<5000	0.167	[154]
porous	75-124	PS	20000-160000	0.12-0.31	[153]
porous silica	8	PS proteins	3600-35000 $10^4$ - $10^5$	0.082-0.144 0.075-0.096	[91,150]
polymeric	10	PEG	200-9230	0.006-0.055	this work



### 3.3.3 Polydispersity

Two different approaches have been used for the determination of the polydispersity of polymers corrected for axial dispersion. They will be discussed separately and the results obtained from both approaches will be compared together later.

In the first approach equation 1.28 is used to evaluate the true polydispersity of the solutes studied in figure 3.24 and 3.25 and the first term for mobile phase dispersion is estimated by three different methods. Two methods have been considered previously[91,150]. First, it is assumed  $\lambda = 1.0$ , when the eddy diffusion contribution to  $H$  will be  $20 \mu\text{m}$  for polyacrylamide packings and  $26 \mu\text{m}$  for the polyether packing. Second, it is assumed that the mobile phase dispersion of a nonpermeating polymer is close to the value of  $H$  for ethanol which is not polydisperse. In this case the eddy diffusion contribution in polyacrylamide packings will be  $54 \mu\text{m}$  corresponding to the average value of  $H$  for ethanol for  $u$  in the range  $0.1 - 1.8 \text{ mm/s}$ . For the polyether packing as the curve obtained for ethanol shows a minima at  $H = 34.9 \mu\text{m}$ , this value will be attributed to the contribution from eddy dispersion. A third method is available for polyacrylamide packings involving the monodisperse solute PDEG. Extrapolation of the data for PDEG in figure 3.24 to  $u = 0$  will give an intercept which arises solely from dispersion due to eddy diffusion, and it is evident in figure 3.24 that this intercept is very close to values of  $H$  for ethanol. Values of the true polydispersity for PEG standards are given in table 3.5, where it can be seen that the values obtained with the

TABLE 3.5

Polydispersities of PEG standards.

standard	$\bar{M}_w/\bar{M}_n$	$[\bar{M}_w/\bar{M}_n]_T$	$[\bar{M}_w/\bar{M}_n]_T$	$[\bar{M}_w/\bar{M}_n]_T$	$[\bar{M}_w/\bar{M}_n]_T$	$[\bar{M}_w/\bar{M}_n]_T$
PEG630	1.080	1.041	1.061	1.048	-----	-----
PEG998	1.060	1.029	1.047	1.035	1.016	1.020
PEG4820	1.040	1.038	1.50	1.041	1.001	1.001
PEG9230	1.080	1.033	1.038	1.034	1.016	1.019

a - SEC characterization with crosslinked PS gels

b - determined with polyacrylamide column packing and equation 1.28 using eddy diffusion term given by plate height for ethanol

c - determined with polyacrylamide column packing and equation 1.28 using  $\lambda = 1$  in eddy diffusion term

d - determined with polyacrylamide column packing and equation 1.28 using eddy diffusion term given by plate height for PDEG extrapolated to  $u = 0$

e - determined with polyether column and equation 1.28 using eddy diffusion term given by plate height for ethanol

f - determined with polyether column and equation 1.28 using  $\lambda = 1$  in eddy diffusion term.

polyether packing are slightly lower than those obtained with a polyacrylamide packing, which are in reasonable agreement with polydispersity results obtained by SEC characterization of PEG standards in THF with crosslinked PS gels[125].

The second approach for determining polydispersity corrected for axial dispersion is based on equation 1.30, suggested by Hamielec[95], which permits the determination of the average MW of polymers, provided the dispersion factor  $h$  and the slope of the calibration curve are known. As  $h$  varies with MW[96], it is important to have the dependence of  $h$  with MW throughout the studied range. For monodisperse solutes,  $h$  can be calculated directly from the chromatogram via equation 1.31 since the only factor responsible for the peak spreading is axial dispersion. When there are no monodisperse solutes available, one of the approaches that can be used to obtain information on  $h$  is to analyse by SEC a standard with known  $\bar{M}_w$  or  $\bar{M}_n$  and find the MW values uncorrected for broadening ( $\bar{M}_w(\infty)$  and  $\bar{M}_n(\infty)$ ). Then, with equation 1.30 and a knowledge of the slope of the calibration curve,  $h$  can be estimated.

Two polymer standards, PEG18000 and PSA12200, specified in table 2.1 were known to have  $\bar{M}_w$  values of 18000 and 12200 respectively[125]. These standards were analysed by SEC and the  $\bar{M}_w$  uncorrected for broadening was determined. With the use of equation 1.30,  $h$  could be estimated for PEG18000 and PSA12200. Three monodisperse solutes ( ethanol, sucrose and raffinose ) were analysed by SEC. The width of the peak was measured at  $h_{0.607}$  ( see figure 1.2 ), and by the use of equation 1.31  $h$  could be estimated. The dependence of  $h$  on  $V_R$ , for the five solutes available for this study is shown in figure 3.27. The calibration curve  $\log MW$  versus  $V_R$  for PEG/PEO and PSA is shown in figure 3.28. The standards PEG630,

FIGURE 3.27

Dependence of the dispersion factor on  $V_R$  for polyacrylamide column packing, serial number JS6-3 in water as eluent at room temperature, flow rate 1 cm<sup>3</sup>/min, ethanol (○); sucrose (Δ); raffinose (▽); PSA12200 (□); PEO18000 (●).

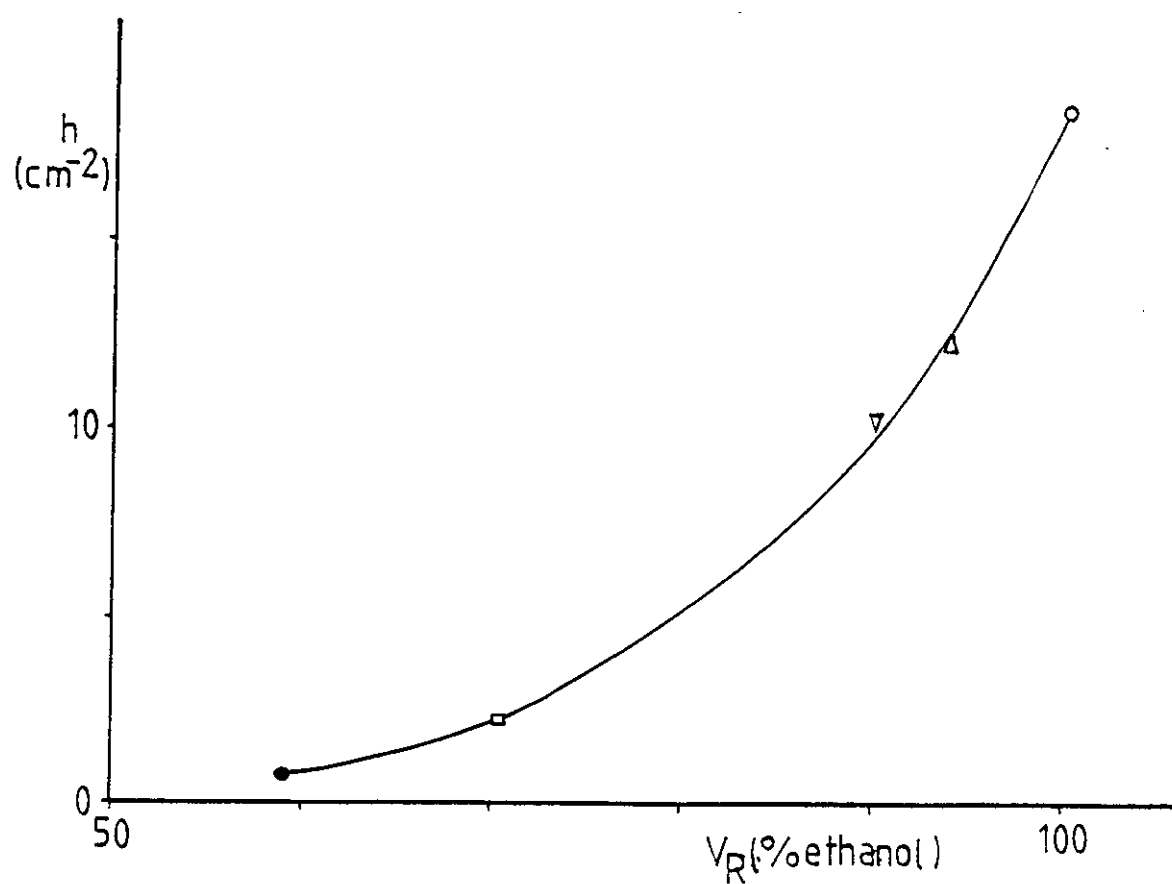
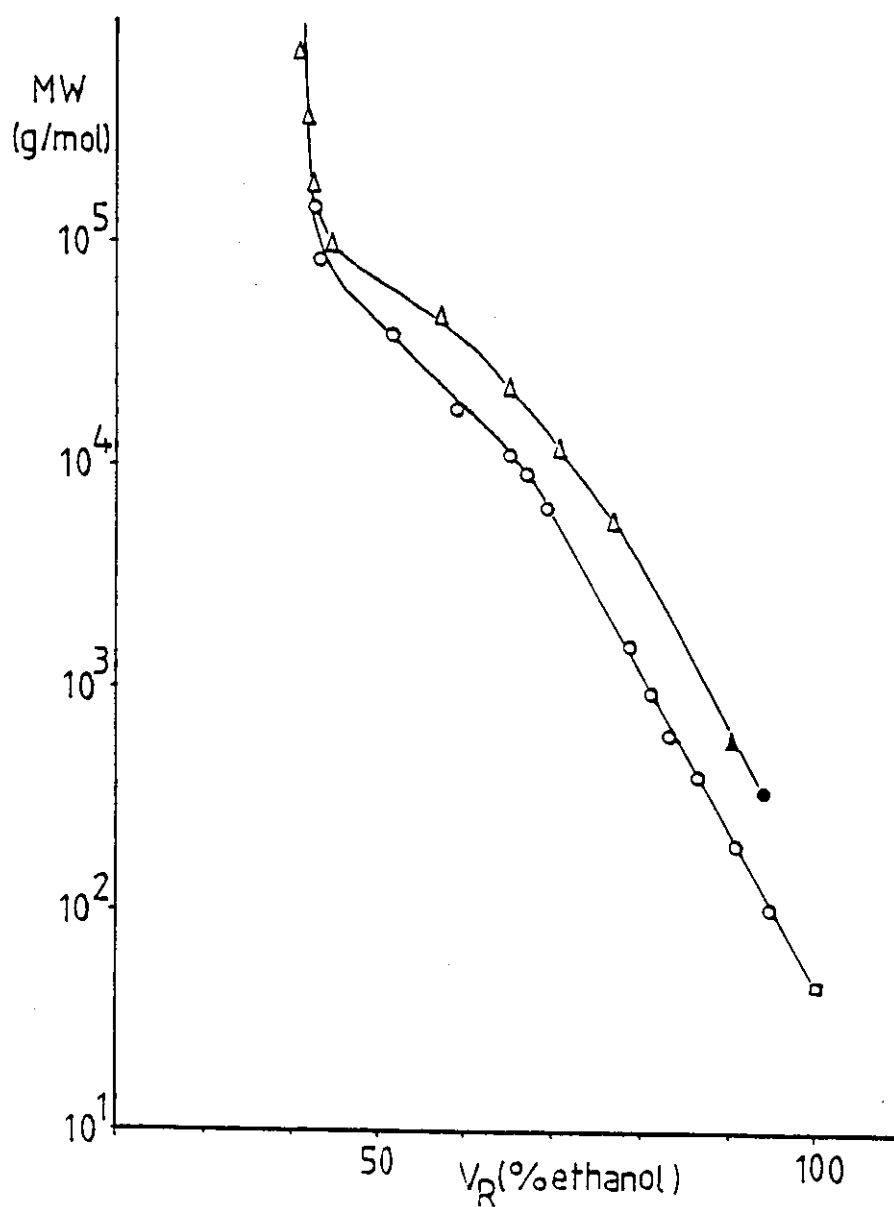


FIGURE 3.28

Log MW versus  $V_R$  calibration curve for polyacrylamide column packing, serial number J56-3 using water as eluent at room temperature, flow rate 1 cm<sup>3</sup>/min. PEG/PEO (○); PSA (Δ); raffinose (▲); sucrose (●); ethanol (◻).



PEG1580, PEG4820, PEG9230 and PEG11250 were then analyzed with this column and the values obtained for the average molecular weight were corrected for axial dispersion with equation 1.30 using the values of  $h$  from figure 3.27 and are listed in table 3.6. The values obtained for  $\bar{M}_n$  for the standards PEG1580 and 4820 are higher than  $\bar{M}_w$ . However, considering the error inherent to SEC as 5% these values can be considered as very similar, for a value for polydispersity near one. The value of  $\bar{M}_n$  obtained for the standard PEG9230 is very low and the polydispersity very high, and this would appear to arise because the chromatogram obtained for this standard displayed a shoulder in the low MW side of the peak. Comparing the polydispersity values obtained after equation 1.30 was applied with the catalogue values, it can be seen that the corrected values of polydispersity are much closer to the catalogue values than the uncorrected values. However, the  $\bar{M}_w$  values obtained after correction are very low, suggesting that this approach is not providing more accurate values for the average molecular weights. The successful use of equation 1.30 depends very much on the use of a reliable value of  $h$ . The effect of the accuracy of the  $h$  value on the average MW and polydispersity of the standard PEG11250 is shown in table 3.7 where  $h$  values found for ethanol, sucrose, raffinose, PSA12200 and PED18000 were employed in equation 1.30. It can be seen that a wide variety of values for  $\bar{M}_w$ ,  $\bar{M}_n$  and  $d$  are obtained, depending on the chosen value for  $h$  and that, as the value of  $h$  decreases, the polydispersity also decreases, tending to 1.07, the catalogue polydispersity value for this standard. So, the availability of a well characterized monodisperse polymer, PDEG (MW 678), made possible to verify the use of equation 1.30 for correcting MW averages of polymers. This polymer was analyzed with another polyacrylamide column (serial number

TABLE 3.6

Comparison of average molecular weights and polydispersities of PEG standards obtained with polyacrylamide column packing corrected ( t ) and uncorrected (  $\infty$  ) for axial dispersion via equation 1.30

standard	$\bar{M}_w$		$\bar{M}_n$		d		
	( $\infty$ )	( t )	( $\infty$ )	( t )	( $\infty$ )	( t )	catalogue
PEG630	738	687	631	677	1.17	1.01	1.08
PEG1580	1582	1429	1319	1460	1.20	1.00	1.06
PEG4820	5240	4369	3747	4498	1.40	1.00	1.04
PEG9230	8807	7570	4756	5532	1.85	1.37	1.08
PEG11250	11319	10369	7711	8417	1.47	1.23	1.07

TABLE 3.7

Effect of different  $h$  values on the average molecular weights of PEG11250, corrected for axial dispersion by the use of equation 1.30

$h$ ( $\text{cm}^{-2}$ )	$\bar{M}_w$	$\bar{M}_n$	$d$
uncorrected	11319	7711	1.47
18.9( ethanol )	11247	7759	1.45
12.5( sucrose )	11212	7784	1.44
10.3( raffinose )	11188	7800	1.43
2.39( PSA12200 )	10769	8105	1.33
1.36( from the curve )	10369	8415	1.23
0.83( PED18000 )	9805	8901	1.10



J70-3 ) and the log MW versus  $V_R$  calibration curve for this column can be seen in figure 3.18. The value of  $h$  obtained by the use of equation 1.30 could not be compared with the  $h$  values in figure 3.27 because they were obtained with a different column. However, when this value was used to correct the MW of a polymer with MW similar to the PDEG, the PEG630 standard, the values obtained shown in table 3.8 provided excellent agreement with the catalogue values. So, it can be concluded that equation 1.30 can provide reliable values for MW corrected for axial dispersion, pending on the availability of well characterized polymers to give accurate  $h$  values.

The comparison of the data obtained in table 3.5 and 3.6, via Dawkins[91,150] and Hamielic[95] methods respectively, shows that the first method provides more accurate values for polydispersity, unless monodisperse or well characterized standards are available, when the second method has the advantage of also providing values for average MW.

TABLE 3.8

Comparison of average molecular weights and polydispersities of PEG630 standard with polyacrylamide column packing, ( serial number J70-3 ) corrected ( t ) and uncorrected (  $\infty$  ) for axial dispersion via equation 1.30.

standard		uncorrected	corrected	catalogue
PEG630	$\bar{M}_w$	665	645	634
	$\bar{M}_n$	581	598	598
	d	1.14	1.08	1.08

### 3.4 PRELIMINARY STUDIES FOR ON-LINE MULTIDIMENSIONAL CHROMATOGRAPHY

#### 3.4.1 Concentration effects

The effect of the concentration of the injected polymer on  $V_R$  was studied for PSS and PBMA samples ( see table 2.2 ) with a PS-DVB column packing using THF as eluent. The calibration curve obtained for this column with PS standards having a concentration of 0.1% in THF is shown in figure 3.29. The results obtained for  $V_R$  by changing the concentration of the injected polymer can be seen in table 3.9. For both polymers there was no large variation in  $V_R$  with concentrations up to 0.6%. The choice of the sample concentration in multidimensional chromatography is very important because low concentrations mean undetectable quantities for system 2 ( see section 2.2.3 ). A high concentration would lead to a shift in the calibration curve, and so the molecules injected in system 2 would not have the correct composition and the results would be misinterpreted. To avoid these problems, it was decided to work with a polymer concentration of 0.6%.

#### 3.4.2 Off-line

The first attempt to perform multidimensional chromatography was

FIGURE 3.29

Log MW versus  $V_R$  calibration curve for PS standards in THF at room temperature, PS-DVB column serial number 17-21, flow rate 0.5 cm<sup>3</sup>/min, instrument 2.

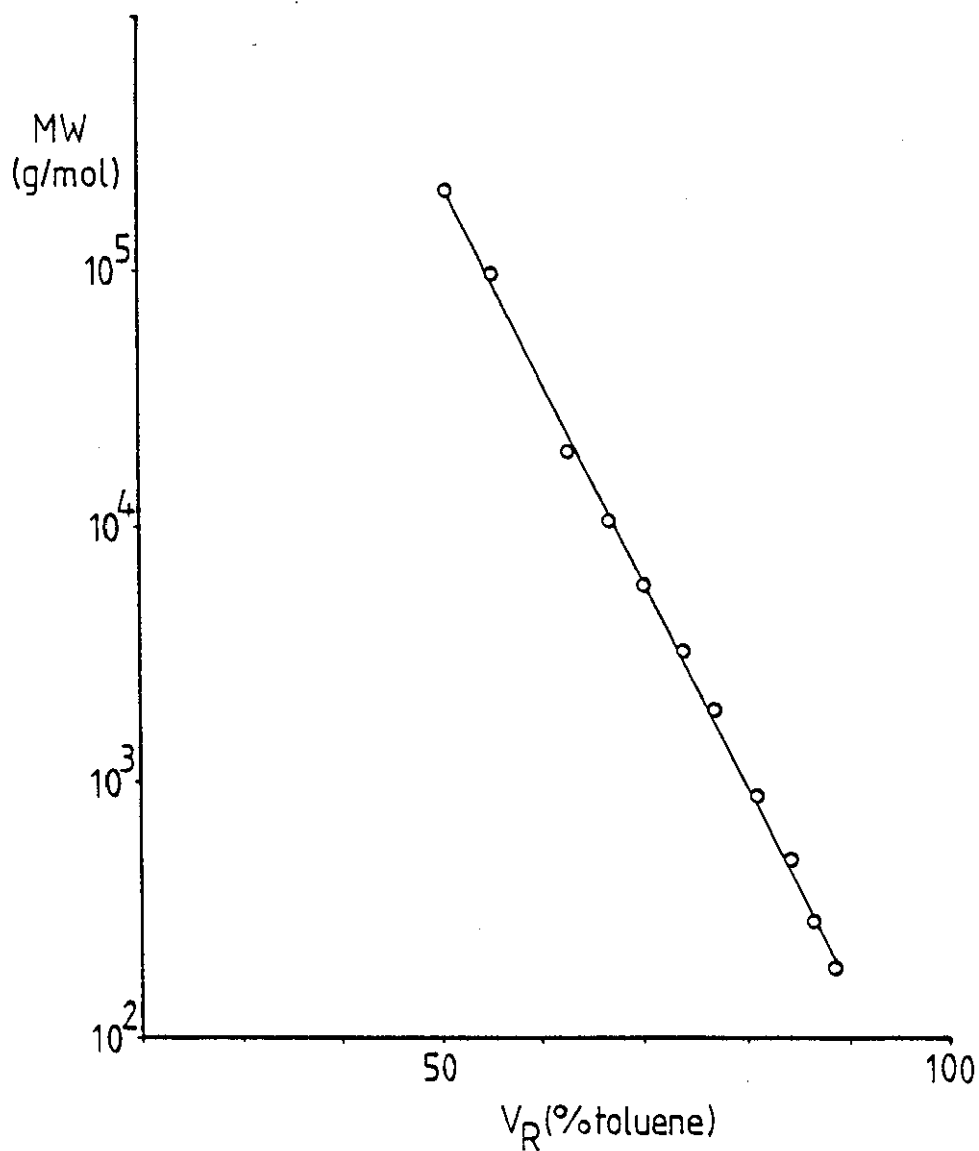


TABLE 3.9

Effect of the concentration of the injected polymer on  $V_R$  for PSS and PBMA ( see table 2.2 ) with a PS-DVB column serial number 17-21, THF as eluent at room temperature, flow rate 0.5 cm<sup>3</sup>/min, instrument 2.

concentration ( g/100 cm <sup>3</sup> )	$V_R$ ( % toluene )	
	PS	PBMA
0.05	74.0	62.1
0.1	74.0	61.8
0.2	74.3	61.8
0.4	74.2	62.1
0.6	74.2	62.3
1.0	77.0	----

made by injecting 100  $\mu$ l of a 0.6% solution of the standard PS32500 in instrument 2, using THF as eluent and a PS-DVB column packing. The chromatogram obtained for this solute is shown in figure 3.30. Ten fractions of this standard were collected and the times in which fraction collection was made are shown in figure 3.30. These fractions were re-injected in the same apparatus, with the same solvent in order to verify if the collected samples were concentrated enough to be detected by the RI detector available with this apparatus. From the ten fractions collected only four ( numbers 4 to 7 ) showed a peak related to the PS32500 chromatogram in figure 3.30. The chromatograms obtained for fractions 4 to 7 are shown in figure 3.31 where it can be seen that the peaks obtained at  $V_R$  around 1000 s were very small. As the sample concentration could not be increased it was decided to collect fractions of several identical injections and concentrate them before re-injection.

The study of the number of injections required to improve detection was performed with a mixture of PS and PBMA ( 0.3% each ) in THF with a PS-DVB column packing. Figure 3.32 shows the chromatogram of each polymer injected separately and figure 3.33 shows the chromatogram of a mixture of the two polymers, indicating the times in which the fractions were collected. It can be seen in figure 3.33 that the mixture of two polymers elutes as a single peak with the peak maximum between the values found for each polymer. The accumulated fractions from 4 or 8 separate injections were treated in the way described in section 2.3.2.1 and re-injected in the same instrument equipped with another PS-DVB column ( serial number 17-23 ). The eluent used to analyse the collected fractions was THF-HEP ( 36.2/63.8 ). This eluent composition was observed to give the best separation between PSS and PBMA polymers by Balke et al[104,114-116] in

FIGURE 3.30

Chromatogram of the standard PS32500 in THF, at room temperature, column packing PS-DVB, serial number 17-21, flow rate 0.5 cm<sup>3</sup>/min, instrument 2, showing the V<sub>w</sub> for fraction collection.

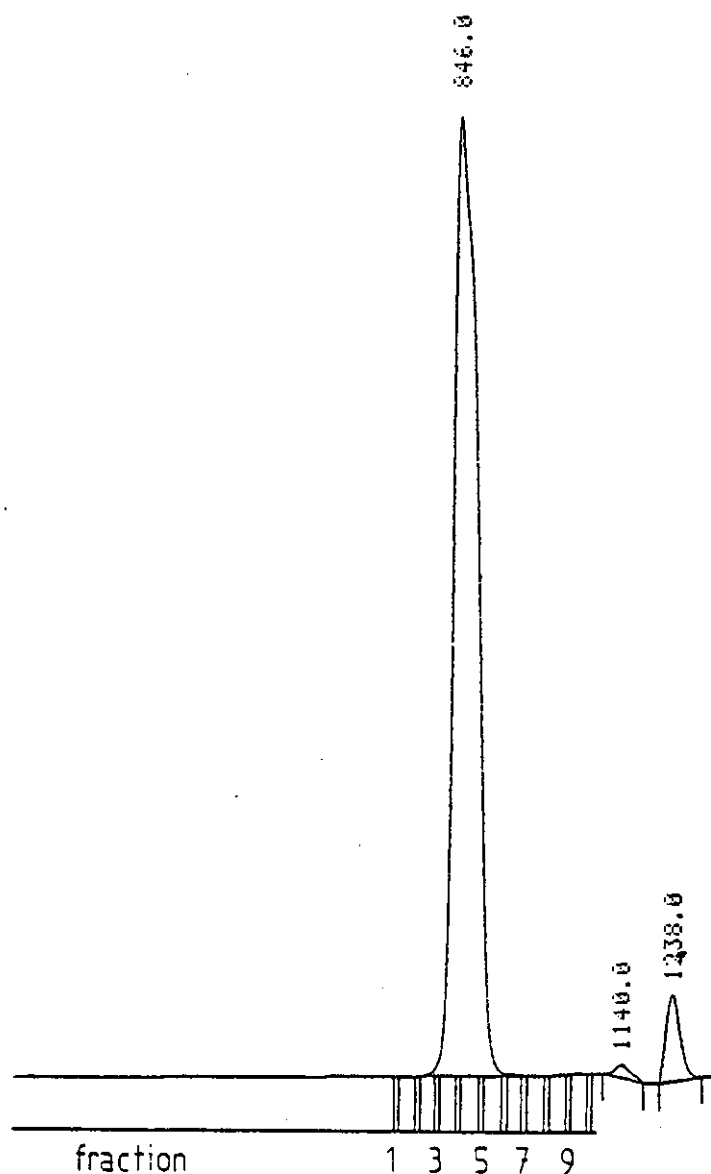


FIGURE 3.31

Chromatograms of the fractions of the standard PS32500 ( specified in figure 3.30 ) in THF, at room temperature, column packing PS-DVB, serial number 17-21, flow rate 0.5 cm<sup>3</sup>/min, instrument 2

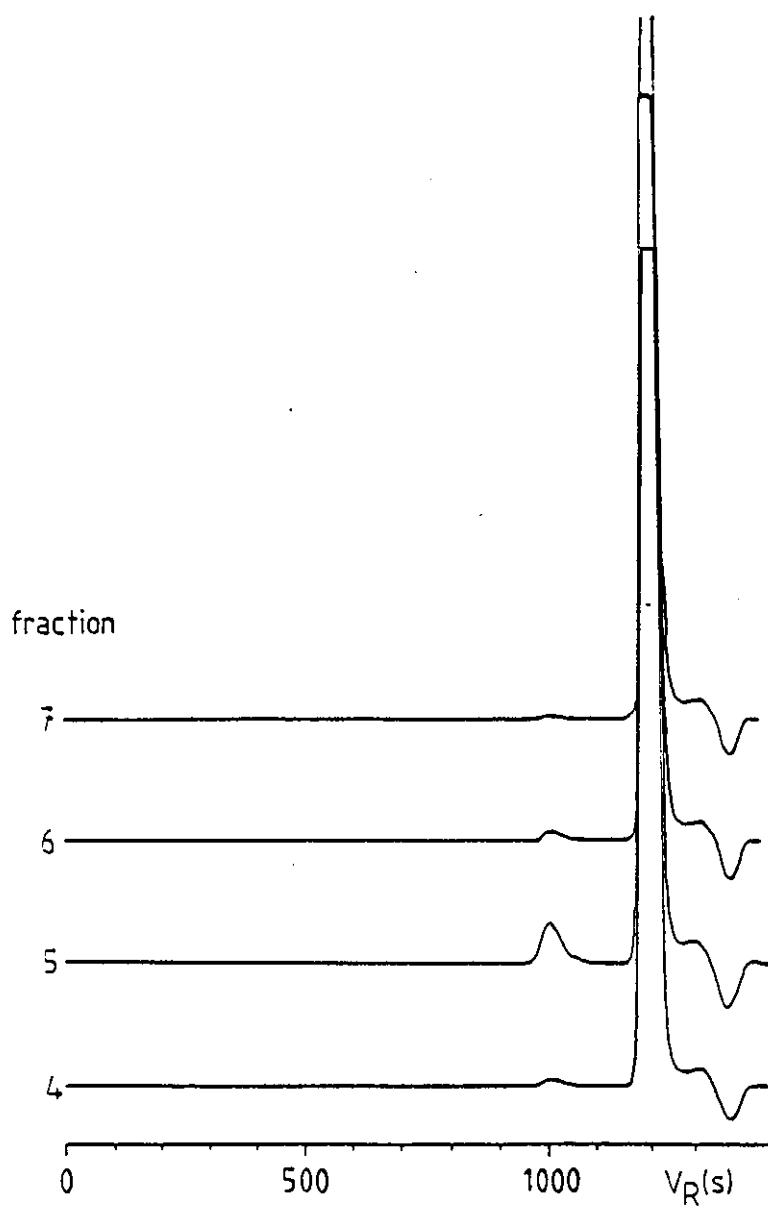




FIGURE 3.32

Chromatogram of PSS (—) and PBMA (---) in THF, at room temperature, column packing PS-DVB, serial number 17-21, flow rate 0.5 cm<sup>3</sup>/min, instrument 2, showing the  $V_R$  used for fraction collection in figure 3.33.

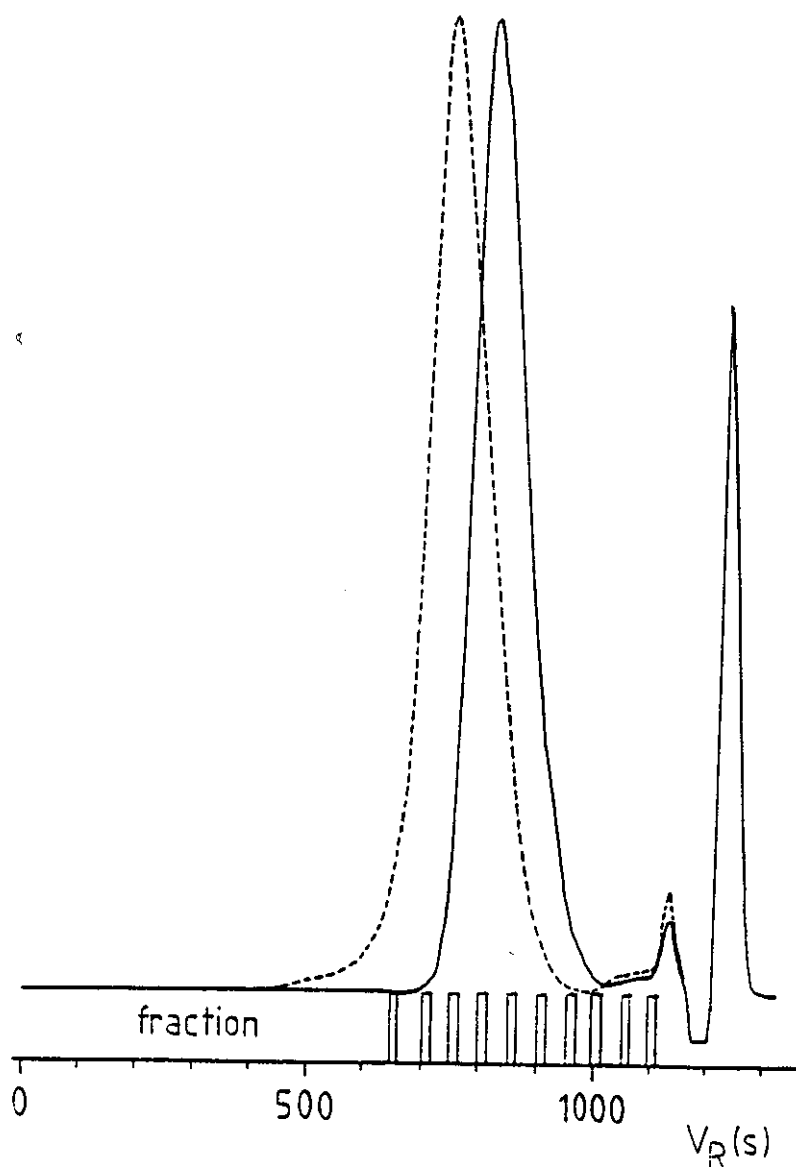
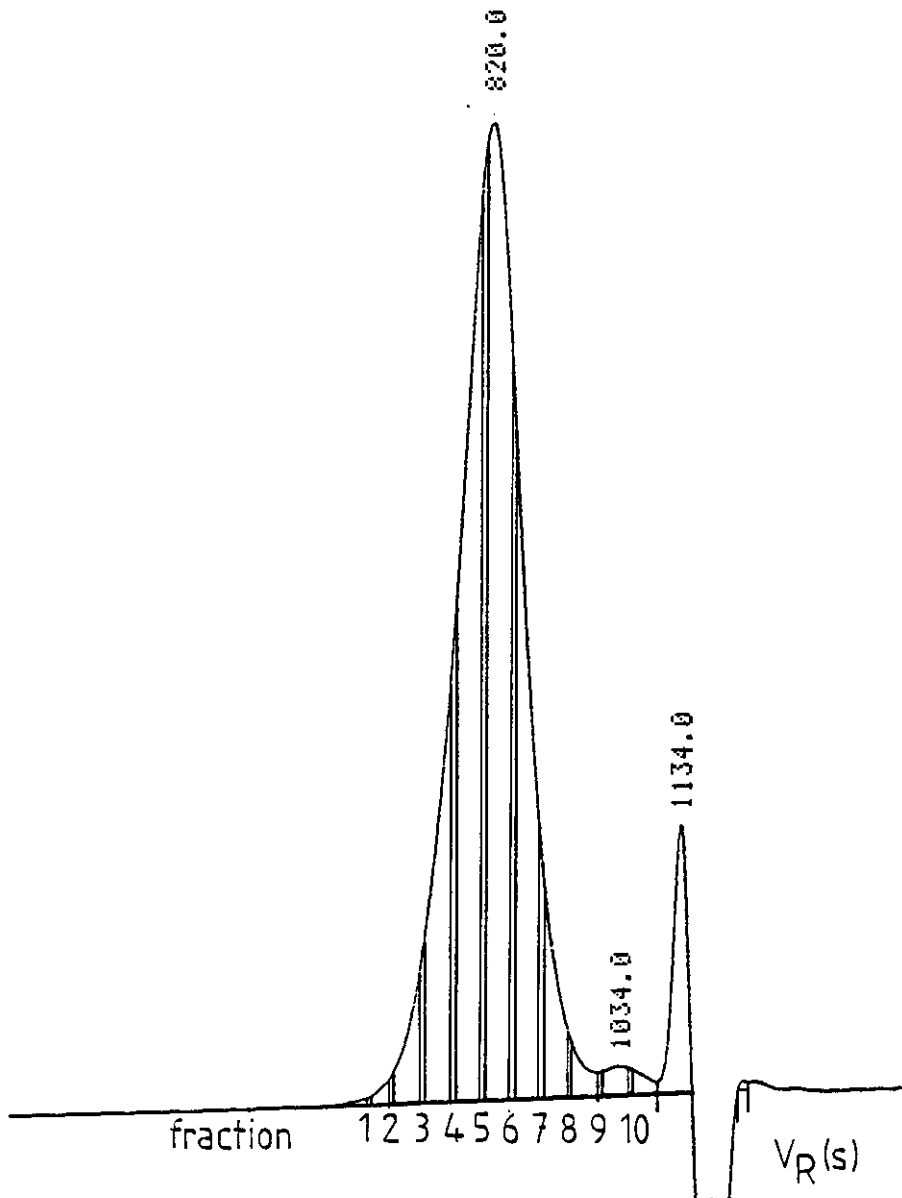


FIGURE 3.33

Chromatogram of a mixture of PSS and PBMA ( 0.3% each ) in THF, at room temperature, column packing PS-DVB, serial number 17-21, flow rate 0.5 cm<sup>3</sup>/min, instrument 2, showing the V<sub>w</sub> for fraction collection.



their multidimensional chromatography experiment with a polyether bonded-phase silica-based column packing. Figures 3.34 and 3.35 show the chromatograms obtained when the collected fractions of 4 and 8 injections were re-injected, respectively. The  $V_R$  obtained for the fractions for the polymer mixture for both 4 and 8 injections is shown in table 3.10. The comparison of figures 3.34 and 3.35 shows that the chromatograms for the fractions are very similar and that there was no increase in peak size when the number of injections to collect the fractions is doubled. Some peaks, such as the peaks obtained for fraction number 6, seem even bigger when the fractions of 4 injections are collected ( see figure 3.34 ). Actually, the solvent peak is so large that the factor governing the size of the polymer peak is mainly the solvent peak. As the solvent peak is extremely large and the computer necessarily reduces this peak to a size which will fit in the printout format, all the other peaks are reduced. So, the size of the peaks obtained when 4 or 8 injections were collected was a function of the solvent peak, which was dependent on several factors such as sample preparation and differences between batches of the eluent being used. One way of solving the problem of the size of the peaks is to use UV detection, which has high sensitivity and does not produce solvent peaks so large as RI detectors.

Analyzing figures 3.32, 3.34 and 3.35 together it seems that the peaks appearing in fractions 1, 2 and 3 are due only to PBMA since PSS which has a lower MW than PBMA is still in the column and has not yet started to elute. Fractions 4 to 6 in figure 3.34 and 3.35 show 2 peaks which comparing with figure 3.32 can be attributed to PBMA ( A ) and PSS ( B ) in order of increasing  $V_R$ . This fact was later confirmed by the injection of PSS alone and PBMA alone. In the first system, the

FIGURE 3.34

Chromatograms of the fractions of a mixture of PBMA ( A ) and PSS ( B ), concentrated from 4 injections, fraction collection times specified in table 2.3, eluent THF-HEP ( 36.2/63.8 ), at room temperature, PS-DVB packing, serial number 17-23, flow rate 0.5 cm<sup>3</sup> /min, instrument 2.

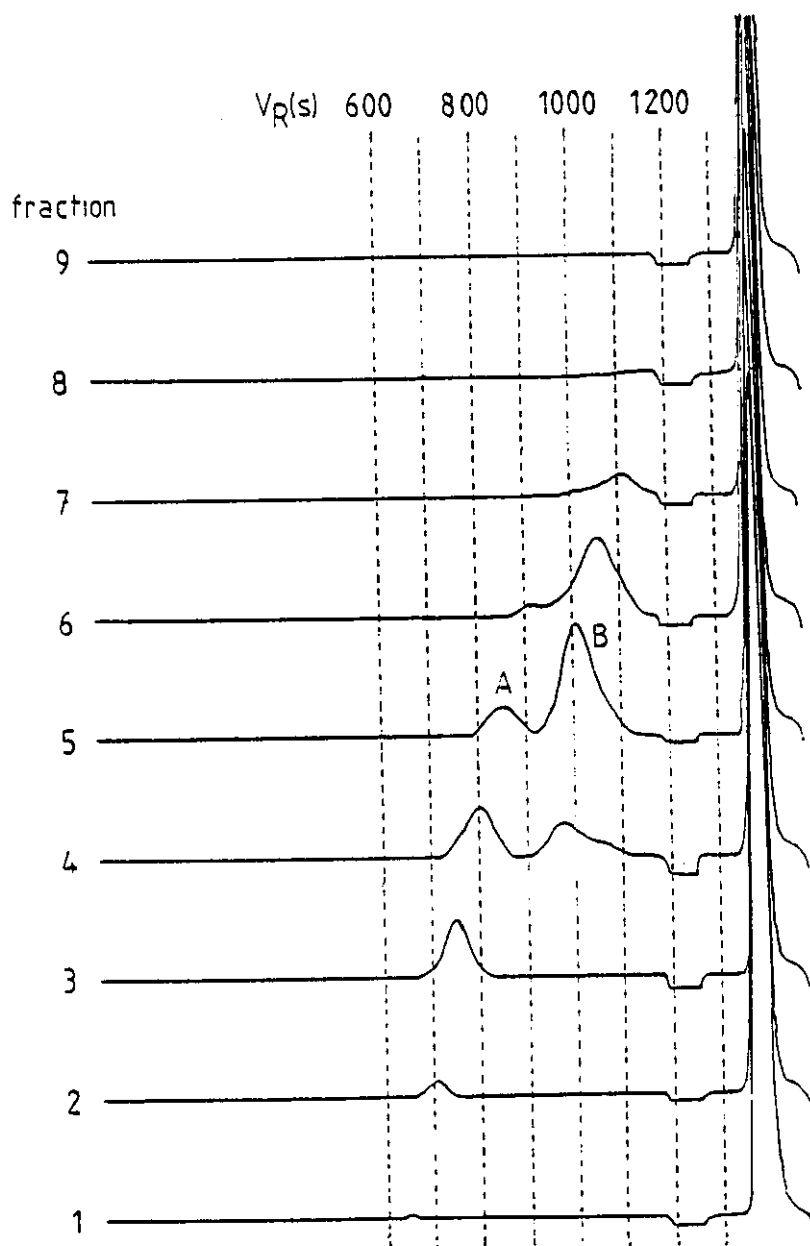


FIGURE 3.35

Chromatograms of the fractions of a mixture of PBMA ( A ) and PSS ( B ), concentrated from 8 injections, fraction collection times specified in table 2.3, eluent THF-HEP ( 36.2/63.8 ), at room temperature, PS-DVB packing, serial number 17-23, flow rate  $0.5 \text{ cm}^3 / \text{min}$ , instrument 2.

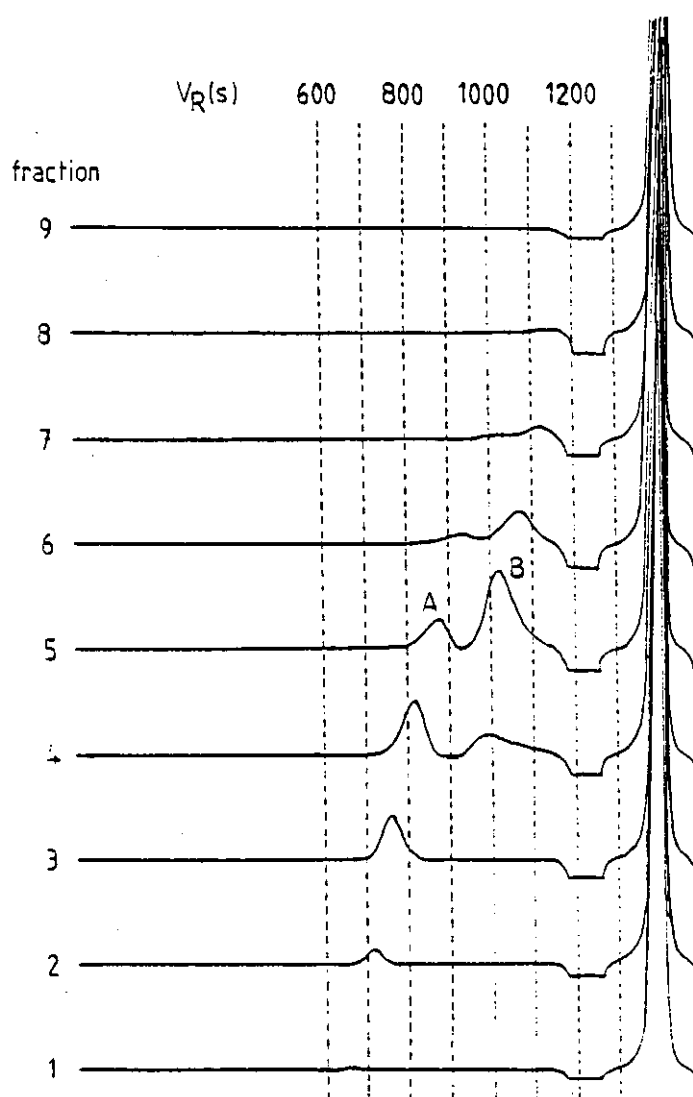


TABLE 3.10

Effect of the number of injections on the  $V_R$  of the fractions of a mixture of PSS and PBMA ( 0.3% each ), fraction collection times specified in table 2.3, eluent THF-HEP ( 36.2/68.2 ), PS-DVB packing, serial number 17-23

fraction number	$V_R$ ( s )					
	4 injections			8 injections		
	PBMA	PS	solvent	PBMA	PS	solvent
1	664	----	1390	666		1384
2	714	----	1390	716		1388
3	758	----	1390	766		1390
4	804	980	1390	820	990	1390
5	856	1014	1388	870	1022	1390
6	---	1066	1388	930	1076	1390
7	---	----	1388	---	1134	1398
8	---	----	1392	---	----	1398
9	---	----	1390	---	----	1394
10	---	----	1390	---	----	1396

chromatographic analysis of the mixture of PSS and PBMA was performed by size exclusion alone, since THF is a good solvent for both polymers and PS-DVB with THF is an inert packing[42]. So, the molecules collected in each slice of the first chromatogram had approximately the same hydrodynamic volume. In the second system PSS and PBMA molecules have changed size and/or are having some kind of interactive behaviour with the packing since they are eluting at different  $V_R$  in system 2. Indeed, the PSS molecules should be smaller in THF-HEP since heptane is a nonsolvent for PS. As heptane is a solvent for PBMA, the mixture THF-HEP is also a good solvent for PBMA. The peak due to PBMA is very small in fractions 6 and 7 and has disappeared completely in fraction 8 as is expected from figure 3.32 where it can be seen that when fraction 8 is collected after all the PBMA molecules had already eluted. The same kind of behaviour was found for PSS, which starts to elute in fraction 4, is larger in fraction 5 and has disappeared in fraction 9, in accordance with that expected from figure 3.32. The small rounded peak shown in figure 3.33 at a  $V_R = 1034$  s is probably due to the solvent since the chromatograms of fractions 9 and 10 do not show any polymer peak.

The results obtained in this system are similar to the results found by Balke et al[104,114-116] where separation was achieved between PS and PBMA, using the same eluent but a polyether bonded-phase silica packing instead of a PS-DVB column packing.

In view of the results obtained in the separation of PSS and PBMA, it was decided to expand the studies of interactive mechanisms operating in system 2. The use of different packings and eluents would allow a more complete investigation of the mechanisms involved in the separation of PSS and PBMA. An on-line multidimensional system was considered to be more

appropriate in terms of analysis time ( see figure 1.4 ) for this work.



### 3.5 ANALYSIS OF POLYMERS BY ON-LINE MULTIDIMENSIONAL CHROMATOGRAPHY

The schematic diagram of the apparatus utilized by Balke et al[104,114-116] for multidimensional chromatography is shown in figure 3.36. With this apparatus the eluent flow in system 1 could be stopped to inject a sample in system 2. The eluent flow in system 1 remained stationary while the analysis in system 2 was being performed. After the run in system 2 was complete, solvent 1 was redirected to column 1, for 1 min at a flow rate of  $0.5 \text{ cm}^3/\text{min}$ , when the flow in system 1 was stopped again and another analysis in system 2 was performed. In this way, several slices of just one injection from system 1 can be analyzed in system 2. The apparatus used in this work ( see figure 2.1 ) did not allow the flow in system 1 to be stopped without switching the pump off, and this procedure would cause undesirable alterations in the solvent flow. Figures 3.37 and 3.38 show the chromatograms of PSS ( 0.4% ) and PBMA ( 0.4% ), respectively, in THF with a PS-DVB column packing when the switching valve ( see figure 2.2 ) is turned to the inject position from 850 to 870 s, in order to inject a fraction of the polymer being analyzed from system 1 in system 2. To avoid this flow disturbance change in  $V_R$  for subsequent fractions, it was decided to collect just one fraction for each injection. From the analysis of figures 3.37 and 3.38, it was decided to choose the fraction eluting between 830 and 850 s to be injected in system 2, since this fraction has a high concentration of both polymers. So, from figure 3.39 onwards, it was always the fraction eluting between 830 and 850 s in system 1 that was injected in system 2.

The column PS-DVB serial number 17-23 and polyacrylamide serial

FIGURE 3.36

Schematic diagram of the equipment used by Balke et al for on-line multidimensional chromatography[112].

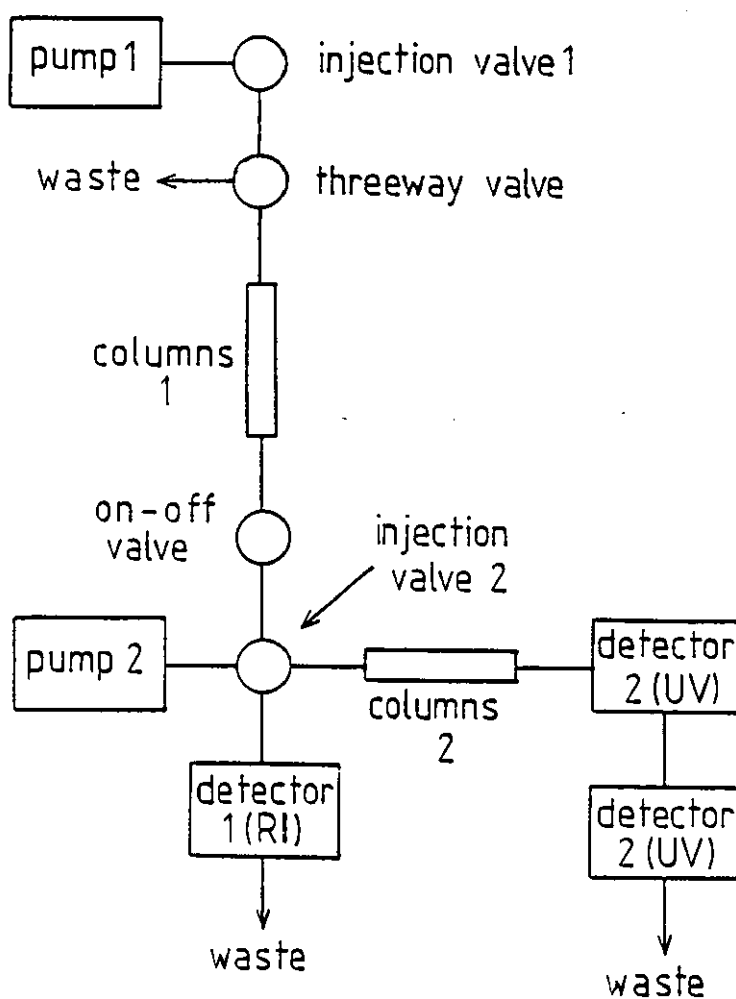


FIGURE 3.37

Chromatogram of PSS ( 0.4% ) in THF with a PS-DVB column packing, serial number 17-21, instrument 3, showing the disturbance in flow rate caused by turning the switching valve to inject position.

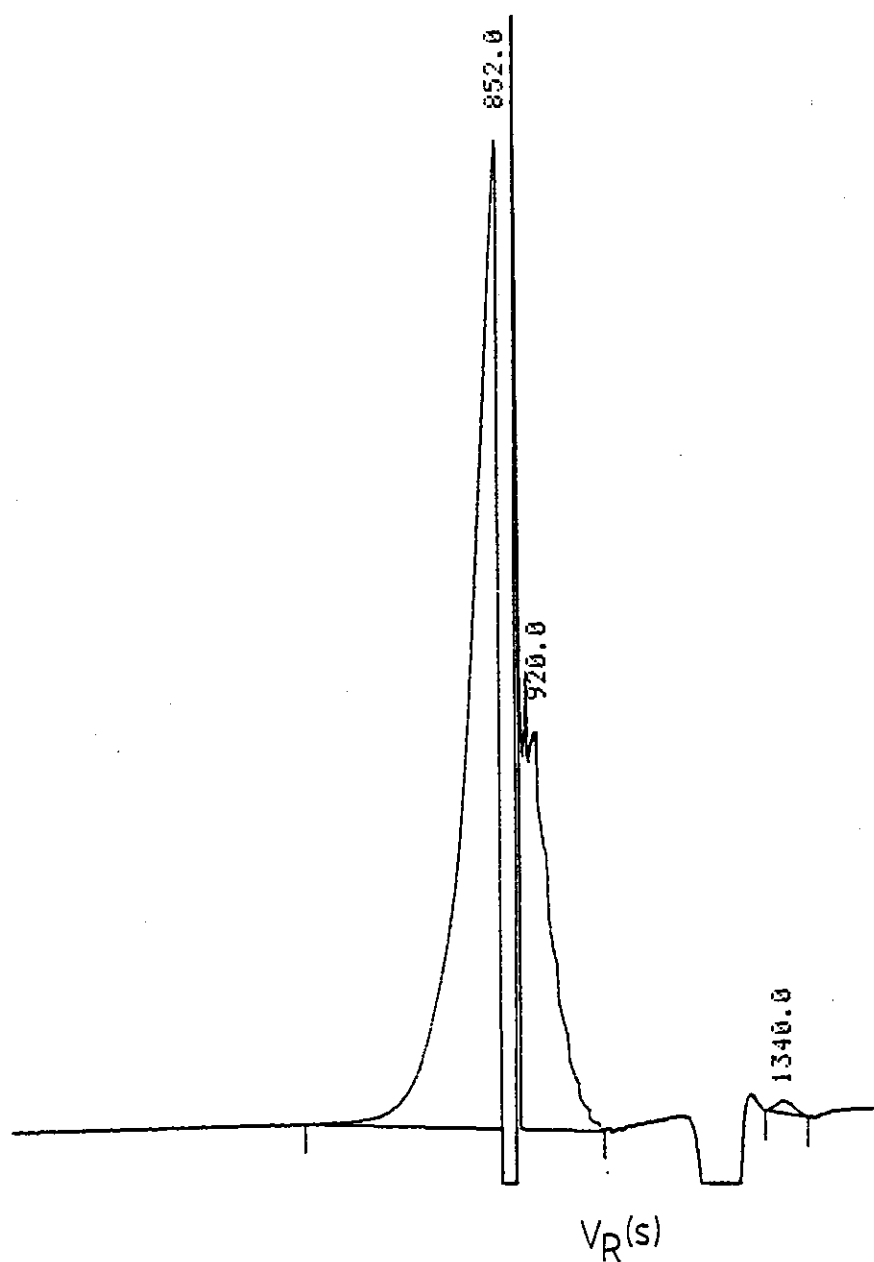
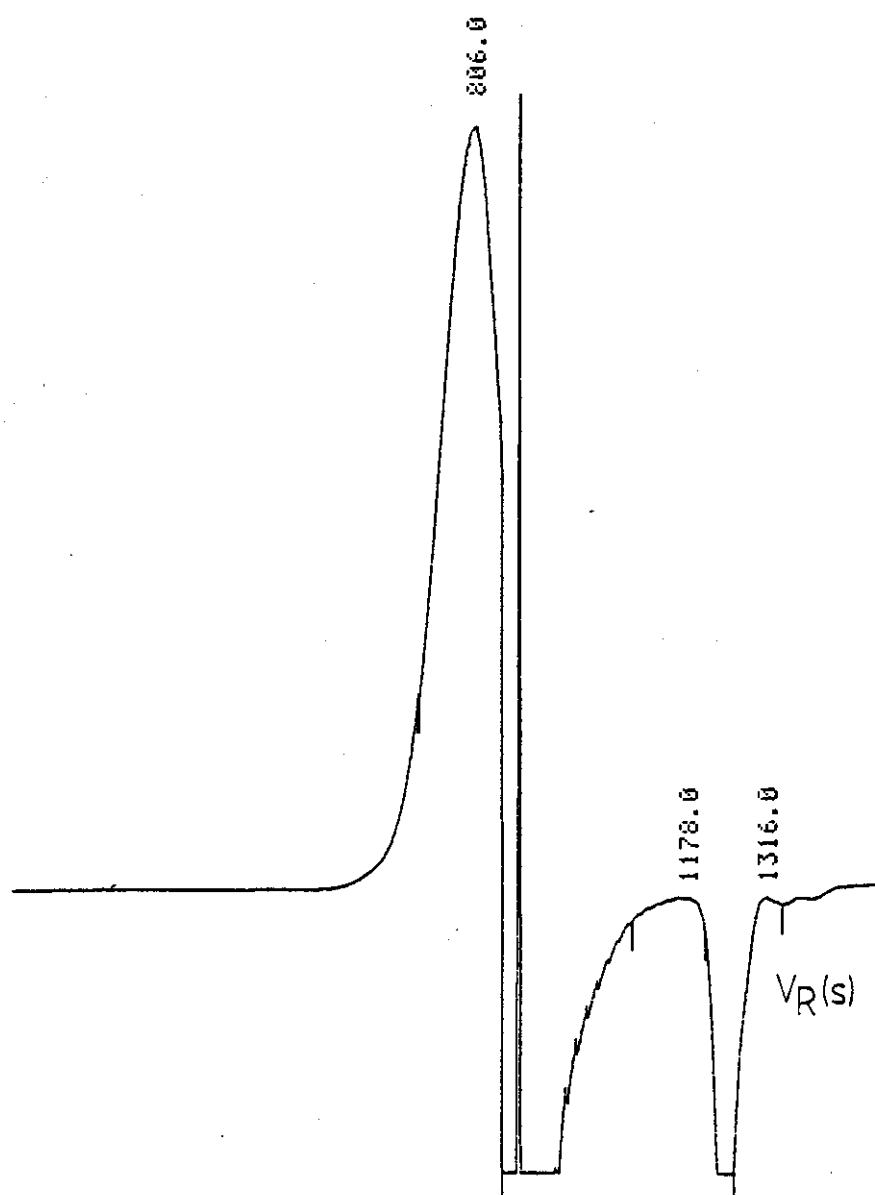


FIGURE 3.38

Chromatogram of PBMA ( 0.4% ) in THF with a PS-DVB column packing, serial number 17-21, instrument 3, showing the disturbance in flow rate caused by turning the switching valve to inject position.



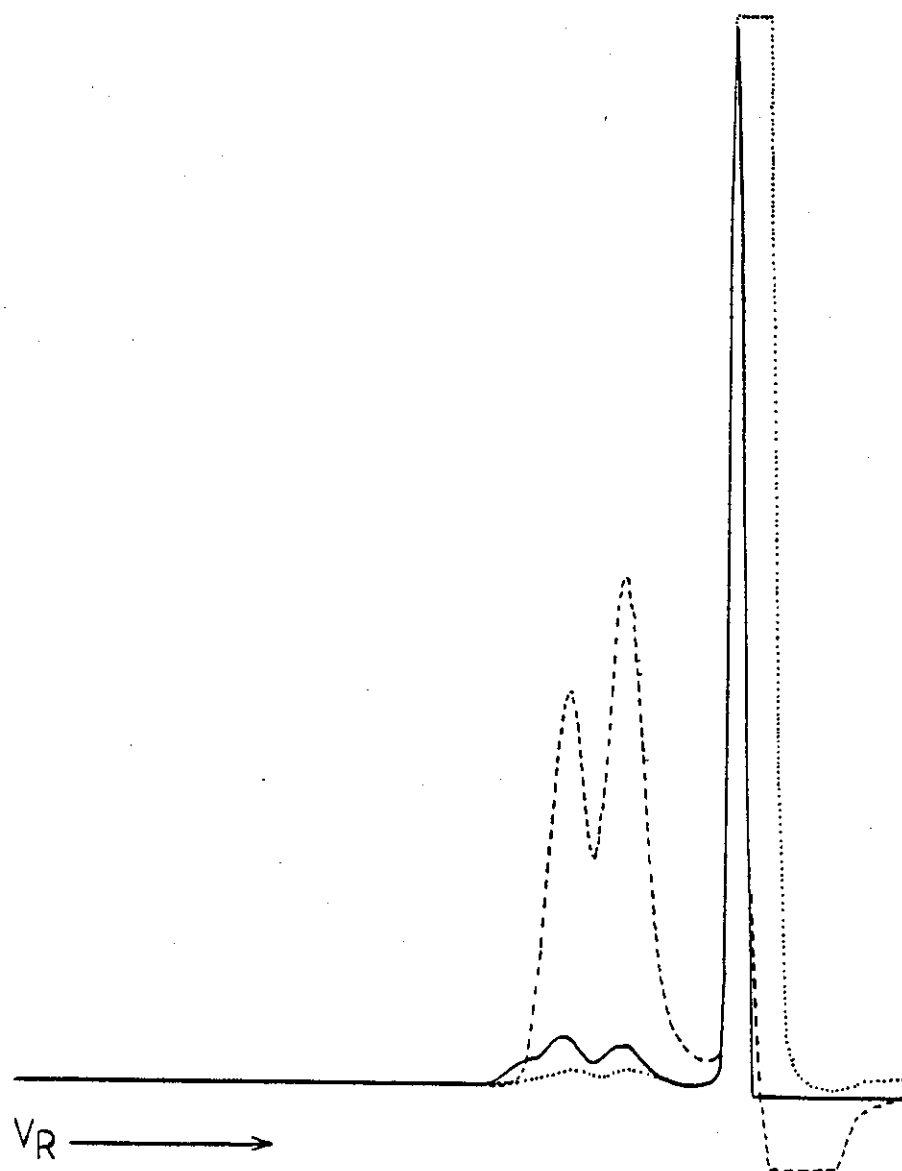
number 8-29 were the only columns used in system 2. Therefore, only the column type employed in the experiment will be mentioned in each chromatogram.

The importance of the use of an appropriate detection method is clearly illustrated in figure 3.39. This figure shows the computer printout for a chromatogram of a slice ( 830-850 s ) of a mixture of PSS, PBMA and the copolymer PSBA8/2 obtained with UV detection at 235 and 260 nm and RI detection. The same plotting factors were used for the three curves. The intensity of the signal obtained from the RI detector is very small and the size of the solvent peak is extremely large due to the injection of a different eluent from system 1 in system 2. The UV detector at 260 nm gives a good signal but fails to recognise the PBMA, since this polymer is transparent in this UV region, showing only two peaks due to PSBA8/2 and PSS, in order of increasing  $V_R$ . At 235 nm, the trace obtained by the detector is small but the shoulder due to PBMA is easily noticeable. This wavelength will be therefore used throughout this work.

The composition of each copolymer slice can be determined quantitatively by the use of dual detection. Both dual UV detectors working at different wavelengths[114] and the combination of UV and RI detectors have been used to determine the composition of copolymers[109,110,156,157]. For PSBA copolymers, the absorbance at 260 nm will reflect only the styrene concentration in the copolymer while the UV absorbance at 235 nm or the RI signal will reflect the concentration of styrene plus the n-butylmethacrylate in the copolymer. If the detectors are previously calibrated by using the corresponding homopolymer, the measurement of the area under the peaks and its use in the appropriate equations[114] will give the copolymer composition.

FIGURE 3.39

Chromatograms obtained in system 2, with a PS-DVB packing, THF-HEP (36/64), for a slice of a mixture of PS, PBMA and the copolymer PSBA8/2, ( $V_R = 830-850$  s); UV detection 235 nm (—); UV detection 260 nm (---); RI detection (.....).

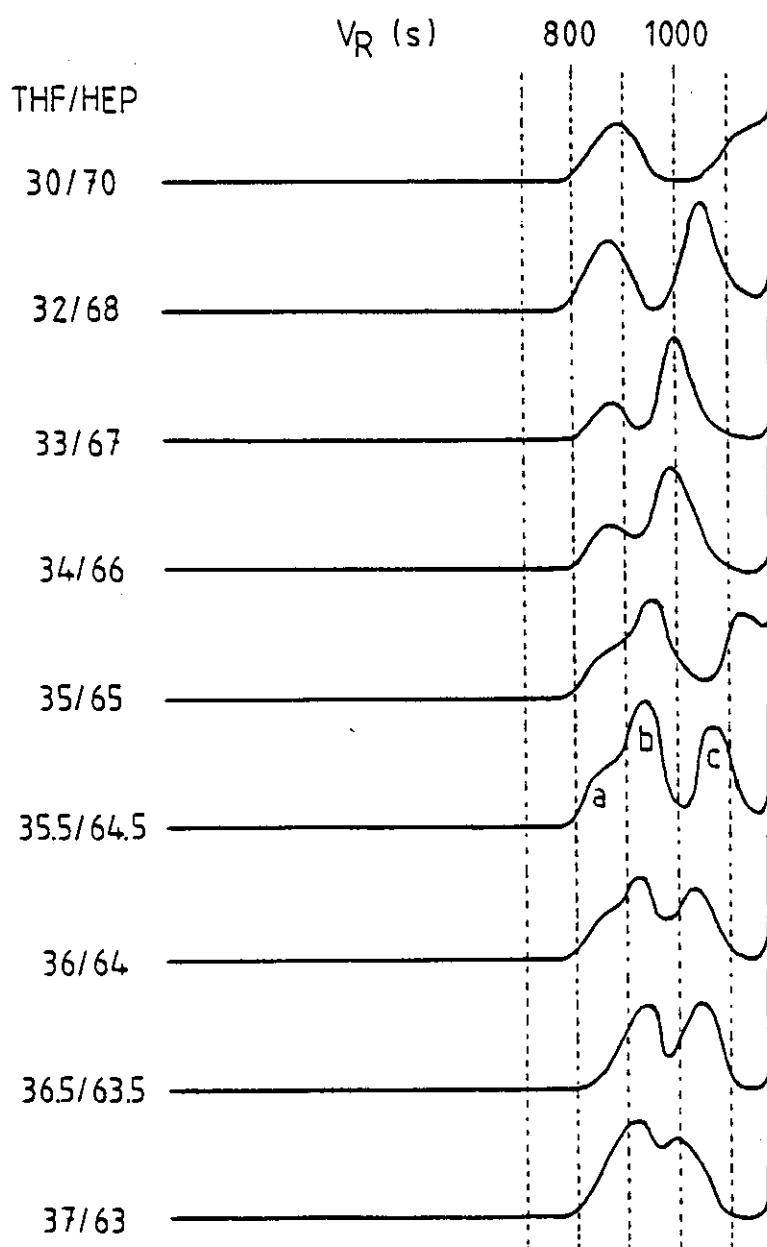


### 3.5.1 Crosslinked polystyrene column packing

The first system chosen to be studied was the system already used in off-line experiments ( see section 3.4.2 ). It was decided to work with eluent concentrations around 63.8%, since this concentration had already proved to give a separation of PSS and PBMA homopolymers. The chromatograms obtained in system 2 for the mixture PSS, PBMA and copolymer PSBA8/2 with the PS-DVB column packing and eluents ( THF-HEP ) varying in composition from ( 37/63 ) to ( 30/70 ) are shown in figure 3.40. These chromatograms showed that all the polymer peaks are displaced towards high elution volume as the concentration of HEP is increased. In all the eluent concentrations studied, PBMA is the first polymer to elute and its  $V_R$  varies only slightly with the concentration of HEP. At THF-HEP concentrations of ( 37/63 ) and ( 37.5/62.5 ) the copolymer PSBA8/2 elutes together with PBMA. At higher HEP concentrations it is possible to see three peaks due to PBMA, copolymer PSBA8/2 and PSS, in order of increasing elution volume, up to the concentration of ( 35/65 ). At higher concentrations of HEP ( 34/66 ) the PSS peak combines with the solvent peak. The same happens to the peak due to PSBA8/2 copolymer, which is being displaced towards high  $V_R$  until THF-HEP ( 30/70 ) when it merges with the solvent peak. So, it can be concluded that the increase of the HEP concentration in the mobile phase markedly increases  $V_R$ , particularly for

FIGURE 3.40

Chromatograms obtained with system 2, for a slice of a mixture of PSS ( c ), PBMA ( a ) and copolymer PSBA8/2 ( b ), PS-DVB column packing, eluent concentration varying from ( 37/63 ) to ( 30/70 ) THF-HEP.





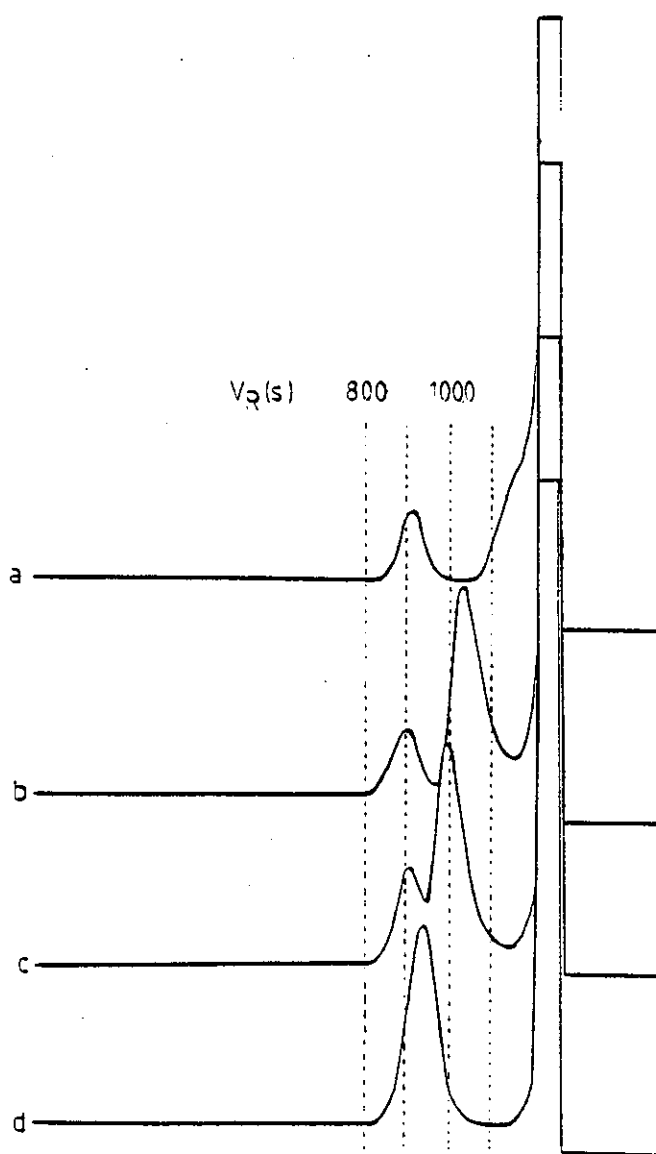
PSS and copolymer PSBA8/2. Separations of 4 different copolymers of PSBA in a mixture with PBMA with the PS-DVB column packing and THF-HEP ( 30/70 ) are shown in figure 3.41. The chromatogram a in figure 3.41 shows the peak of PBMA eluting first and the peak due to the copolymer PSBA8/2 merging with the solvent peak. As the content of styrene in the copolymer decreases, the  $V_R$  of the copolymer peak also decreases. Chromatograms b and c in figure 3.41 show two peaks each, due to PBMA and the copolymers PSBA6/4 and 4/6 respectively eluting in order of increasing  $V_R$ . In chromatogram d, the copolymer PSBA2/8, which has low styrene content, elutes together with PBMA.

These results prove that PSBA copolymers can be separated according to their composition, with a PS-DVB column packing and THF-HEP as eluent. However, a mobile phase with gradient elution would be necessary for a full characterization procedure.

Balke et al[104,114-116] obtained similar results with a polyether bonded-phase silica-based column packing and to explain these results suggested that four possible mechanisms may be taking part in the separation. They proposed that a size exclusion mechanism will contribute to the late elution of PSS and its copolymers since HEP is a nonsolvent for PS, and so PS and styrene-rich copolymers will decrease in size when the concentration of HEP is increased. As the PBMA molecules will not be affected in the same way, an immediate size distribution will be present, and the smaller PSS and styrene rich copolymers will enter more pores of the column packing than PBMA. A second mechanism that was suggested to be participating in the separation was adsorption. Balke[114] performed cloud point experiments which showed that PSS precipitates beyond concentrations THF-HEP ( 35/65 ), but the concentrations of polymer used were not

FIGURE 3.41

Chromatograms obtained with system 2, for a slice of a mixture of PBMA homopolymer with a series of copolymers: PSBA8/2 ( a ), PSBA6/4, ( b ), PSBA4/6 ( c ), PSBA2/8 ( d ) in PS-DVB column packing, THF-HEP ( 30/70 ).



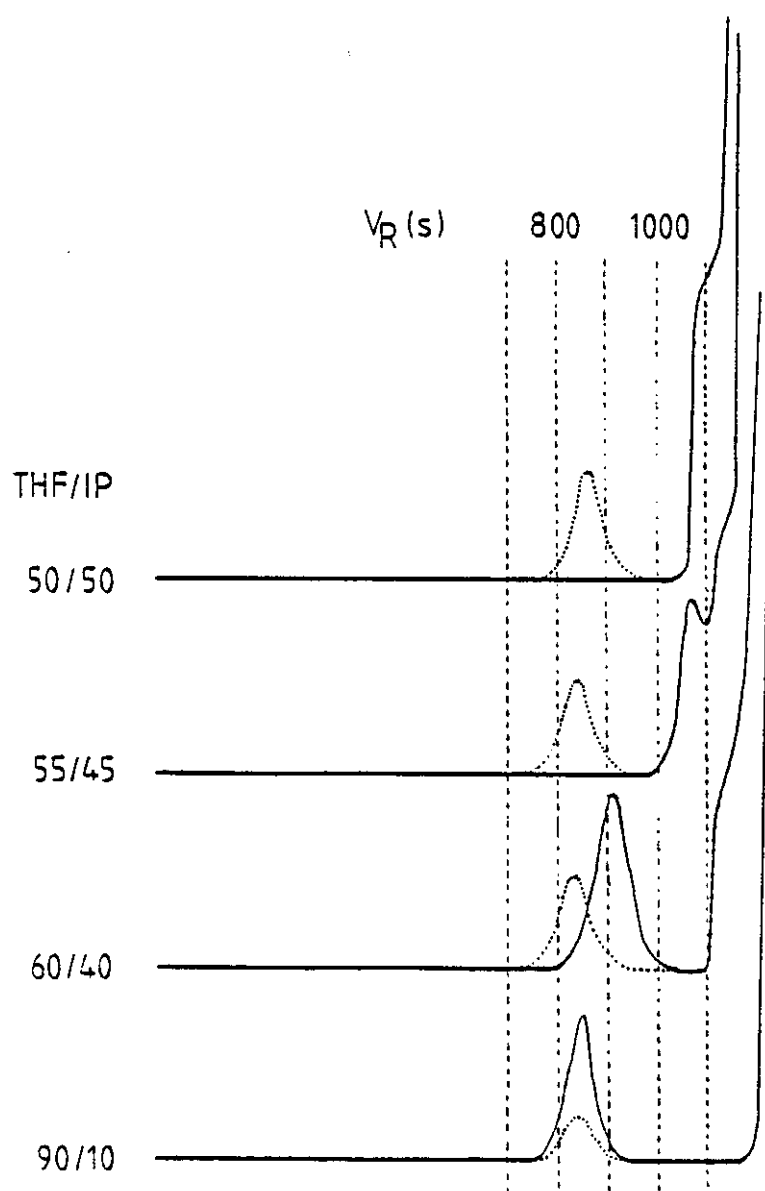
mentioned. Indeed, attempts to dissolve the PSS used in this work in THF-HEP ( 35/65 ) at a concentration of 1% were not successful. So, since the eluent is a poor solvent for PSS, interactions between column packing and PSS will be favoured[30]. A third possibility was pointed out by Balke[144]. The eluent injected from system 1 ( pure THF ) affected the separation in the system 2, forming a solvent gradient that participates in the separation. The lack of precipitation of PSS at high nonsolvent compositions in system 2 was considered to be evidence for this effect. The final possible mechanism has been noted in Balke's[158] most recent paper, where he suggested that HPPLC is also participating in the separation. A tentative explanation is that the polymer is visualized to continually reprecipitate and redissolve as the solvent front gradient repetitively overtakes and then loses the polymer.

An attempt to understand more about the interactions occurring in system 2, was made by changing the eluent in system 2 to THF-IP, a solvent more polar than THF, which should change the elution power of system 2. Figure 3.42 shows the chromatogram obtained in system 2, for a slice ( 830-850 s ) of separate injections of PSS and PBMA homopolymers with a PS-DVB column packing and various compositions of THF-IP. The trend in the elution behaviour of the polymers is very similar to the behaviour found with THF-HEP, the only difference being the peak of PSS merging with the solvent peak earlier, at a concentration equal or smaller than 50%. The PBMA peak shows a smaller variation with the eluent composition. Solution viscosity measurements showed that the mixture THF-IP ( 60/40 ) is a poorer solvent than a theta solvent for PSS and a good solvent for PBMA.

It is known that to increase the adsorption in active packings, the polarity of the solvent has to be decreased[62]. This is true for figure

FIGURE 3.42

Chromatograms obtained with system 2, for a slice ( 830-850 s ) of separate injections of PSS (—) and PBMA (-----) homopolymers with a PS-DVB column packing and eluent composition varying from ( 90/10 ) to ( 50/50 ), THF-IP.



3.40, where the increase of HEP concentration ( the polarity of the mobile phase decreases ) causes an increase of the retention of PSS. However, for THF-IP, in figure 3.42, the opposite is verified, since the increase in the mobile phase polarity causes the increase in the adsorption of PSS.

It can be concluded from figures 3.40 and 3.42 that in PS-DVB column packings, the main factor controlling the elution behaviour of PSS is the solubility of PSS in the mobile phase. In figure 3.40, as the concentration of HEP, a nonsolvent for PSS, increases, a layer of eluent which is THF rich should form around the packing. This quasistationary layer will be more attractive to PSS, which will be progressively more retained until PSS elutes with the solvent peak. There is no proof that PSS is precipitating in the column, or even eluting after the  $V_T$  of the column, since there was no peak after the solvent peak. PSS was shown to be insoluble in THF-HEP ( 65/35 ) at concentrations of 1%, but this does not necessarily mean that PSS will precipitate at the low concentrations involved in system 2.

For PBMA, as the peak in figures 3.40 and 3.42 is not displaced as the eluent composition changes, it can be supposed that there is no change in the solvent quality of the mobile phase for PBMA throughout the studied range and that the main mechanism influencing the separation is size exclusion.

### 3.5.2 Polyacrylamide column packing

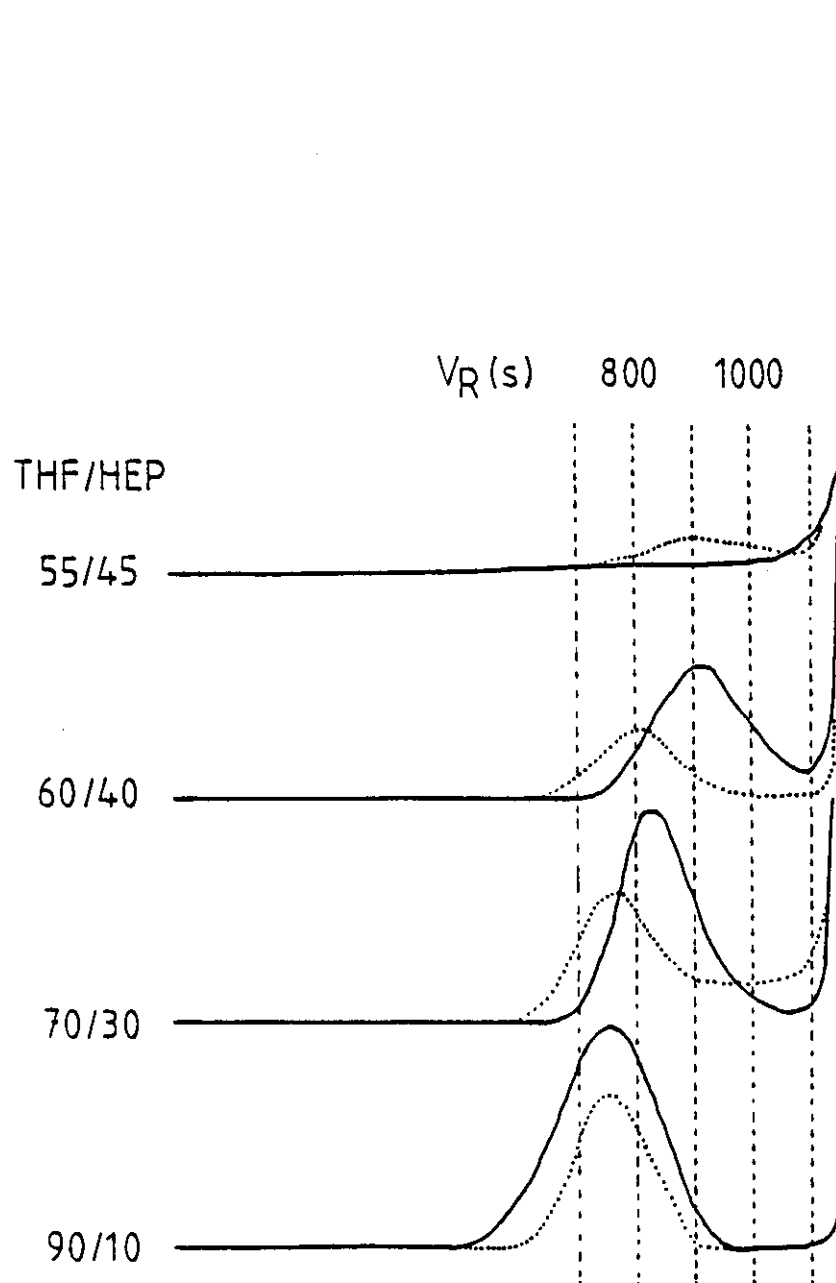
The use of a packing more polar than PS-DVB, such as a polyacrylamide packing, should provide a different behaviour in the elution of PSS, PBMA and its copolymers since this packing in organic eluents showed an interactive behaviour ( see section 3.2.3 ). The chromatograms obtained with system 2, for a slice ( 830-850 s ) of different injections of PSS and PBMA with a polyacrylamide column packing and various THF-HEP compositions is shown in figure 3.43. Comparing this figure with figure 3.40, where the column packing is PS-DVB with THF-HEP used as eluent, it can be seen that the PSS is displaced to high  $V_R$  much earlier. At concentration THF-IP ( 55/45 ), in figure 3.43 the PBMA shows a deformed peak, suggesting that some adsorption is taking place. This behaviour was not shown with PS-DVB ( see figure 3.40 ), where PBMA eluted at concentrations of HEP as high as 70% without being adsorbed.

It has been seen in section 3.2.3 that polyacrylamide packings in THF show some kind of interactive behaviour with polymeric solutes. The addition of HEP to the THF makes the mobile phase less polar and decreases solvent-packing interactions. So, solute-packing interactions are increased, leading to the elution of PSS together with the solvent peak at lower HEP concentrations and to the adsorption of PBMA.

Size exclusion mechanisms should also be taking place in a polyacrylamide packing since the considerations about the size of PS molecules in eluents of increasing concentration of HEP are also valid. However, no precipitation of PSS is occurring because PSS is soluble in

FIGURE 3.43

Chromatograms obtained with system 2, for a slice of different injections of PS (—) and PBMA (.....), polyacrylamide column packing and eluent composition varying from THF-HEP ( 90/10 ) to ( 55/45 ).



THF-HEP ( 55/45 ) mixtures.

The possibility of copolymer fractionation in this system is proved in figure 3.44 with the chromatogram obtained in system 2 for a slice ( 830-850 s ) of separate injections of PSS, PBMA and PSBA copolymers in THF-HEP ( 55/45 ). It can be seen that the PSBA copolymers are separated by composition and that the separation obtained in polyacrylamide packings is similar to those obtained in PS-DVB column packing at higher HEP concentration.

The effect of the use of a more polar eluent in the separation of PSS and PBMA with the polyacrylamide packing is shown in figure 3.45, for a chromatogram of a slice ( 830-850 s ) of separate injections of PSS and PBMA with a polyacrylamide column packing and THF-IP composition varying from ( 90/10 ) to ( 30/70 ). It can be seen in figure 3.45 that PSS elutes at a concentration of THF-IP ( 50/50 ) without merging with the solvent peak. This IP concentration is above the PSS precipitation point. One explanation for this behaviour is that IP being more polar than THF should form a quasistationary layer around the polar packing. PSS molecules do not approach this layer and tend to elute in a THF rich mobile phase of preferential adsorption of IP onto the polyacrylamide packing. This would justify the broad peaks obtained for PSS. The same kind of explanation would be valid for PBMA, for which IP is a theta solvent at 23 °C[49]. So, PBMA should not approach the packing and when the concentration of IP increases up to 70% is carried through the column in the same way as PSS.

Another effect that should be influencing the analysis of PSS, PBMA and PSBA copolymers is the change in the volume of the polyacrylamide packing in different eluents. This effect can be very important for polyacrylamide packings ( see section 3.2.2 ) but there was no data



FIGURE 3.44

Chromatograms obtained with system 2, for a slice of separate injections of PBMA ( a ), PSBA2/8 ( b ), PSBA4/6 ( c ), PSBA6/4 ( d ), PSBA8/2 ( e ), PSS ( f ) with a polyacrylamide column packing and THF-HEP ( 55/45 ).

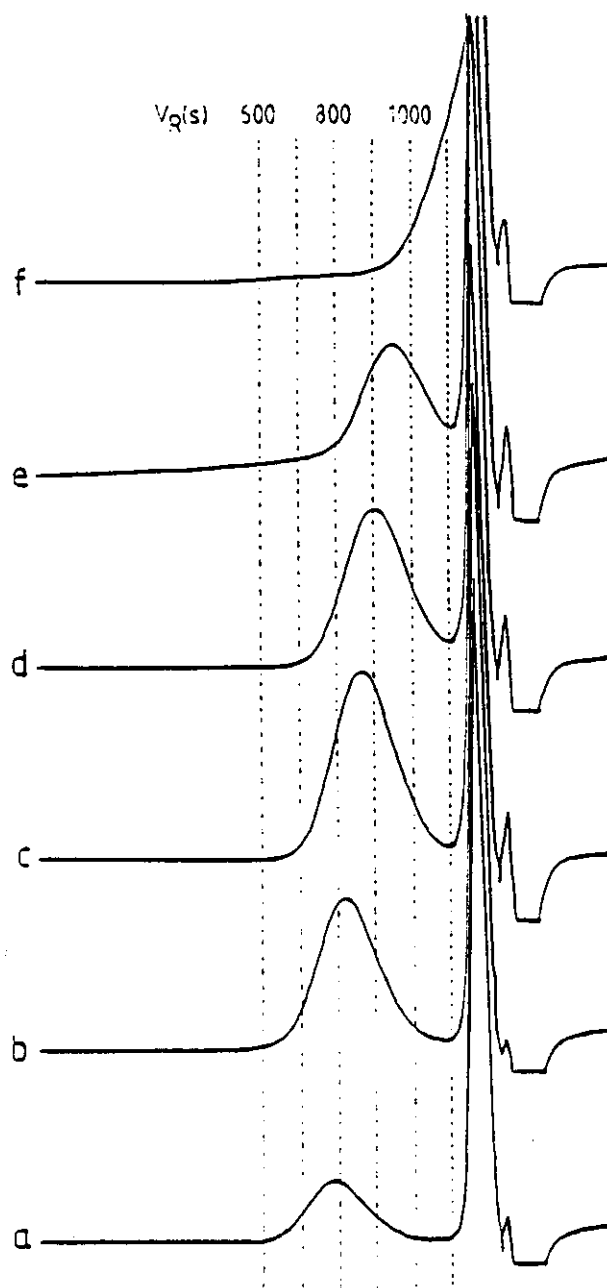
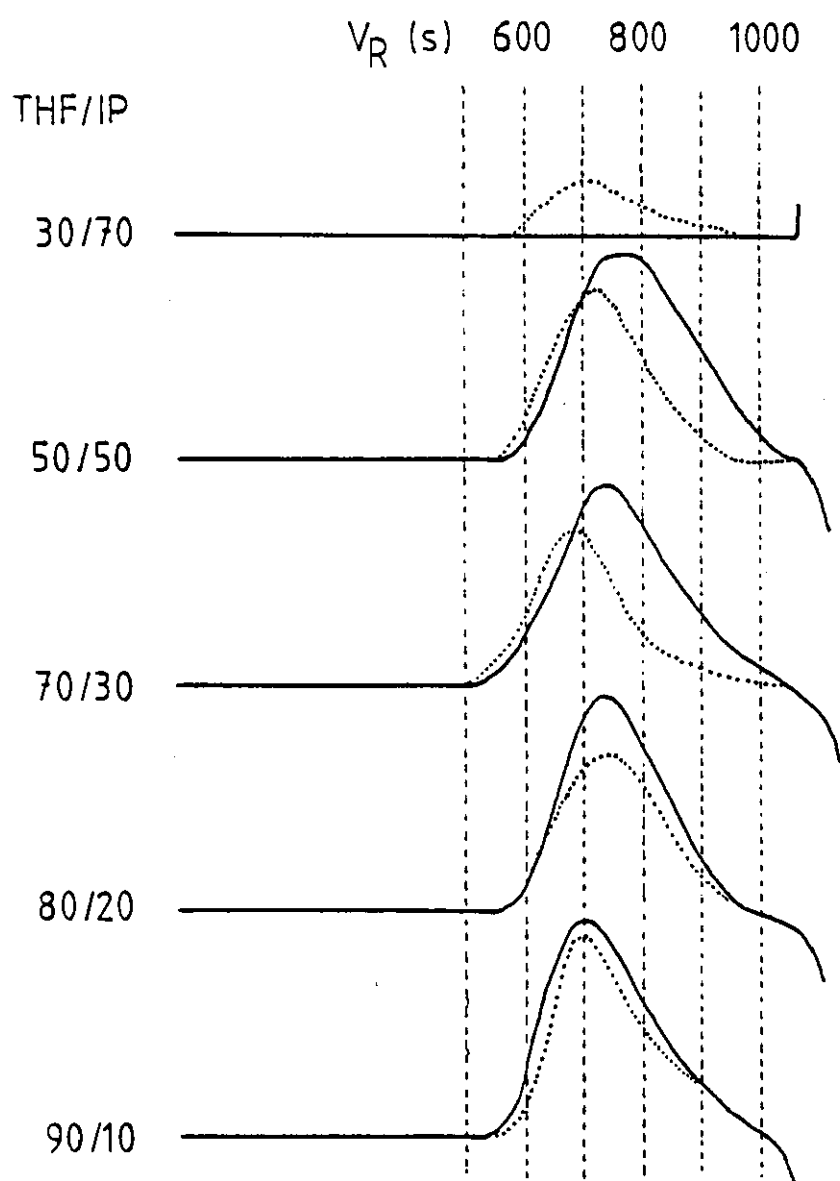


FIGURE 3.45

Chromatograms obtained in system 2, for a slice of separation injections of PSS (—) and PBMA (.....), with a polyacrylamide column packing and THF-IP composition varying from ( 90/10 ) to ( 30/70 ).



available in this study to interpret this variation.

It can be concluded from the 4 different systems studied that PSBA copolymers can be separated according to the copolymer composition and that several mechanisms are operating in each system. The use of polar packings ( polyacrylamide ) in THF-HEP seems to provide better results than nonpolar ( PS-DVB ) packings or even polyacrylamide in THF-HEP, in the separation of PSS and PBMA since the separation of the polymers occurs without precipitation. The size exclusion mechanism can be eliminated by using packings with very small pores so that none of the solute molecules can enter, as suggested by Glockner[103,111] and Mori[116]. In order to analyse quantitatively the CCD of copolymers, adsorption should be the only mechanism operating in the composition separation and a mobile phase with gradient elution would be necessary to provide better separation.

#### 4. CONCLUSIONS AND RECOMMENDATIONS

The chromatographic behaviour of a new column packing for HPSEC based on crosslinked polyacrylamide particles was studied. PEG/PEO standards were analysed with a polyacrylamide column packing in water, water-MeOH ( 80/20 ), and water-MeOH ( 60/40 ) mixtures, and the universal calibration method was shown to be valid for PEO with MW below  $10^5$ . The availability of a polyacrylamide column packing with larger pores would enable the extension of these studies to high MW polymers. This column packing is therefore highly favoured for aqueous separations of poly( ethylene glycol ), because PEG/PEO adsorbs onto silica packings and also onto silica-based packings having bonded-phases[15-17,77,79]. For PSA standards in water and water-MeOH ( 80/20 ) with polyacrylamide column packings, the universal calibration method is valid for MW above  $4 \times 10^3$ , showing that separations are dominated by the size exclusion mechanism. Below this value, secondary mechanisms appear to be taking part in the separation since water-MeOH ( 80/20 ) is a poor solvent for PSA, and solute-packing interactions are favoured[30]. In the future the use of

polyacrylamide packings for the chromatographic analysis of polyelectrolytes should be tested, since another polymeric packing (polyether based) has proved to offer clear advantages over glass or silica based packings in the analysis of charged polymers[15].

Polyacrylamide packings with organic solvents, THF and DMF, and PS and PEG/PEO standards showed an interactive behaviour and the comparison with the universal calibration curve obtained with PEO/PEG in water did not agree. As the adsorptive behaviour of polyacrylamide columns with PEG/PEO in THF and DMF was not reproducible, further work is required to understand whether these interactions depend on variations in the method of gel manufacture or in changes to the pore surfaces occurring during extensive use of the gels for chromatographic separations. Further work should be performed to test whether crosslinked polyacrylamide packings would be suitable for separations of polar polymers in DMF.

Column efficiency data were obtained for PEG standards with polyacrylamide and polyether column packings. The increase in column efficiency for polyacrylamide packings with a decrease in the flow rate or an increase in column temperature was confirmed by the injection of cocktail samples of PEG/PEO. These high column efficiencies and the high pore volume, as shown by the retention times of small solutes on calibration curves, indicate that these polyacrylamide packings are suitable for aqueous high resolution separations of small molecules. In particular, high resolution separation of oligosaccharides have been demonstrated with these polyacrylamide gels[155].

The diffusion coefficient of a solute, obtained from the interpretation of plate height data, and its comparison with the literature values for the diffusion coefficient of the same solute in free solution

showed a predominance of dispersion caused by solute mass transfer in the stationary phase for polyacrylamide and polyether packings in relation to silica based packings[91,150]. It was also concluded, from a comparison of the  $D_s/D_m$  values obtained for polyacrylamide and polyether packings that the restricted diffusion of solutes during mass transfer is higher for polyacrylamide than for polyether column packings. This suggests that studies should be performed to determine porosity formation in the preparation of polyacrylamide packings, in order to change the pore volume characteristics to obtain a more homogeneous pore size distribution.

Two methods were tested for the determination of polydispersities of polymers corrected for axial dispersion. The method developed by Dawkins et al[91,150], based on the interpretation of plate height data, provided reliable values for the polydispersity of PEG standards corrected for axial dispersion. The method developed by Hamielec et al[95], could be tested with confidence for only one polymer ( PEG630 ), since the analysis of the data obtained for a series of PEG standards showed unreliable results. Further work on the method proposed by Hamielec requires much better characterized standards of water-soluble polymers to become available.

A system was developed to perform off-line and on-line multidimensional chromatography. The off-line system was used to provide preliminary information on the detector response of solute injected into system 2 as a function of the injected solute concentration. The dilution of the sample zone as it diverges during separations in the two systems required optimization of the injection and column switching procedures.

The on-line experiments were performed with two columns ( PS-DVB and polyacrylamide ) and two types of mobile phases in order to provide

interactive chromatography in system 2. The results obtained for PS-DVB, a nonpolar column packing, showed that in both solvents ( THF-HEP, THF-IP ) the separation was affected by the action of several mechanisms. The main effect controlling the separation was the solubility of the PSS in the mobile phase. When the concentration of the nonsolvent ( HEP or IP ) was increased, the  $V_m$  of the PSS was increased. When the concentration of nonsolvent is high enough, to make the mixture of THF and HEP ( or IP ) a nonsolvent for PSS, PSS retention was increased and the PSS eluted with the solvent peak. The separation of PSBA copolymers by chemical composition was performed with PS-DVB column packings and THF-HEP ( 30/70 ) and these results were similar to those obtained by Balke et al[104,114-116] using PS, PBMA and PSBA copolymers in THF-HEP with a polyether bonded-phase silica-based column packing. This work therefore confirms that crosslinked polystyrene gels may be used for the interactive chromatography of copolymers according to composition.

The use of the more polar polyacrylamide column packing with THF-HEP showed different results, where the main factor controlling the separation was adsorption and not the precipitation of the polymer in the column. However, in polyacrylamide packings with THF-IP as eluent, the possible formation of a quasistationary layer of IP around the packing, and the incompatibility of PSS and PBMA with IP, prevented the solutes approaching the packing and adsorbing. Whilst these results demonstrate that separations according to copolymer composition can be achieved, it is clear that for a heterogeneous copolymer the molecular size separation in system 1 will be influenced by MW and composition and the separation in system 2 according to solubility changes will also be influenced by MW and composition. To achieve a quantitative characterisation of a heterogeneous

copolymer, it is necessary to perform a separation according to one variable only in system 1 and according to a second variable only in system 2. Consequently, separations by composition involving solubility and/or partition because of their MW dependence are not likely to be satisfactory. Polymer adsorption behaviour is not very sensitive to chain length. Therefore, polar packings such as silica-based packing should be preferred for the copolymer separations according to composition by gradient elution methods[108,116]. Furthermore, if the silica-based packing contains pores which are small enough so that none of the solute molecules can enter, as suggested by Glockner[103,111] and Mori[116], there will only be an adsorption mechanism in system 1 and no size exclusion. Silica-based packings, as used in the experiments of Mori[116] and Danielewicz[108], should provide an ideal choice for system 1. Then, a conventional SEC column would be employed for system 2 to perform size exclusion separations on slices containing copolymer chains having constant composition. With this type of multidimensional chromatography together with adequate detectors, automated quantitative determinations of compositions in copolymers will be possible.



## 5. REFERENCES

1. R. E. Majors, Int. Lab. 1972, Jul/Aug, 25-35.
2. R. E. Majors, J. Chromatogr. 1977, 15, 334-351.
3. E. P. Otocka, Anal. Chem. 1973, 45, 1969-1970.
4. J. Cazes, J. Chem. Ed. 1970, 47, A461-A471.
5. R. E. Majors, Int. Lab. 1975, Nov/Dec, 11-35.
6. R. E. Majors, Anal. Chem. 1982, 54, 323R-363R.
7. L. R. Snyder & J. J. Kirkland, Introduction to Modern Liquid Chromatography, John Wiley & Sons, New York, 1979, p 173.
8. R. E. Majors, LC, HPLC Mag. 1985, 3, 774, 776, 780.
9. See ref. 7, p 21.
10. R. E. Majors, J. Chromatogr. Sci. 1980, 18, 488-511.
11. W. W. Yau, J. J. Kirkland & D. D. Bly, Modern Size-Exclusion Liquid Chromatography, John Wiley & Sons, New York, 1979, p 166.
12. J. V. Dawkins, in J. Janca (Ed.), Steric Exclusion Liquid Chromatography of Polymers, Marcel Dekker, New York, 1984, chapter 2.
13. See ref. 11, p 173.

14. T. Hashimoto, H. Sasaki, M. Aiura & Y. Kato, J. Polym. Sci. Part A-2, 1978, 16, 1789-1800.
15. P. L. Dubin & I. Levy, Polym. Preprints, 1981, 22, 132-134.
16. H. G. Barth, J. Chromatogr. Sci. 1980, 18, 409-429.
17. P. L. Dubin, Sep. and Purif. Methods 1981, 10, 287-313.
18. Y. Kato, H. Sasaki, M. Aiura & T. Hashimoto, J. Chromatogr. 1978, 153, 546-549.
19. Y. Kato, K. Komiya, H. Sasaki & T. Hashimoto, J. Chromatogr. 1980, 193, 311-315.
20. Y. Kato & T. Hashimoto, J. Chromatogr. 1982, 235, 539-43.
21. Y. Kato, T. Matsuda & T. Hashimoto, J. Chromatogr. 1985, 332 39-46.
22. T. Kato, T. Tokuya & A. Takahashi, J. Chromatogr. 1983, 256, 61-69.
23. R. M. Alsop & G. J. Vlachogiannis, J. Chromatogr. 1982, 246, 227-240.
24. P. L. Dubin & I. Levy, J. Chromatogr. 1982, 235, 377-387.
25. PL catalogue, Polymer Laboratories Ltd., Shropshire, U. K.
26. J. V. Dawkins & N. P. Gabbot, Polymer 1981, 22, 291-292.
27. C. Quivoron, in J. Janca (Ed.), Steric Exclusion Liquid Chromatography of Polymers, Marcel Dekker, New York, 1984, chapter 5.
28. J. Janca, in J. Janca (Ed.), Steric Exclusion Liquid Chromatography of Polymers, Marcel Dekker, New York, 1984, chapter 1.
29. J. V. Dawkins, in C. F. Simpson (Ed.), Techniques in Liquid Chromatography, John Wiley & Sons, Chichester, 1982, chapter 12.
30. J. V. Dawkins & M. Hemming, Makromol. Chem. 1975, 176, 1795-1813.
31. J. V. Dawkins, J. Polym. Sci. Part A-2, 1976, 14, 569-571.

32. F. Rodriguez & O. K. Clark, Ind. Eng. Chem. Prod. Res. Develop.  
1966, 5, 118-121.
33. W. W. Yau & S. W. Fleming, J. Appl. Polym. Sci. 1968, 12, 2111-2116.
34. L. H. Tung, Sep. Sci. 1970, 5, 429-436.
35. F. W. Billmeyer, Jr., Textbook of Polymer Science,  
Wiley-Interscience, New York, 2nd. edition, 1971, p 6.
36. J. V. Dawkins, Br. Polym. J. 1972, 4, 87-101.
37. See ref. 35, p 78.
38. See ref. 11, p 289.
39. See ref. 11, p 294.
40. See ref. 11, p 285.
41. J. Janca, J. Chromatogr. 1980, 187, 21-26.
42. Z. Grubisic, P. Rempp & H. Benoit, J. Polym. Sci. Part B, 1967, 5,  
753-759.
43. K. A. Boni, F. A. Sliemers & P. B. Stickney, J. Polym. Sci. Part  
A-2, 1968, 6, 1567-1578, 1579-1591.
44. H. Coll & L. R. Prusinowski, J. Polym. Sci. Part B, 1967, 5,  
1153-1156.
45. H. Coll & D. K. Gilding, J. Polym. Sci. Part A-2, 1970 8, 89-103.
46. J. V. Dawkins, J. Macromol. Sci.-Phys. Part B-2, 1968, 4, 623-639.
47. J. V. Dawkins & M. Hemming, Polymer 1975, 16, 554-560.
48. See ref. 11, p 291.
49. J. Brandrup & E. H. Immergut (Eds.), Polymer Handbook,  
Wiley-Interscience, New York, 2nd. edition, 1975.
50. J. Janca, Adv. Chromatogr. 1981, 19, 37-90.
51. R. Audebert, Polymer 1979, 20, 1561-1566.

52. S. Mori, in J. Janca (Ed.), Steric Exclusion Liquid Chromatography of Polymers, Marcel Dekker, New York, 1984, chapter 4.
53. S. Mori, Anal. Chem. 1978, 50, 745-748.
54. B. G. Belenkii, L. Z. Vilenchik, V. V. Nesterov, V. J. Kolegov & S. Ya. Frenkel, J. Chromatogr. 1975, 109, 233-238.
55. J. Lecourtier, R. Audebert & C. Quivoron, J. Chromatogr. 1976, 121, 173-183.
56. A. Campos & J. Figueruelo, Makromol. Chem. 1977, 178, 3249-3252.
57. J. V. Dawkins, Polymer 1978, 19, 705-708.
58. J. V. Dawkins, J. Liq. Chromatogr. 1978, 1, 279-289.
59. R. B. Walter, & J. F. Johnson, J. Liq. Chromatogr. 1980, 3, 315-327.
60. D. Berek & D. Bakos, J. Chromatogr. 1974, 91, 237-245.
61. D. Berek, T. Bleha & Z. Pevna, J. Polym. Sci., Part B, 1976, 14, 323-327. 62. D. Berek, D. Bakos, T. Bleha & L. Soltes, Makromol. Chem. 1975, 176, 391-398.
63. H. J. Mencer & Z. Vajnaht, J. Chromatogr. 1982, 241, 205-211.
64. J. V. Dawkins & M. Hemming, Makromol. Chem. 1975, 176, 1777-1793.
65. J. V. Dawkins & M. Hemming, Makromol. Chem. 1975, 176, 1815-1828.
66. A. Campos, V. Soria & J. E. Figueruelo, Makromol. Chem. 1979, 180, 1961-1974.
67. J. E. Figueruelo, V. Soria & A. Campos, J. Liq. Chromatogr. 1980, 3, 367-380.
68. J. E. Figueruelo, V. Soria & A. Campos, in Liquid Chromatography of Polymers and Related Materials II (Chromatographic Science Series, Vol. 13, J. Cazes & X. Delamare, eds. ), Marcel Dekker, New York, 1980, p 49-71.

69. J. E. Figueruelo, V. Soria & A. Campos, Makromol. Chem. 1981, 182, 1525-1532.
70. D. Bakos, T. Bleha, A. Ozina & D. Berek, J. Appl. Polym. Sci. 1979, 23, 2233-2244.
71. K. Chitumbo & W. Brown, J. Chromatogr. 1973, 80, 187-197.
72. B. Stenlund, Adv. Chromatogr. 1976, 14, 37-74.
73. J. Janca, J. Chromatogr. 1977, 134, 263-272.
74. J. Janca & S. Pokorny, J. Chromatogr. 1978, 148, 31-36.
75. J. Janca & S. Pokorny, J. Chromatogr. 1978, 156, 27-33.
76. J. Janca, Anal. Chem. 1979, 51, 637-641.
77. J. Janca, J. Chromatogr. 1979, 170, 309-318.
78. J. Janca & S. Pokorny, J. Chromatogr. 1979, 170, 319-324.
79. J. Janca, S. Pokorny, M. Bleha & O. Chiantore, J. Liq. Chromatogr. 1980, 3, 953-970.
80. L. Letot, J. Lesec & C. Quivoron, J. Liq. Chromatogr. 1980, 3, 1637-1655.
81. M. J. R. Cantow, R. S. Porter & J. F. Johnson, J. Polym. Sci., Part B, 1966, 4, 707-711.
82. S. Mori, J. Appl. Polym. Sci. 1976, 20, 2157-2164.
83. A. Rudin & H. W. Hoegy, J. Polym. Sci., Part A-1, 1972, 10, 217-235.
84. A. Rudin, J. Appl. Polym. Sci. 1976, 20, 1483-1490.
85. N. Friis & A. E. Hamielec, Adv. Chromatogr. 1975, 13, 41-70.
86. See ref. 11, p 53.
87. See ref. 11, p 91.

88. J. V. Dawkins, in Liquid Chromatography of Polymers and Related Materials II (Chromatographic Science Series, Vol. 13, J. Cazes and X. Delamare, eds. ), Marcel Dekker, New York, 1980, p 19-39.
89. J. C. Giddings, Dynamics of Chromatography, Part 1, Marcel Dekker, New York, 1965.
90. J. V. Dawkins, & G. Yeadon, Polymer 1979, 20, 981-989.
91. J. V. Dawkins, & G. Yeadon, Faraday Symp. 1980, 15, 127-138.
92. J. V. Dawkins, & G. Yeadon, J. Chromatogr. 1980, 188, 333-345.
93. L. H. Tung, J. Appl. Polym. Sci. 1966, 10, 375-385.
94. A. E. Hamielec in J. Janca (Ed.), Steric Exclusion Liquid Chromatography of Polymers, Marcel Dekker, New York, 1984, chapter 3.
95. A. E. Hamielec & W. H. Ray, J. Appl. Polym. Sci. 1969, 13, 1319-1321.
96. L. H. Tung & J. R. Runyon, J. Appl. Polym. Sci., 1969, 13, 2397-2409.
97. L. H. Tung, Separ. Sci. 1970, 5, 339-347.
98. K. S. Chang & R. Huang, J. Appl. Polym. Sci. 1972, 16, 329-335.
99. G. Glockner, J. Liq. Chromatogr. 1984, 7, 1769-1788.
100. J. H. Duerksen & A. E. Hamielec, J. Appl. Polym. Sci. 1968, 12, 2225-2255.
101. R. E. Majors, J. Chrom. Sci. 1980, 18, 571-579.
102. D. H. Freeman, Anal Chem. 1981, 53, 2-5.
103. G. Glockner, J. H. M. van den Berg, N. L. J. Meijerink, T. G. Scholte & R. Koningsveld, Macromolecules 1984, 17, 962-967.
104. S. T. Balke, Sep. Purif. Methods 1982, 11, 1-28.

105. S. Teramachi, A. Hasegawa, Y. Shima, M. Akatsuka & M. Nakajima, *Macromolecules* 1979, 12, 992-996.
106. L. H. Garcia Rubio, J. F. MacGregor & A. E. Hamielec, in C. D. Craver (Ed.), *Polymer Characterization - Spectroscopic, Chromatographic, and Physical Instrumental Methods*, ACS 203, Washington, 1983, p 311-344.
107. M. Danielewicz, M. Kubin & S. Voska, *J. Appl. Polym. Sci.* 1982, 27, 3629-3631.
108. M. Danielewicz, & M. Kubin, *J. Appl. Polym. Sci.* 1981, 26, 951-956.
109. S. Teramachi, A. Hasegawa, M. Akatsuka, A. Yamashita & N. Takemoto, *Macromolecules* 1978, 11, 1206-1210.
110. S. Teramachi, A. Hasegawa, F. Sato & N. Takemoto. *Macromolecules* 1985, 18, 347-350.
111. G. Glockner, J. H. M. van den Berg, N. L. J. Meijerink, T. G. Scholte & R. Koningsveld, *J. Chromatogr.* 1984, 317, 615-625.
112. S. T. Balke & R. D. Patel, in T. Provder (Ed.), *Size Exclusion Chromatography ( GPC )*, ACS Symposium series 138, Washington, 1980, chapter 8.
113. S.T. Balke & R. D. Patel, *J. Polym. Sci., Part B*, 1980, 18, 453-456.
114. S. T. Balke & R. D. Patel, in C. Craver (Ed.), *Polymer Characterization - Spectroscopic, Chromatographic and Physical Instrumental Methods*, ACS 203, Washington, 1983, chapter 16.
115. S. T. Balke, *Polymer News* 1983, 9, 6-8.
116. S. Mori, Y. Uno & M. Suzuki, *Anal. Chem.* 1986, 58, 303-307.
117. L. Fisher, *An Introduction to Gel Chromatography-Experimental Technique in Column Gel Chromatography*, North-Holland, 1974, p 233.

118. W. P. Edwards, J. Liq. Chromatogr. 1985, 8, 2625-2640.
119. H. H. Teo, R. H. Mobbs & C. Booth, Eur. Polym. J. 1982, 18, 541-544.
120. S. G. Yeates, H. H. Teo, R. H. Mobbs & C. Booth, Macromol. Chem. 1984, 185, 1559-1563.
121. G. N. Patel & H. H. Stejny, J. Appl. Polym. Sci. 1974, 18, 2069-2073.
122. G. N. Patel & H. H. Stejny, J. Appl. Polym. Sci. 1974, 18, 3537-3542.
123. B. Gibson - Private Communication, Loughborough University, U. K.
124. S. Mori & T. Suzuki, J. Liq. Chromatogr. 1980, 3, 343-351.
125. F. P. Warner - Private Communication, Polymer Laboratories, Shropshire, U. K.
126. See ref. 11, p 79.
127. British Standard BS 2000 Part 71, 1982, Designation IP 71/80.
128. E. A. Collins, J. Bares & F. W. Billmeyer, Experiments in Polymer Science, John Wiley & Sons, New York, 1973, p 394.
129. See ref. 35, p 71.
130. E. J. Meehan, J. Polym. Sci. 1946, 1, 175-182.
131. T. Kato, T. Okamoto, T. Tokuya & A. Takahashi, Biopolymers 1982, 21, 1623-1633.
132. A. L. Sparatorico & G. L. Beyer, J. Appl. Polym. Sci. 1975, 19, 2933-2945.
133. H. Engelhardt & D. Mathes, J. Chromatogr. 1979, 185, 305-319.
134. H. Engelhardt & D. Mathes, J. Chromatogr. 1977, 142, 311-320.
135. J. V. Dawkins, J. W. Maddock & A. Nevin, Eur. Polym. J. 1973, 9, 327-343.



136. U. Bianchi & A. Peterlin, J. Polym. Sci., Part A-2, 1968, 6, 1759-1772.
137. T. Kato, N. Nakamura, M. Kawaguchi & A. Takahashi, Polym. J. 1981, 13, 1037-1043.
138. C. Rossi & C. Cuniberti, J. Polym. Sci., Part B, 1964, 2, 681-684.
139. J. V. Dawkins, J. Chromatogr. 1977, 135, 470-472.
140. Bio-Rad Laboratories, Gel Chromatography, 2nd. Ed., Richmond, 1975.
141. E. P. Otocka & M. Hellman, J. Polym. Sci., Part B, 1974, 12, 331-338.
142. T. C. Laurent & J. Killander, J. Chromatogr. 1964, 14 317-330.
143. See ref. 11, p 386.
144. H. J. Mencer & Z. G. Gallot, J. Chromatogr. 1982, 241, 213-216.
145. P. L. Dubin & K. L. Wright, Polym. Preprints 1974, 15, 673-675.
146. P. L. Dubin, S. Koontz & K. L. Wright, J. Polym. Sci., Part A-1, 1977, 15, 2047-2057.
147. K. Nakamura & R. Endo, J. Appl. Polym. Sci. 1981, 26, 2657-2664.
148. S. Mori & A. Yamakawa, J. Liq. Chromatogr. 1980, 3, 329-342.
149. See ref 11, p 233.
150. J. V. Dawkins & G. Yeadon, J. Chromatogr. 1981, 206, 215-221.
151. TSK catalogue, Toyo Soda Manufacturing Co., Ltd., Tokyo, Japan.
152. J. H. Knox & F. McLennan, J. Chromatogr. 1979, 185, 289-304.
153. M. E. van Kreveld & N. van den Hoed, J. Chromatogr. 1978, 149, 71-91.
154. J. C. Giddings, L. M. Bowman Jr. & M. N. Myers, Macromolecules, 1977 10, 443-449.
155. L. L. Lloyd & F. P. Warner, unpublished work.

156. W. W. Law, C. M. Burns & R. Y. Huang, J. Appl. Polym. Sci. 1985, 30, 1187-1194.
157. F. J. Burgess, A. V. Cunliffe, J. V. Dawkins & D. H. Richards, Polymer 1977, 18, 733-740.
158. S. T. Balke, Orthogonal Chromatography, presented at the ACS New York City National Meeting, April 12-13, 1986, New York.

